PREPARATION AND CHARACTERIZATION OF CONTROLLED RELEASE FERTILIZERS USING ALGINATE-BASED SUPERABSORBENT POLYMER FOR PLANTATIONS IN MALAYSIA

YONG TZYY JENG

MASTER OF ENGINEERING SCIENCE

FACULTY OF ENGINEERING AND GREEN TECHNOLOGY
UNIVERSITI TUNKU ABDUL RAHMAN
MAY 2015

PREPARATION AND CHARACTERIZATION OF CONTROLLED RELEASE FERTILIZERS USING ALGINATE-BASED SUPERABSORBENT POLYMER FOR PLANTATIONS IN MALAYSIA

By

YONG TZYY JENG

A dissertation submitted to the Department of Petrochemical Engineering,
Faculty of Engineering and Green Technology,
Universiti Tunku Abdul Rahman,
in partial fulfillment of the requirements for the degree of
Master of Engineering Science
MAY 2015

ABSTRACT

PREPARATION AND CHARACTERIZATION OF CONTROLLED RELEASE FERTILIZERS USING ALGINATE-BASED SUPERABSORBENT POLYMER FOR PLANTATIONS IN MALAYSIA

Yong Tzyy Jeng

Superabsorbent polymers (SAPs) were synthesised through graft-copolymerisation of acrylic acid (AA) and acrylamide (AM) onto sodium alginate (NaAlg) using ammonium persulfate (APS) as initiator, *N,N'*-methylenebisacrylamide (NMBA) as crosslinking agent and calcium chloride (CaCl$_2$) as precipitating agent. The SAPs were synthesised using different molar ratio of AA and AM monomers; 85:15, 70:30; 55:45; 40:60; 25:75 and three different concentration of CaCl$_2$; 1M, 2M and 3M. Self-prepared pure fertilizers with NPK ratio of 15:15:15 were imbedded in the SAPs. The effect of molar ratio of AA and AM and the concentration of CaCl$_2$ on the swelling capacity, biodegradability and rate of release of fertilizer were investigated. Infrared spectroscopy shows a successful grafting of AA and AM onto NaAlg backbones. The grafting efficiency and grafting percentage of AA and AM onto NaAlg were found increasing as the concentration of AM increased. Furthermore, thermogravimetric analysis (TGA) shows that the grafting of AA and AM had improved the thermal stability. Differential scanning calorimetry (DSC) shows that the T_g has increased as the concentration of AM increases and this can be proven by X-ray diffraction study (XRD). XRD study also

shows that the crystallinity of grafted polymers could be influenced by the increment concentration of $CaCl_2$. On the other hand, scanning electron microscopy (SEM) was done on the grafted polymers and it can be deduced that the surface of grafted polymer was more compact with less folds and pinholes as the concentration of AM increased. This directly affected the swelling capacity, biodegradability and release rate of fertilizer from graft polymers. In addition, the water retention of soil also improved with the addition of graft polymers into soil sample.

ACKNOWLEDGEMENT

Date: _____

PERMISSION SHEET

It is hereby certified that **YONG TZYY JENG** (ID No: **12AGM00022**) has completed this dissertation entitled "PREPARATION AND CHARACTERIZATION OF CONTROLLED RELEASE FERTILIZERS USING ALGINATE-BASED SUPERABSORBENT POLYMER FOR PLANTATIONS IN MALAYSIA" under the supervision of Assoc. Prof. Dr. Yamuna Munusamy (Supervisor) from the Department of Petrochemical Engineering, Faculty of Engineering And Green Technology, and Asst. Prof. Dr. Chee Swee Yong (Co-Supervisor) from the Department of Chemical Science, Faculty of Science.

I hereby give permission to my supervisors to write and prepare a manuscript of these research findings for publishing in any form, if I did not prepare it within six (6) months times from this date, provided, that my name is included as one of the authors for this article. Arrangement of names will depend on my supervisors.

APPROVAL SHEET

This dissertation entitled "**PREPARATION AND CHARACTERIZATION OF CONTROLLED RELEASE FERTILIZERS USING ALGINATE-BASED SUPERABSORBENT POLYMER FOR PLANTATIONS IN MALAYSIA"** was prepared by YONG TZYY JENG and submitted as partial fulfillment of the requirements for the degree of Master of Engineering Science at Universiti Tunku Abdul Rahman.

Approved by:

_____

(Assoc. Prof. Dr. Yamuna Munusamy)   Date:…………………..

Supervisor

Department of Petrochemical Engineering

Faculty of Engineering and Green Technology

Universiti Tunku Abdul Rahman

_____

(Asst. Prof. Dr. Chee Swee Yong)   Date:…………………..

Co-supervisor

Department of Chemical Science

Faculty of Science

Universiti Tunku Abdul Rahman

DECLARATION

I <u>YONG TZYY JENG</u> hereby declare that the dissertation is based on my original work except for quotations and citations which have been duly acknowledged. I also declare that it has not been previously or concurrently submitted for any other degree at UTAR or other institutions.

Name _____

(Yong Tzyy Jeng)

Date _____

LIST OF TABLES

LIST OF FIGURES

LIST OF APPENDICES

LIST OF ABBREVIATIONS

AA	acrylic acid
Alg-*g*-P(AA-*co*-AM)	alginate-*g*-poly[(acrylic acid)-*co*-acrylamide]
AM	acrylamide
AN	acrylonitrile
APS	ammonium persulfate
Ca^{2+}	calcium (II) ion
$CaCl_2.2H_2O$	calcium chloride dihydrate
CMC	carboxymethylcellulose
COD	chemical oxygen demand
-COO$^-$	carboxylate
-COOH	carboxylic acid
DSC	differential scanning calorimtery
G	(1,4)-α-L-gulopyranuronic acid
IPN	interpenetrating network
IR	Infra-red
IUPAC	International Union of Pure and Applied Chemistry
KBr	Potassium bromide
kDa	kiloDalton
kPa	Kilopascal
M	(1,4)-β-D-mannopyranuronic acid
m	monomer molecule
$M_1\bullet$	chain initiating species
mPa.s	millipascal seconds
NaAlg	sodium alginate
NaAlg-*g*-P(AA-*co*-AM)	sodium alginate-*g*-poly[(acrylic acid)-*co*-acrylamide]
N-MBA	N,N'-methylenebisacrylamide
PAA	poly(acrylic acid)
PAM	polyacrylamide
PHR	phosphate rock

PMMA	poly(methacrylic acid)
PVP	polyvinylpyrolidone
R•	initiator radical
rpm	revolutions per minute
SAP	superabsorbent polymer
SEM	scanning electron microscopy
Semi-IPN	semi-interpenetrating network
SGF	simulated gastric fluid
SH	sodium humate
SIF	simulated intestinal fluid
TGA	thermogravimetric analysis
wt.%	weight percent
XRD	x-ray diffraction
μL	microlitre

TABLE OF CONTENTS

Page

CHAPTER 1.0

INTRODUCTION

1.1 Introduction

The cultivation of high yield crops requires adequate supply of nutrients for sustained and better crop performance and yield. Thus, fertilizer and water are important factors that limit the production of agriculture, so it is extremely important to improve the utilization of water resources and fertilizer nutrients which are the highest variable costs items in crop production budget.

According to the statistics provided by the Malaysia Government Agency, Fertilizer Industry Association of Malaysia (**FIAM**), the consumption of NPK fertilizer for oil palm plantations in Malaysia for year 2008 alone is around 1.289 million tonnes. Besides that, the analysis report from The World Bank also shows that the fertilizer consumption on arable land in Malaysia is about 1570.70 kilograms per hectare which is extremely high.

However, about 40-70% of nitrogen, 80-90% of phosphorus and 50-70% of potassium of the applied normal fertilizers is lost to the environment and cannot be absorbed completely due to the fact that it will be washed or leached out by rain water, causing not only substantial economic and resource losses but also very serious environmental pollution (Trenkel, 1997; Saigusa, 2000).

As a solution for this problem, controlled release fertilizer using biodegradable superabsorbent polymer is the best idea to be developed not only can release the nutrient contents gradually in order to save its consumption but also can minimize environmental pollution (Wu and Liu, 2008).

1.2   Biodegradable Superabsorbent Polymers

About 90% of traditional superabsorbent polymers are petroleum-based and used in disposable articles. Most of them are disposed in landfills or by incineration (Kiatkamjornwong, Mongkolsawat and Sonsuk, 2002) that can cause serious environmental pollution. Thus, it is the common consensus that non-biodegradable waste has to be evaded, and biodegradable products have to be fully-utilized as much as possible under reasonable economical and ecological conditions in order to build a friendly environment that can lead sustainable development for a country.

Therefore, in recent years, synthesis of biodegradable superabsorbent polymers (SAPs) is attracting researchers' interest in polymer-based production due to their exclusive environmental benefits. Among them, carbohydrates have attracted huge growing interest for the development of biodegradable SAPs.

Biodegradable SAPs are loosely crosslinked networks of hydrophilic polymers that can absorb, swell and retain a very large volume of water or other biological aqueous fluids up to thousands times of their own weight for

certain period and the fluid absorbed is hardly removable even under some pressure.

Moreover, the macromolecules of these polymers are able to break down into smaller compounds or completely degrade in biologically active environment (Baker *et* al., 2009). The biodegradation process is not only caused by microorganisms, but also through hydrolysis and oxidation process in biological environment (Cosgrove *et al.*, 2007). Because of their excellent characteristics, biodegradable SAPs had been widely used not only in agriculture and horticulture but also in other applications.

1.3   Polysaccharides

Carbohydrates are extremely abundant due to their incorporation more than 90% of the dry mass of all biomass, and more than 90% of carbohydrate mass is in the form of carbohydrate polymers which are polysaccharides (Zohuriaan and Shokrolahi, 2004). Polysaccharides, which are the stereoregular polymers of monosaccharide, are distinctive raw materials. The uniqueness of polysaccharides is that they are natural, affordable and available worldwide. Being stable, hydrophilic and amenable to both chemical and biochemical modification (Crini, 2005) caused polysaccharides to be largely exploited for decades in numerous applications.

In addition, polysaccharides carry excellent biological and chemical properties too. These include biodegradability, non-toxicity, high chemical

reactivity, biocompatibility, polyfunctionality and adsorption capacities. The extraordinary adsorption property of polysaccharides involve high hydrophilic characteristic of the polymer due to hydroxyl groups of glucose unit, a large number of functional groups such as acetamido, primary amino and/or hydroxyl groups, high chemical reactivity of the functional groups and flexible structure of the polymer chain (Crini, 2005).

1.4   Polysaccharides For Superabsorbent Polymers

Superabsorbent polymers (SAPs) were first introduced into the agriculture and diaper industries about four decades ago (Omidian *et al.*, 2005). Since then, the application of SAPs have been extended to other industries due to their primary concern: excellent water-holding ability.

SAPs are structurally crosslinked hydrophilic polymer networks which can highly swell after absorbing a large amount of water or aqueous saline fluids, practically 10 to 1000 times of their original weight or volume (Ramazani-Harandi *et al.*, 2006), in short periods. SAPs are not dissolved in the media due to their three-dimensional structure. The electrostatic repulsion force of the ionic charges of the polymer networks stimulates the swelling by dissociation of the carboxylic group (-COONa or -COOK) in the solution (Karadag and Saraydin, 2002), allowing the water to penetrate into the matrix.

The desired features of SAPs include high swelling rate, high swelling capacity and excellent strength of swollen gel (Kabiri *et al.*, 2003; Ramazani-

Harandi *et al*., 2006). The water absorbency of a SAP is greatly affected by its composition, molecular weight, degree of crosslinking, the molecular conformation of the polymer and by the properties of liquids to be absorbed (Chen and Tan, 2006).

Usually SAPs are synthesised using acrylic monomers such as acrylic acid, salts of the acrylic acid and acrylamide (Omidian *et al*., 1998). SAPs are produced with acrylic acid as key material in commercial field. (Lanthong *et al*., 2006). Due to the excellent swelling behaviour, SAPs were used in some water absorbing applications such as feminine napkins, disposable diapers, absorbent pads, agriculture, horticulture and cosmetic.

In recent years, various applications of SAPs are still being expanded to many fields such as horticulture, agriculture and sealing composites, drilling, medicine, fluid additives, artificial snow etc. (Li and Wang, 2005). Van de Velde and Kiekens (2002) mentioned that the applications found in medical field can be divided into three common categories: wound closure and healing products, surgical implant devices and drug delivery systems.

Diapers or other absorbent articles incorporated with biodegradable SAPs might be disposed in municipal composting facilities or directly flushed down the toilet to degrade at municipal wastewater treatment plants or degrade in domestic septic tanks. Therefore, SAP manufacturers have paid their attention to develop biodegradable SAPs in order to fulfill the growing demand for biodegradable products.

1.5 Problem Statements

The problem statements of this research study are as follows:

(i)   The nutrients from the fertilizers are leached out during rain. Plants such as oil palm and rubber trees are unable to fully assimilate most of the nutrients released from fertilizers.

(ii)   Excessive loss of fertilizers to the environment result substantial economic and resources losses.

(iii)   Unabsorbed nutrients release from fertilizer cause environmental pollution.

1.6 Objectives of Research Study

The objectives of this research study are as follows:

(i)   To synthesise a biodegradable SAP derived from sodium alginate, namely crosslinked NaAlg-g-P(AA-co-AM).

(ii)   To study the effects of the molar ratio of monomers (AA and AM) and the concentration of precipitating agent ($CaCl_2$) on the swelling capacity of the sodium alginate-based SAPs.

(iii)   To characterize the grafted SAPs by determining the functional groups, thermal stability, surface morphology, crystallinity, glass transition temperature and melting temperature, biodegradability through Fourier

transform infrared (FTIR), thermogravimetric analysis (TGA), scanning electron microscopy (SEM), X-ray diffraction study (XRD), differential scanning calorimetry study (DSC) and weight loss test using soil burial, respectively.

(iv)   To formulate controlled release fertilizers using NaAlg-based SAPs.

(v)   To study the release rate of NPK fertilizer from biodegradable SAPs through soil burial test and the water retention of the plantation soil samples.

CHAPTER 2.0

LITERATURE REVIEW

2.1 Polymer, Copolymer and Graft Copolymer

The term "polymer" derives from *polus* or *poly* mean many and *meros* mean parts is used to describe macromolecules, whose structure is composed of a minimum of several hundred repeating chemical subunits (Murray, 1977) and its relative molecular masses in excess of 5000 g/mol. The repeating chemical units which make up a polymer are named as monomer molecules. A polymer is then a substance with high molecular mass composed of molecules with repeating chemical structural unit, or monomers, which are connected strongly by chemical covalent bonds.

Macromolecules are classified according to different criteria. The criterion is according to the number of different types of monomers (Braun *et al*., 2005). Homopolymers are the polymers when they are produced from a single type of monomer. If there is a second or third type of monomer involved in the polymer synthesis, the products are named as "binary, ternary, … copolymers". Different arrangement of monomers in copolymer chains are categorized into alternating-, block-, statistic- and graft-copolymers.

Graft copolymer is one kind of copolymer in which one or more blocks

of homopolymer *X* are grafted onto main chain of homopolymer *Y*. This means that a branched copolymer with one or more side chains of a homopolymer *X* attached to the homopolymer *Y* backbone. The grafted copolymer is given a name by mentioning the main chain first, with the word "*-graft-*" in between the names of the corresponding homopolymers. For example: poly*Y-graft-*poly*X* (Odian, 1991).

2.2   Alginates

2.2.1   Source of Alginic Acid

Alginic acid is a natural acidic polysaccharide extracted from *phylum Phaeophyta* which is brown algae. It exists as the most abundant polysaccharide in the brown algae which consists up to 40% of the dry matter (Draget, 2009). The extracts of polysaccharides from marine macroalgae are named as hydrocolloids or phycocolloids because they show colloidal properties when dissolved in water and are extracted from phykos (the Greek word 'phykos' refers to seaweed) (Lewis *et al*., 1988).

Even though this polysaccharide is found in all kind of species of brown seaweeds (Chandia *et al*., 2005), the main species of commercial purposes are *Ascophyllum nodusum*, *Durvillaea antartica*, *Eclonia maxima*, *Laminaria digitata*, *Laminaria hyperborea*, *Laminaria japonica*, *Lessonia nigrescens*, *Macrocystis pyrifera*, and *Sargassum spp* (Cui and Wang, 2006). Besides that, Davis *et al*. (2003) also mentioned that alginic acid can also be found in the family *Corallinaceae* of the red algae (*phylum Rhodophyta*).

Alginate appears within the inner layer of the cell wall matrix and in the mucilage or intercellular matrix as a gel containing barium, calcium, magnesium, sodium and strontium ions (Davis *et at*., 2003; Draget, 2009). As the major structural polysaccharide of brown seaweed, alginate carries its flexibility in order to conduce to the strength of the cell wall. The abundance of alginic acid alters between 10% and 40% of the dry weight of untreated brown algae. This alteration depends on the seasonal variation and the depth at which the brown algae grow in the water (Davis *et al*., 2003; Sabra and Deckwer, 2004).

Moreover, alginic acid is also synthesized as capsular polysaccharides by two types of soil bacteria, *Azotobacter vinelandii* and *Pseudomonas aeruginosa* (Robyt, 1998; Draget *et al*., 2005) in addition to be in natural brown seaweeds that can be found in the shallow waters of temperate zones. All the commercial alginates are extracted from algae sources (Draget, 2009). Even if the mechanism involved in producing alginate is not nouveau, but the fact that these bacteria-synthesised alginic acid corresponds to alginates from brown algae is incontrovertible.

2.2.2 Chemical Structure of Alginic Acid

Alginic acid is an unbranched block copolymer consisting of two distinct monosaccharide residues, (1,4)-β-D-mannopyranuronic acid (M) (Figure 2.1) and (1,4)-α-L-gulopyranuronic aicd (G) (Figure 2.2). Though Robyt (1998) mentioned that the amounts of M and G are in the ratio of 2:1 for

most alginic acids, the ratio of the uronic acids can deviate widely with the algal species, type of tissue, habitat, season and age of the plant (Robyt, 1998; Chandia *et al.*, 2005; Leal *et al.*, 2008).
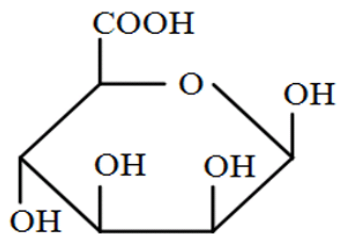
Figure 2.1: **(1,4)-β-D-mannopyranuronic acid (M)**
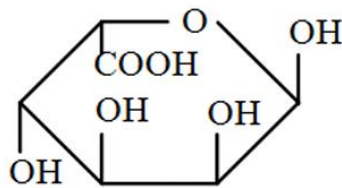
Figure 2.2: **(1,4)-α-L-gulopyranuronic aicd (G)**

Draget *et al.* (2005) described that the polymer can be described into three distinct portions through partial acid hydrolysis. The repeating units of the respective M and G molecules form the homopolymeric M- and G- blocks. These homopolymeric regions of M- and G- blocks are separated in proper order by alternating repeating units of M and G (so-called the MG blocks) (Figure 2.3).
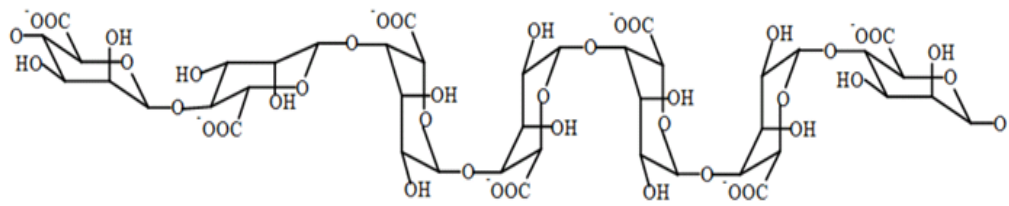
Figure 2.3:   Chain conformation of MG block

Painter *et al*. (1968), Smidsrød and Whittington (1969), Larsen *et al*. (1970) and Draget *et al*. (2005) described that the sequential structure of an alginic acid polymer does not have regular pattern, hence the Bernoullian statistics could not give the explanation regarding the distribution of monomers along the polysaccharide chain. This finding was supported by Orive *et al*. (2006). However, Larsen *et al*. (1970) suggested that a second-order Markov model would be more suitable to describe the monomer sequence in alginates.

Alginates are the salts and derivatives of alginic acid. The polysaccharide is called alginic acid which is water-insoluble if the acid groups are in the carboxylic form (-COOH), whereas, it is known as the alginate or sodium alginate if the acid groups are in the carboxylate form (-COO⁻) (Figure 2.4). Glicksman (1953) stated that alginic acid is insoluble and thus the sodium, potassium and ammonium salts are more preferable for industrial area and food purposes. Among all of these salts, sodium alginate is the compound that most widely used in most of applications.
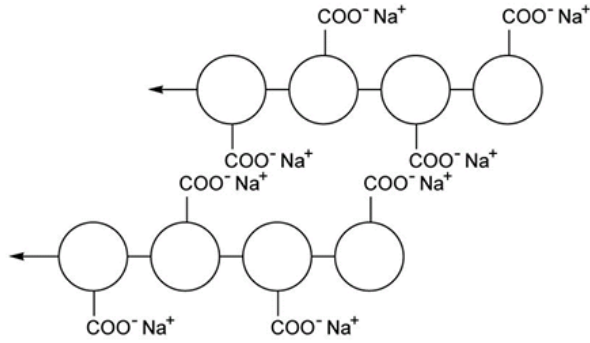
Figure 2.4: **Model of sodium alginate**

2.2.3 Physical Properties of Alginate

Generally, the molecular masses of alginates range between 500 and 1000 kDa. They are soluble in hot and cold water. Their solubility is affected by some factors such as pH, concentration of solution, ions in solution, the presence of divalent ions (Moe *et al.*, 1995) and ionic forces (Rioux *et al.*, 2007). The viscosities of alginates could reach up to 5000 mPa.s for 1 wt.% of solution. Alginate solutions are known as pseudoplastic, therefore a drop in viscosity is expected as higher shear is applied. Concentration of polymer, size of polymer, temperature and rate of shear are those known physical variables that can influence the flow characteristics of alginate solutions, while chemical variables like monovalent salts, polyvalent cations, pH and sequestrants (Lewis *et al.*, 1988).

Alginates gels are well-known to be cold setting if compared with other gelling polysaccharides. This denotes that alginate gels are independent of temperature but the kinetics of the gelling process may be strongly altered by a

temperature change. Being non-equilibrium gels, alginates are dependent upon the history of formation. Therefore, the properties of the gel product will be modified if the gelation process falls on different temperature (Draget, 2009). The thermoirreversibility of alginate gels also shows that the gels are thermally stable and thus they can only be heat-treated without melting though they may degrade in the end (Cui and Wang, 2006).

The most noteworthy physical properties of alginate is its selective binding of multivalent cations (Draget *et al*., 2005). Sodium ions in sodium alginate will be substituted by the divalent metal ions whenever it interacts with divalent metal ions. The polysaccharide is then crosslinked by the divalent metal ions (such as barium, cadmium, calcium, cobalt, copper, lead, nickel, strontium or zinc) to form gels. Among all of these divalent ions, calcium is most frequently used to form gels (Figure 2.5).
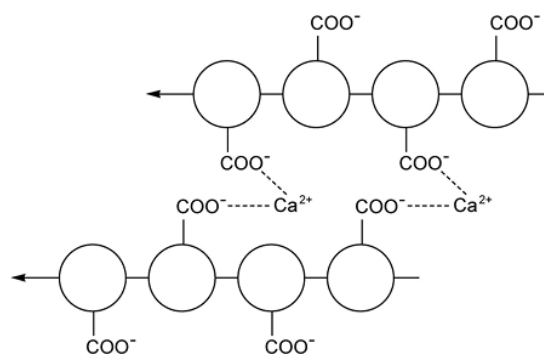
Figure 2.5:   Model of calcium alginate

Robyt (1998) mentioned that the alginate gels formation and the affinity force of divalent cations are predominately due to the presence of G residues.

The binding sites for the calcium ions are believed to be formed by two axially linked G residues. That sequence of G between two or more alginate molecules builds a gel network of calcium to crosslink the alginate molecules. This is known as the "egg-box" model, since the calcium ions resembled eggs fitting into a box made by the alginate chains (Figure 2.6).
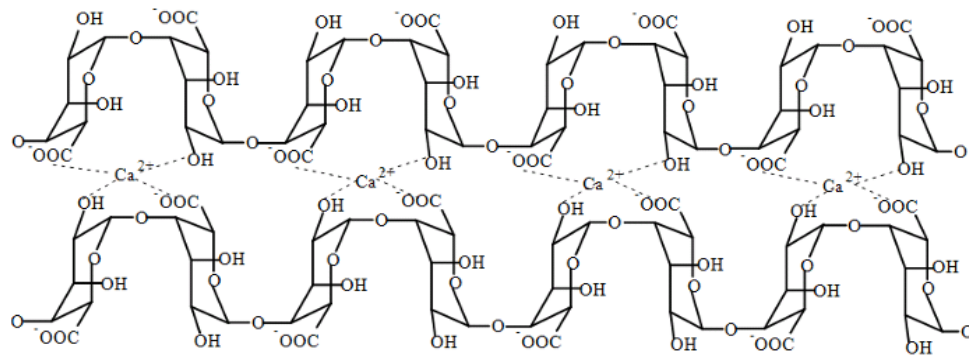
Figure 2.6:   "Egg-box" model

2.2.4   Applications of Alginate

Sabra and Deckwer (2004) stated that about 50% of alginate has been used in the food industry and this has witnessed the fast growing demand of alginates in the global market. The alginates used in the food industry are products mostly from harvested brown algae, and global market for this polysaccharide is approximately 30,000 tons.

Although alginates do not carry any nutritional value, there are still often used as additives to modify and stabilise the texture of foods. Due to the ability of gel formation and stabilising aqueous mixtures and emulsions (Torres

et al., 2007), alginates are widely used as additives in foods such as dessert gels, bakery products, salad dressings, beverages, fabricated foods, dairy products and frozen desserts (Lewis *et al.*, 1998) through the ability of viscosifying, stabilising, emulsifying and gelling aqueous solutions. Alginate is also used in ice cream making in order to prevent crystallisation and shrinkage, therefore giving a more homogenous product (Sabra and Deckwer, 2004).

Some toxicology studies have already verified the high safety level of alginates in food industry. The U.S. Federation of American Societies for Experimental Biology (FASEB) established the alginates as "generally recognized as safe" in year 1982. The European common market (EC) regulations and the Codex Alimentarius Commission of the United Nations Food and Agriculture Organisation/World Health Organisation also legalized the application of alginates in food industry (Lewis *et al.*, 1988).

Furthermore, alginates are also widely used in medical applications. It acts as an assisting agent in human-health for some decades. Thomas (2004) revealed that the salts of alginic acid have a very long history in the wounds management and large amounts of alginates are used for the exuding wounds treatment like pressure ulcers, leg ulcers and infected surgical wounds. Other than traditional wound dressings, alginates are also applied in dental impression material and in some formulations to prevent gastric reflux (Draget *et al.*, 2005).

The drastic increment in the usage of alginate in the medical field

started with the acknowledgment of its usage as a scaffold for encapsulation and immunoprotection of transplanted cells. According to Wong (2004), alginates are known as immobilisation matrices in various biotechnological processes.

Sabra and Deckwer (2004) stated that calcium alginate gels is the most widely used medium to immobilize living cells like bacteria, algae, yeast, and animal and plant and cells. The immobilisation of living cells is accomplished in a single-step procedure through cells entrapment within calcium alginate gel-spheres under very mild conditions and therefore it is compatible with most cells (Draget *et al*., 2005). From production of ethanol by yeast, to production of monoclonal antibodies by hybridoma cells, to mass production of artificial seed by entrapment of plant embryos, the use of this immobilisation technique is immense.

In addition, Wong (2004) also stated that alginate has been used to immunoprotect recombinant cells delivering tumor-suppressing agents and growth hormone. Cell types like chondrocytes, islets, bone-marrow stromal cells, fibroblasts, myoblasts, kidney cells and epithelial cells have been achieved as stable cultures in alginate beads.

2.3 Poly(acrylic acid) and Polyacrylamide

The polymers and copolymers of acrylic acid ($C_3H_4O_2$; IUPAC name: prop-2-enoic acid; common synonyms: vinylformic acid, acroleic acid, propene

acid, ethylenecarboxylic acid, propenoic acid) and acrylamide (C_3H_5NO; IUPAC name: prop-2-enamide; common synonyms: acrylic amide, 2-propenamide) are categorised in the acrylic family of polymers.

Polyacrylamide (Figure 2.7) is used as flocculants in papermaking, mining and treatment of municipal drinking water and industrial wastes whereas the crosslinked polyacrylamide is also used in gel electrophoresis (Odian, 1991).

Poly(acrylic acid) (Figure 2.8) is used as adhesives, crosslinked ion-exchange resins, and it is found useful as dispersants for inorganics pigments in paint. Furthermore, it is used as flocculants to aggregate suspended particles in metal recovery and clarification of waste and potable waters. Other than that, it is also used as thickening agent to increase the viscosity of a solution without modifying its properties and also improve the suspension and emulsion which can increase the stability of related product (Odian, 1991).
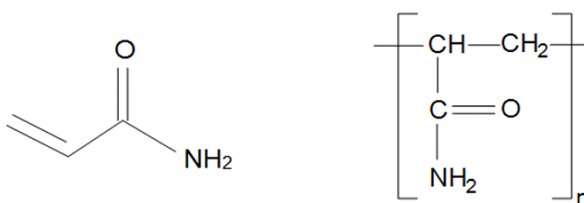
Figure 2.7:   Acrylamide (AM) and Polyacrylamide (PAM)
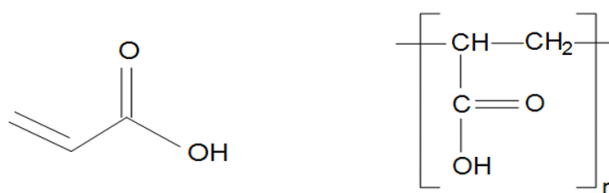
Figure 2.8: **Acrylic Acid (AA) and Poly(acrylic acid) (PAA)**

PAA is generally acknowledged as a polyelectrolyte which has been widely utilised in the area of site-specific drug delivery to specific regions of the gastrointestinal tract. However, due to its great water solubility, PAA which acts as drug carrier, has been restricted to a certain level because of the dissolution before the drug can be delivered. Huang *et al*. (2007) mentioned that PAA is normally crosslinked with organic cross-linkers to form interpenetrating networks (IPNs) to overcome this disadvantage, but this seems to have some limitation in the morphology and properties such as morphological inhomogeneity and mechanical weakness in the systems.

Yin *et al* (2008) cited Huang *et al*. (2007) as proving that the carboxylic acid groups in PAA allow it to build different types of intermolecular interaction such as hydrogen bonding, electrostatic force and dipole-ion with other polymers, especially ionic natural polysaccharides. After some various investigations from researchers, the swelling property of the hydrogels is greatly affected by these mentioned interactions, and hence the PAA hydrogels are applied in pharmaceutical purposes, especially in drug delivery systems.

2.4   Graft Copolymerisation

Graft reaction involves the copolymerisation of a monomer onto the polymer backbone – it originates from the formation of an active site at a point on a polymer chain other than its end, followed by the exposure of this site to a monomer (Han *et al*., 2003).

2.4.1   Advantages of Graft Copolymerisation

Modification of polymers has gained lots of attention in recent years. Grafting method is one of the universal, accessible, effective and promising methods of chemical modification of high molecular weight compounds especially natural polymers (Lee *et al*., 2005a). Işıklan *et al*. (2010) emphasized that grafting is a well-established and powerful method for the synthesis of natural-synthetic polymer hybrid materials. Grafting method may improve the functional properties of polymers by modifying their physical and chemical properties. With polymer grafting, the properties of the pendant chains can be enforced to those substrate polymers without changing the latter to a great extent (Lee *et al*., 2005a).

Zhu *et al*. (1996) described that the polymer grafting allows the conversion of commodity-based polymers to value-added specialty polymers. For example, the grafting of maleic anhydride oligomers onto polyolefins (PO) to enhance the adhesive properties of the polymers to metals and glass fibers grafting of elastomers, the grafting onto polypropylene (PP) to improve the

impact strength for applications in the automobile industry and the grafting of highly charged ionic polymers onto high molecular weight polyacrylamide (PAM) to have better flocculation effects.

Alginate-based graft copolymers are getting more important due to their high potential in industry. The wide availability of vinyl and other monomers implies that the polymer grafting is a powerful method to affect substantial modifications to alginate properties and thus expand its applications and utilisation. Işıklan *et al*. (2010) also mentioned that the desired properties could be introduced by graft copolymerised of vinyl monomers onto alginate. A variety of types of side chains leads the development of application of alginates.

The grafting of vinyl monomers such as methyl acrylate (Patel *et al*., 1999), acrylamide (Tripathy *et al*., 1999; Xu *et al*., 2006), acrylonitrile (Lee *et al*., 2005b; Pourjavadi and Zohuriaan-Mehr, 2002), acrylic acid (Yin *et al*., 2008) and itaconic acid (Işıklan *et al*., 2010) onto alginate has attracted a huge attention and shown its precious value in developing new polymeric materials with unique properties and increasing the range of its utilisation. In this research study, instead of grating either one type of the monomer onto alginate, the grafting reaction was carried out by grafting acrylic acid and acrylamide altogether on alginate backbone. This is due to different monomers have different kinds of nature. Incorporation of AM together with AA in grafting process can manipulate the controlled release system by delaying the biodegradation and reducing the water absorbency.

2.4.2 Methods for Synthesis of Graft Copolymerisation

Braun *et al*. (2005) described that the methods for the synthesis of graft copolymers can be classified into three divisions The first method of preparation of graft copolymers is the homo- and copolymerisation of macromonomers, such as monofunctional polyethylene oxides (PEO) or methacrylic acid esters of long chain aliphatic alcohols, via anionic polymerisation where the reactive chain end is modified with a reactive vinyl monomer (Figure 2.9).
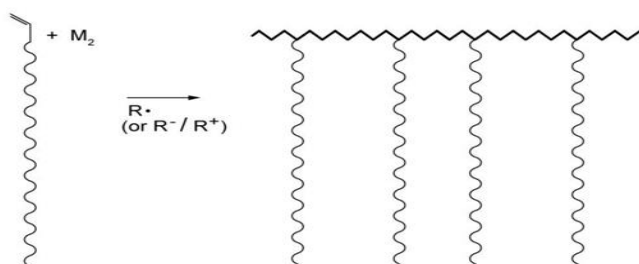
Figure 2.9: **Copolymerisation of macromonomers (Braun *et al*., 2005)**

The second way of synthesising graft copolymers is named as "grafting form". The long chain branches are formed when the active sites brought forth at the polymer X backbone initiated the polymerisation of monomer Y (Braun e*t al*., 2005) as shown in Figure 2.10. The radical center on the polymer X backbone could be with irradiation using UV radiation or with any other high energy radiation such as electron beam radiation.
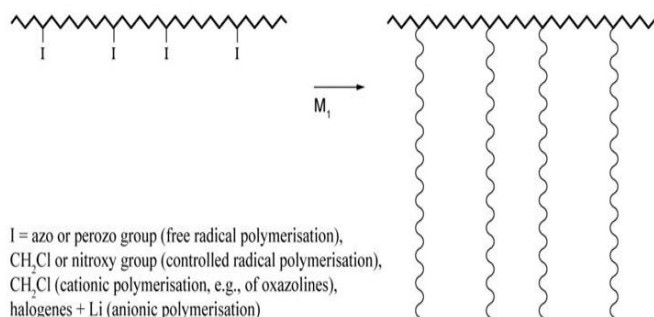
Figure 2.10: Copolymer grafted from polymer X (Braun *et al*., 2005)

The last method is termed as "grafting onto", in which a long branch is formed when the polymer X backbone is attacked by a growing chain of monomer Y via chain-transfer, in polydienes (Figure 2.11). The reaction of monofunctional oligomers with the reactive side groups of a polymer backbone is also one kind of "grafting onto" reaction.
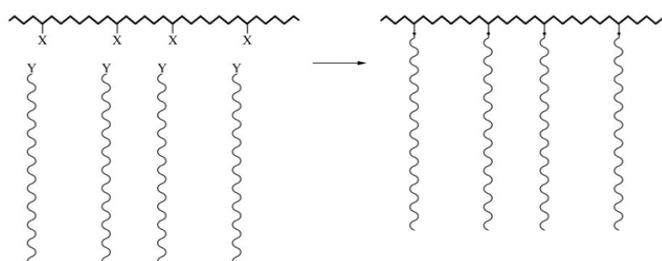
Figure 2.11: Grafting of growing chain Y onto polymer backbone X

(Braun et al., 2005)

Da Silva *et al*. (2007) mentioned that the copolymerisation reaction of AM grafting onto polysaccharides using persulphate as the initiator, is decomposed to produce sulphate ion radicals which are known as chain carriers (refer to Section 2.5.2.1 for more details). Hydrogen radical is then abstracted

from hydroxyl group of the polysaccharide to generate alkoxy radicals on the substrate and results in active centres on the substrate to initiate radical polymerization reaction of AM and form to a graft copolymer.

Meanwhile, Saboktakin *et al*. (2009) carried a free radical graft copolymerisation of poly(methacrylic acid) (PMMA) onto carboxylmethyl starch (CMS) at 70ºC, using bis-acrylamide as the crosslinker and persulfate as an initiator. The authors studied the equilibrium swelling studies in enzyme-free simulated gastric and intestinal fluids (SGF and SIF, respectively). They found that the swelling and hydrolytic behaviour of the hydrogels was dependent on the content of MAA group, which resulted an increase in gel swelling in SIF or a decrease in gel swelling in SGF.

Tripathy *et al*. (1999) had grafted PAM onto NaAlg using a ceric ion initiated solution polymerisation technique at 27±1ºC. Six graft copolymers had been prepared with a variation in the number and length of grafted PAM chains. The results showed that graft copolymers containing longer PAM chains were having the highest flocculation-efficiency. After few years, Xu *et al*. (2006) carried on the previous work and they found out that the graft copolymer was much more flocculation-efficient in kaolin suspension, in removal capacities for chemical oxygen demand (COD) and colority in dyeing wastewater.

2.5 Chain Growth Polymerisation

Chain growth polymerisation or addition polymerisation is a technique where activated species (initiators) add onto active centers of growing polymer chain. The molecules are linked together through double or triple chemical bonds or are cyclic and having sufficiently high ring strain. Braun *et al* (2005) stated that the chain growth polymerisation is divided into three different categories based on the mechanism of initiation, whether the chains initiation occurs via ionic (Cationic or anionic), radical or coordinative-acting (which can be found in transition-metal mediated polymerisation) initiators. Ebewele (2000) also mentioned that those initiators are regularly but inaccurately identified as catalysts and it is noteworthy that those initiators are used up in the reaction, whereas catalysts are regenerated at the end of the reaction.

As the initiation system, which is made up of redox system that could generate radicals in the initiation step in this research study, the chain growth polymerisation naturally proceeds through the radical polymerisation pathway. Hence, only radical polymerisation is going to be described in the following section.

2.5.1 Radical Chain Polymerisation

Braun *et al* (2005) stated that there are three distinctive kinetic steps involved in free radical chain reaction: initiation step, propagation step and termination step. Once the active centers are produced in the initiation step, the

reaction will immediately propagate rapidly through the action of macroradicals or macroions until the termination stage that forms inactive macromolecules is accomplished.

The initiation step of free radial chain polymerisation involves two reactions: formation of initiator radical (which is the rate-determining step in initiation stage) and addition of the initiator radical to monomer. The initiator radicals of chain reactions are produced by the hemolytic dissociation of the relatively weak covalent bond in the initiator to acquire a pair of initiator or so-called primary radicals, R•. The primary radical, R• then binds together with the first monomer molecules (m) to form a new radical, M_1• (chain initiating species).

Odian (1991) described that the rapid growth of M_1• by the consecutive additions of hundreds or thousands of monomer molecules indicated the beginning of the propagation step. With each addition of monomer molecules, there is a new radical that is larger by one monomer unit than the previous primary radical is formed.

The reaction continues to propagate at the reactive chain ends in the chain-reaction polymerisation. It only stops during the termination reaction whereby the reaction deactivates the chain ends or causes the monomer to be completely consumed. According to Odian (1991), the termination reaction could either happen by molecular reaction between radicals by combination (coupling), or disproportionation in which a β-hydrogen radical of one radical

centre is shifted to another radical centre.

Braun *et al.* (2005) cited Buchhloz and Graham (1998) as proving that both disproportionation and combination reactions are kinetically indistinguishable. The only difference of these two termination reactions depends on the products formed. The combination reaction produces a single polymer chain whereas the disproportionation reaction generates in two chains, each with half the molecular mass of the product from recombination.

2.5.2 Thermal Initiation Using Ammonium Persulfate as Initiator

Ammonium persulphate (as shown in Figure 2.12; common synonyms: diammonium persulfate, ammonium peroxydisulfuric acid, ammonium peroxydisulfate), which is an inorganic peroxo compound, is used in the initial stage of this research study. It is a thermal initiator that decomposes at high temperature.
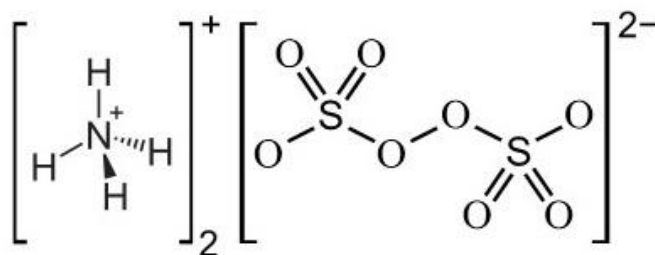
Figure 2.12:   Ammonium persulfate; $(NH_4)_2S_2O_8$

Ammonium persulfate (APS) is used regularly in the polymerization reaction because this initiating agent (concentration $0.1 - 1.0$ wt.% with respect

to monomer) could be thermally decomposed into radicals (Figure 2.13) that can initiate the polymerisation reaction even at low temperature at 30°C (Braun *et al.*, 2005), therefore it is known as a thermal initiator.

Sulphate Anion Radical

△ = Thermal Initiation
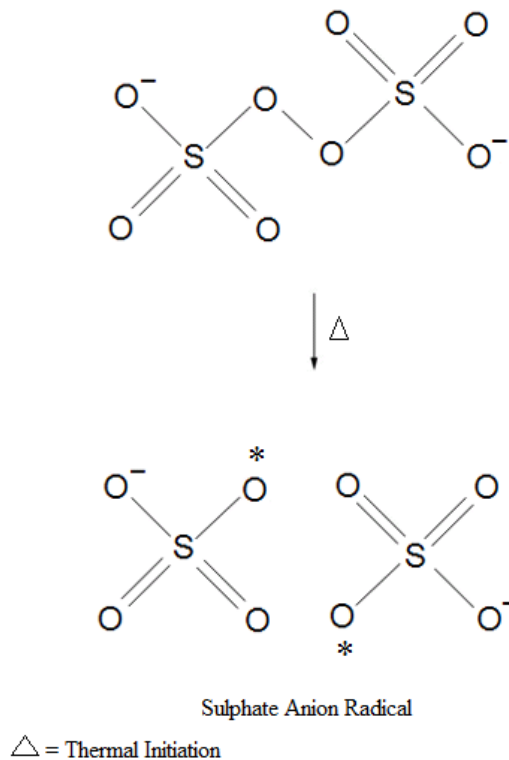
Figure 2.13:   Thermal Initiation of APS

The decomposition of persulphate ions in the polymerisation reaction (initiation stage) proceeds according to Equation 2.1 – 2.3 (Rudin, 1999; Braun *et al.*, 2005). Each initiators molecule decomposes to produce two types of primary radicals (sulphate and hydroxyl radicals). Rudin (1999) suggested that these radicals work well at the temperature range of 40 to 90 °C, whereas Braun *et al.* (2005) also proposed that the desired temperature for every polymerisation reaction is at the temperature range of 40 to 90 °C for the radicals.

$$S_2O_8^{2-} \rightarrow 2 \cdot OSO_3^-$$ …… (2.1)

$$\cdot OSO_3^- + H_2O \rightarrow HSO_4^- + \cdot OH$$ .... (2.2)

$$2 \cdot OH \rightarrow H_2O + \tfrac{1}{2} O_2$$ ……. (2.3)
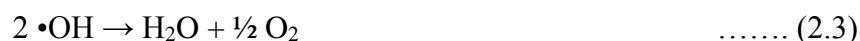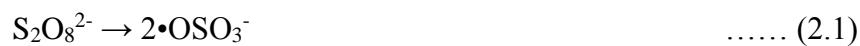
2.6   Crosslinking

It is worth mentioning that the crosslinks' nature significantly affects the properties of SAPs. Elastic gels are formed when SAPs absorb any liquid (e.g water). The gel formed is then a soft, deformable solid composed of the expanded polymer chains and water (Buchholz and Graham, 1998). Ionic, covalent and hydrogen bonds are the three major bonding types that connect the polymer chains together to form ionic, covalent and physical gels.

Buchholz and Graham (1998) stated that there are two methods to form covalent gels; the first type of covalent crosslinks are introduced via condensation or addition reaction when a di- or tri- functional reagent reacts with performed polymer chains, for instance the carboxylic acids, whereas the second type of covalent crosslinks are formed through a free-radical initiated addition polymerisation when a di-, tri-, or tetra-vinyl monomer such as N, N'-methylenebisacrylamide (N-MBA) (Figure 2.14) is used to copolymerise the major monomer, for instance, AA.
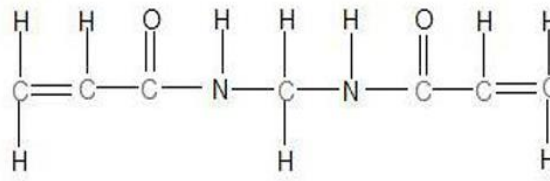
Figure 2.14: *N, N'*-methylenebisacrylamide (N-MBA)

Due to the association of unlike charges, ionic crosslinks are produced through reaction of a polyvalent ion of opposite charge and the charged polymer chains. If ionic crosslinks compared to covalent crosslinks, the placement of the crosslinks is less affected by the chemical structure of the crosslinker because the bond is formed by ion association. The main disadvantage of ionic gels is that the ion exchange might happen between the ionic crosslinks and the ionic components present in the liquid, as the result, the nature of the crosslinks and behavior of the SAP are modified. Moreover, Buchholz and Graham (1998) also stated that the incorporation of the crosslink and the final structure of the SAP are difficult to control due to the rapid interionic reaction.

Physical gel is formed when the hydrogen bonds are formed between segments of one chain with the segments of another chain. Due to the presence of polypeptide chains, the gelling of gelatin solution is a typical example of physical gel which allows the strong hydrogen bonds forming between their chains. Physical crosslinks have their disadvantage as well. Aside from the reduction of the mass efficiency of the crosslinker due to the extension of the multiple segments of the polymer chains, simple heating of the polymer can

also demolish the crosslinks (Buchholz and Graham, 1998).

2.6.1   Gels Crosslinking by Copolymerisation

Small amounts of crosslinkers are certainly required in order to modify the properties and characteristics of superabsorbent polymers. Crosslinking agents are used to introduce crosslinks or so-called intermolecular bridges between polymer chains. Unlike branched polymer in which the side growth of each polymer chain is terminated before the polymer chain could have a chance to interconnect with another polymer chain in a crosslinked (Figure 2.15) polymer, the growing polymer chains are chemically bonded (Ebewele, 2000).
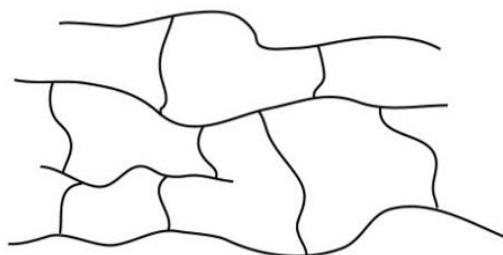
Figure 2.15:   Crosslinked Polymer

Buchhloz and Graham (1998) had ranged the copolymerisable crosslinkers in superabsorbent polymers widely from functional compounds (N, N'-methylenebisacrylamide, allymethacrylate and diacrylate esters) to trifunctional compounds (1, 1, 1-trimethylol-propanetriacrylate and triallylamine) and to tetra-functional compounds (tetraallyloxyethane).

The efficiency of crosslinking agents relies on respective factors and there are steric hindrance and reduced mobility at the site of pendant double bonds, solubility of the crosslinker in the monomer mixtures and the tendency of a crosslinker to undergo intermolecular addition reaction, for example: cyclopolymerisation (Buchholz and Graham, 1998).

2.6.2   Crosslinking of hydrogels with *N, N'*-methylenebisacrylamide

The bifunctional compound *N, N'*-methylenebisacrylamide (*N*-MBA, $C_7H_{10}N_2O_2$, IUPAC name: *N*-[(Prop-2-enoylamino)methyl]prop-2-enamide) is a most often used water soluble crosslinking agent.

A new macro-radical, which has four reactive sites, is produced from N-MBA crosslinker in any polymerisation reaction involving the crosslinking agent (Figure 2.16) due to the poly-functionality of N-MBA (Singh *et al.*, 2007)
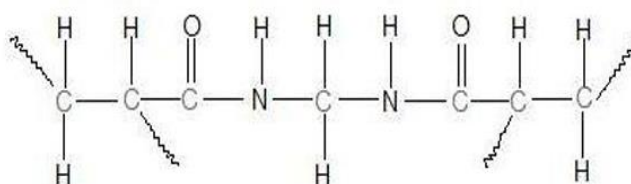
Figure 2.16:   Linking sites of *N, N'*-methylenebisacrylamide

These mentioned reactive sites (Figure 2.15) are the sites that can be linked both with the radicals on the natural polysaccharide (NaAlg) and the

synthetic polymers (PAA and PAM) used in the synthesis of the SAP in this research study. As a result, a three-dimensional network is formed.

From the research article presented by Wang (2007), the author proposed that in the synthesis of cellulose-based SAP with N-MBA as the crosslinking agent, the polymerization mechanism is shown in Figure 2.17. With this epistemology, the mechanism of the crosslinking reaction between NaAlg-based SAP and N-MBA in this research study could be developed.
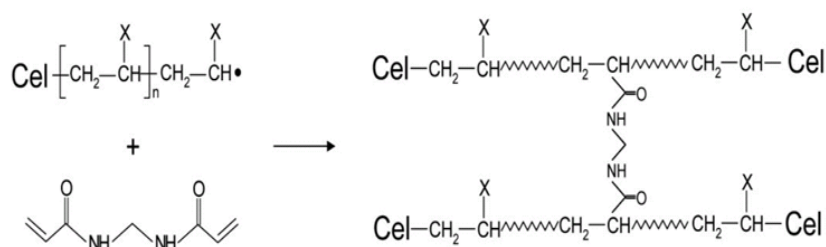
Figure 2.17: Crosslinking mechanism of cellulose-based SAP by N-MBA (Wang, 2007)

SAP hydrogels are synthesised from synthetic polymers without natural polymers that have AA as the main component. Kabiri *et al*. (2003) carried out their research regarding the effect of the concentration and type of crosslinker on the porosity and adsorption rate of highly porous SAP hydrogels formed from high concentration of AA/potassium acrylate aqueous solutions using N-MBA and 1,4-butanedioldiacrylate as crosslinkers. It was concluded that both crosslinkers showed same effects on water absorbency in distilled water and saline. The gelation time decreased with increasing concentration of the crosslinker especially N-MBA.

Mahdavinia and co-workers (2004) graft copolymerised AA and AM onto chitosan using potassium persulfate (KPS) as a free radical initiator in the presence of N-MBA as a crosslinker. The concentration of N-MBA and ratio of AA/AM on the water swelling capacity had been investigated. The authors also revealed that the hydrogels exhibited salt-sensitivity and cation exchange properties.

In year 2007, Singh and co-workers synthesised psyllium (common name for the plant genus *Plantago*) and PAM based hydrogel polymeric networks in the presence of *N*-MBA as crosslinker. The authors found that the equilibrium swelling was dependent on both structural features of the polymers and swelling environment. The increase of concentration of N-MNBA in the polymeric networks was found to result the decrease of swelling capacity.

In 2008, Yin and co-workers prepared a series of hydrogels through graft copolymerisation of AA and NaAlg by using *N*-MBA as a crosslinker. The dynamic swelling experimental results showed that an extraordinary overshooting effect was revealed in the swelling process of P(NaAlg-*g*-AA) hydrogels in the buffer solutions at pH $\leq$ 4.0. The authors ascribed that the phenomenon to a cooperative physical crosslink which was caused by the formation of hydrogen bond between the carboxyl groups of the hydrogels. The swelling capacity decreased due to hydrogen bond crosslinking and thus resulted the water expulsion during the dynamic swelling process.

Özeroglu and Birdal (2009) proposed meso-2,3-dimercaptosuccinic

acid-Ce(IV) redox couple for crosslinking polymerisation of AM with N-MBA as crosslinker in acid aqueous medium. The authors concluded that the swelling ratio and rate of swelling of the hydrogels in distilled water decreased with the increase of concentration of the acid, initiator and crosslinker.

Wang and Wang (2010) synthesised a pH-sensitive semi-interpenetrating network (semi-IPN) SAP composed of NaAlg-*g*-poly(sodium acrylate) (NaA) network and liner polyvinylpyrolidone (PVP) via free-radical solution polymerisation. Ammonium persulphate and N-MBA were used as the initiator and crosslinker, respectively in this reaction. The authors concluded that the introduction of PVP and the formation of the semi-IPN structure improved the swelling capacity and rate of swelling of the hydrogel.

2.7 Preparation of Biodegradable SAPs

In order to save the environment from synthetic polymers, graft copolymerisation of synthetic polymer on natural polymers such as starch and NaAlg was introduced as an alternative method to produce SAPs. As a result of this, countless research papers on syntheses of such SAPs swarmed the research literature world. Basically, these SAPs could be categorised into crosslinked and non-crosslinked SAPs and these two categories of literatures are shown as next few paragraphs.

There were some research articles which focused on syntheses of polymer without using any crosslinker. In Brazil, Da Silva *et al*. (2007)

synthesised a cashew-*g*-PAM polymer at 60 °C by a radical polymerisation using KPS as the redox initiator under nitrogen atmosphere. A series of graft copolymers was prepared by varying the concentration of AM and keeping the concentrations of the initiator and polysaccharide at constant. The authors concluded that even with a low acrylamide/gum ratio, high percentages of AM conversion (%C) and grafting efficiency (%E) were still obtained.

In 2009, Yang and co-workers carried out the synthesis of carboxymethylcellulose (CMC)-*g*-PAM in an aqueous medium by using ammonium persulphate and sodium sulfite redox system as initiator. The effects of reaction conditions, such as monomer concentration, initiator concentrations, initial reaction temperature, and pH value, on the weight-average molecular weight of the copolymers were investigated, and the optimal conditions for the grafting reaction were established.

Pourjavadi *et al*. (2010b) graft copolymerised polyacrylamide-*co*-poly-2-acrylamido-2-methylpropane sulfonic acid (PAM-*co*-PAMPS) chains onto NaAlg through a free radical polymerisation method, to produce novel types of highly swelling hydrogels. The results showed that the biodegradable SAP could successfully deliver a drug to the intestine without losing any drug in the stomach and thus acting as potential candidate as an orally administrated drug delivery system.

In addition, there were some articles which focused on the syntheses of crosslinked-SAPs too. Chen and Tan (2006) synthesised a novel

carboxymethylchitosan-*g*-PAA SAP through graft polymerisation of AA onto the carboxymethylchitosan chain and subsequent crosslinking. In the polymerisation reaction, ammonium persulphate and N-MBA were used as initiator and crosslinking agent. Optimisation conditions for SAP with the highest swelling ratio were found by studying the swelling ratio of the polymer synthesised under different conditions.

In 2006, Lanthong and coworkers prepared biodegradable SAPs by graft copolymerisation of AM/IA onto cassava starch via a redox initiator system of APS and *N*, *N*, *N'*, *N'*-tetramethylethylenediamine (TEMED), in the presence of N-MBA as crosslinking agent, sodium bicarbonate as foaming agent and a triblock copolymer of (polyoxyethylene / polyoxypropylene / polyoxyethylene) as a foam stabilizer They found out that the water absorption of SAPs was affected by acrylamide-to-itaconic acid ratio, starch-to-monomer ratio and concentration of the crosslinking agent and iniatiator.

Chang *et al*. (2010) successfully synthesised novel SAPs from carboxymethylcellulose sodium (CMC) and cellulose in the NaOH/urea aqueous system using epichlorohydrin (ECH) as crosslinker. The results showed that cellulose acted as a strong backbone in the hydrogel to support it for retaining the shape while the CMC improved the size of pores. The maximum swelling ratio in water reached an exciting level of 1000 as the hydrogels keep a stable appearance.

Spagnol *et al*. (2012) developed superabsorbent hydrogel composite

using cellulose nanofibrils and chitosan-graft-poly(acrylic acid), in the presence of N-MBA as crosslinking agent and KPS as initiator. The authors evaluated the crosslinker and filler amounts were the main factors controlling the water uptake. Besides that, swelling capacity was also improved by adding cellulose nanofibrils in the polymerisation reaction.

Liu and coworkers (2013) synthesised a chitin-based acrylate superabsorbent by grafting copolymerisation chitin and acrylic acid with APS and N-MBA as initiator and crosslinker, respectively in NaOH/urea solution without nitrogen protection. The authors revealed that chitin which possesses more hydrophilic group in the graft copolymerisation reaction, significantly enhanced the water absorption of the product. Acrylic acid was expected to simplify the procedures and reduce the water consumption whereas NaOH and urea play the role of solvent and reaction reagents. Thus, the final product exists as a hydrogel without excess reagent emissions, which is conductive to reducing the environmental pollution.

Ge and Wang (2014) prepared chitosan-acrylic acid SAPs through thermal reaction without or with N-MBA and potassium peroxydisulfate as crosslinker and radical initiator respectively, under air or nitrogen atmosphere. The authors concluded that SAPs were successfully synthesised by the thermal reaction without using radical and crosslinker in air at atmospheric pressure. The results also showed that the yield of thermal reaction in air was similar to reaction in nitrogen atmosphere (radical and crosslinker were used) and the thermal reaction without using crosslinker and initiator was suggested since

both of them are harmful or toxic to human body and environment.

2.8   Recent Development of Application of SAPs

Nowadays, many researchers are focusing their work on obtaining environmentally friendly SAPs, such as starch, cellulose and NaAlg-based, to be implemented in diaper application, medical, tissue engineering application, drug delivery system and controlled release fertilizer system.

Safaa *et al*. (2012) developed a new superabsorbent system in diaper industry using Tara gum/acrylic acid (TG/AAc) via gamma irradiation. The results showed that the presence of Tara gum with acrylic acid in the hydrogel had caused an increase in the crosslink density. This was proven as there was an increase in the elastic modulus. Thus, a higher elastic modulus value signified a more rigid structure of TG/AAc hydrogel. From the swelling capacity result, TG/AAc hydrogel showed that pressure ($0.6N/m^2$) did not change its swelling capacity in urea (major component of urine) solution up to 6 hours.

Upadhyaya *et al*. (2014) successfully provided a comprehensive introduction to various types of carboxymethyl chitosan (CMCS) based on formulation for delivery of therapeutic agents and tissue regeneration and preparation procedures and applications in different tissues/organs. The results revealed that CMCS has improved the dissolution of rate of many otherwise poorly soluble drugs and thus can be exploited for bioavailability improvement

of drugs. In addition, therapeutic agents such as anticancer, anti-inflammatory, antibiotics, antithrombotic, proteins and amino acids have been incorporated in CMCS-based system effectively to increase the bioavailability and to achieve the targeted controlled release.

Bhattacharya *et al*. (2013) prepared an interpenetrating polymer network (IPN) hydrogel microspheres of xanthan gum (XG) based SAP and poly(vinyl alcohol)(PVA) using water-in-oil (w/o) emulsion crosslinking method for sustained release of ciprofloxacin hydrochloride (CIPRO). The results revealed that the formulation which containing lower amount of glutaraldehyde gave a higher rate of release. This confirms that the formation of a denser network structure can reduce the swelling and the rate of drug release from the SAP matrix.

Mogoşanu and Grumezescu (2014) emphasized that the dressing protects injury and contributes to the recovery of dermal and epidermal tissues in the wound healing process. The results concluded that polysaccharides (e.g. chitin, chitosan, alginates, heparin, chondroitin), proteoglycans and proteins are used extensively in wounds management. This is due to their biocompatibility, biodegradability and similarity to macromolecules recognized by the human body. Furthermore, by electrospinning technique, some synthetic polymers like biomimetic extracellular matrix micro or nanoscale fibers based on polyglycolic acid, polyactic acid, polyacrylic acid, poly-ε-caprolactone, polyvinylpyrrolidone, polyvinyl alcohol, polyethylene glycol, exhibit *in vivo* and *in vitro* wound healing properties and enhance epithelialisation.

Liang, Liu and Wu (2007) synthesized a SAP which possessed the core/shell structure which is urea formaldehyde (UF) and polyphosphate potassium, and the poly(acrylic acid-*co*-acrylamide)/kaolin respectively. The results showed that its water absorbency was up to 91g/g in tap water. The SAP contained 11.3, 21.1 and 8.6 wt. % for N, P and K respectively. The NPK nutrient release of the SAP was not above 75% on the 30th day and this concluded that it had a good slow release property in soil and water holding ability and water retention properties of the soil could be greatly improved. Availability of fertilizer and water resource to crops could be improved simultaneously.

Wu, Liu and Liang (2008) prepared a double-coated slow-release NPK compound fertilizer with SAP using (acrylic acid)/diatomite (AA/DT) which contains urea, chitosan and water-soluble granular fertilizer NPK which were in the outer coating, the inner coating and the core respectively. The double coated SAP was undergone its swelling test and it was found that it could swell 75 times of its own weight at room temperature for 2 hour. Besides, the SAP contained 8.47% of potassium, 8.51% of phosphorus and 15.77% of nitrogen through AAS and elemental analysis. The results showed that the slow release ratio of the effective nutrient in it was not exceeding 75% on the 30th day. This can be concluded that chitosan and diatomite in the production of coating material can reduce the production cost and the technique is environmental-friendly. Its slow release property could be useful in agricultural and horticultural purposes.

Wu and Liu (2008) prepared a three-layer structured SAP which is chitosan-coated nitrogen, phosphorus and potassium compound fertilizer. The three layer structures included the core which was water-soluble NPK fertilizer granular, the inner coating which was chitosan and the outer coating was poly(acrylic acid-*co*-acrylamide). The results showed that the chitosan-coated SAP had a good control release property since the release of NPK nutrients did not exceed 75% on the 30th day. In addition, the product could improve the water holding ability and retention property of the soil.

Zhong *et al*. (2012) synthesized an eco-friendly SAP using modified sugarcane bagasse/poly (acrylic acid) embedding phosphate rock (MSB/PAA/PHR) in order to improve the water-fertilizer (NPK) utilization ratio. The result showed that MSB/PAA/PHR had an excellent water absorption capacity which achieved 414g/g in distilled water and 55 g/g in 0.9wt. % of NaCl solution, a preferable sustained-release property and this could also mitigate the environmental contamination.

Zhong *et al*. (2013) synthesized an agricultural SAP based on sulfonated corn starch/poly (acrylic acid) embedding phosphate rock (SCS/PAA/PHR) due to the difficulty of utilization of plants since phosphate rock is abundant. The result showed that SCS/PAA/PHR possessed an excellent sustained-release property of plant nutrient and the SCS/PAA improved the release of phosphorus nutrient.

Hemvichian *et al*. (2014) synthesized a SAP by using radiation-induced

grafting of acrylamide (AM) onto carboxymethyl cellulose (CMC) and this SAP was loaded with potassium nitrate (KNO_3) as an agrochemical model which has a highly potential of controlled release system. The results showed a very high swelling ratio of 190g/g of dry SAP. However, the swelling ratio and control release rate of KNO_3increased with decreasing of AM and irradiation dose.

CHAPTER 3.0

MATERIALS AND RESEARCH METHODOLOGY

3.1   Materials

Graft copolymerization process for this research was carried out by using sodium alginate (NaAlg) as polymer backbone which was provided by R&M, UK. Acrylic acid (AA) and acrylamide (AM) were used as monomers. Both of them were supplied by SRL, India. N,N'-methylenebisacrylamide (N-MBA) was used as crosslinking agent while ammonium persulfate (APS) was used as initiator. Both were obtained from SRL, India. Calcium chloride dihydrate, $CaCl_2.2H_2O$ was used as precipitating agent which was obtained from R&M, UK.

For NPK fertilizer preparation, extra pure urea and potassium chloride, which were purchased from SRL, India, were used to produce nitrogen and potassium respectively and phosphate rock powder, which was obtained from China National Analysis Center, China, was used to produce phosphorus. These three main elements act as the resources for NPK fertilizer.

3.2   Synthesis of Biodegradable SAPs

3.2.1   Gelatinisation of Sodium Alginate

6.0 g of sodium alginate was dispersed in 150 ml distilled water. The

system was heated at 80 ± 2 ºC with mechanical stirring, using an overhead metal stirrer at 1000 rpm for 30 minutes to form a homogenous, gelatinised NaAlg paste (shown in Figure 3.1).
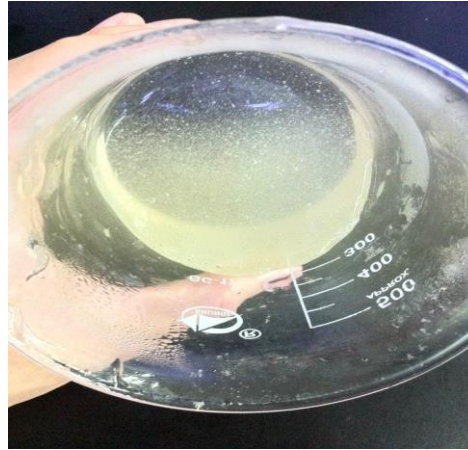
Figure 3.1: Gelatinised NaAlg paste

3.2.2   Graft Copolymerisation of Poly[(acrylic acid)-*co*-acrylamide] onto Sodium Alginate (Phase 1a)

After cooling the gelatinised sodium alginate paste to 60 ºC, liquid ammonia was then added to adjust its pH to 9. A total of 21g of AA and AM in different concentration ratio and N-MBA were added into the gel paste, followed by APS to initiate the reaction (Table 3.1). The system was then left stirring at 1000 rpm for 90 minutes.

During the process, an aluminium foil was used to cover the beaker in order to prevent water evaporation and to achieve better heat stability. The polymerization reaction was done for 120 minutes. The complete recipe for the graft copolymerization of NaAlg-*g*-poly[(acrylic acid)-*co*-acrylamide] is shown

45

in Table 3.1. At this phase, the ratio of AA and AM on graft polymers was varied and the effect on the properties of grafted polymers were studied.

3.2.3   Precipitating of Product Solution (Phase 1b)

After 120 minutes of polymerization reaction, the product gel was then precipitated by dropping the product gel from a separating funnel into a beaker with different concentration of $CaCl_2$ solution (Table 3.2) under stirring to form the final product which is in spherical bead form (Figure 3.2 and 3.3). These grafted polymer beads were then dried overnight in an oven at 60°C.

Figure 3.2   Product gel was dropped from separating funnel to beakers with different concentration of CaCl$_2$

Table 3.1: Recipe for graft copolymerisation of NaAlg-*g*-poly[(acrylic acid)-*co*-acrylamide]

Ingredient	Quantity
NaAlg Solution	
NaAlg	6.0 g
Distilled water	150.0 cm^3
Monomers Solution	
AA + AM	21.0 g
Distilled Water	200.0 cm^3
Monomers Ratio (AA:AM)	
Grafted Polymer A	85:15
Grafted Polymer B	70:30
Grafted Polymer C	55:45
Grafted Polymer D	40:60
Grafted Polymer E	25:75
Crosslinker	
NMBA	0.1 wt.%
Initiator	
APS	1.0 g
Distilled water	30 cm^3

Figure 3.3 **Spherical grafted polymer beads were formed in the CaCl$_2$ solution**

At this phase, the effect of concentration of CaCl$_2$ solution on grafted polymer beads was studied.

3.3 Synthesis of Controlled Release Fertilizer Using Superabsorbent Polymers

Nitrogen (N) from urea, phosphorus (P) from phosphate rock and potassium (K) from potassium chloride were calculated in Appendix A and its recipe is recorded in Table 3.2, and mixed well together in a beaker and shake for 10 minutes to obtain a homogenous powder. The well-mixed NPK powder was then transferred into the NaAlg-g-poly[AA-*co*-AM] solution. The mixture was then stirred vigorously until uniform and slowly transferred from a separating funnel to beakers with 1M, 2M and 3M CaCl$_2$ solution. The spherical grafted polymer beads were left in the CaCl$_2$ solution for half an hour to ensure complete gelling. The beads were then taken out from the solution, rinsed twice with distilled water and dried at 60°C overnight. The fertilizer-

imbedded grafted polymer beads (Figure 3.4) were formed.

Table 3.2: **Ingredients used for gelatinization and fertilizer encapsulation of superabsorbent polymer**

Ingredient	Quantity
Gelatinizing/Precipitating Agent	
Calcium Chloride solution (mol/dm^3)	
1	73.51 g in 500ml distilled water
2	147.02 g in 500ml distilled water
3	220.53 g in 500ml distilled water
Molar Mass of CaCl$_2$.2H$_2$O	147.02 g/mol
NPK Fertilizer	
Ratio of N:P:K	15:15:15
Urea, CH_4N_2O	2.549 g
(molar mass: 60.06 g/mol)	
Phosphate Rock, $Ca_3(PO_4)_2$	5.949 g
(molar mass: 310.17 g/mol)	
Potassium Chloride, KCl	2.265 g
(molar mass: 74.55 g/mol)	

Calculation for preparation of NPK fertilizer is attached in **Appendix A**.

Figure 3.4:   **Fertilizer-imbedded grafted polymer beads**

3.4   Characterisation

3.4.1   Grating Efficiency Determination

The obtained NaAlg-grafted polymer with different ratio of AA and AM was washed with distilled water several times, and poured into excess non-solvent ethanol for dehydration. After extraction with acetone for one day at room temperature to dissolve the homopolymers, the gel was cut into small pieces and dried at 70 ºC to constant mass.

The grafting percentage (*G%*) and grafting efficiency (*E%*) of 5 small pieces of each sample were calculated by using equations 3.1 and 3.2 respectively (Huang *et al*, 2005):

$$G\% = \frac{W_1 - W_0}{W_0} \times 100 \qquad \text{...........................} \qquad (3.1)$$

$$E\% = \frac{W_1 - W_0}{W_2} \times 100 \qquad \text{............................} \qquad (3.2)$$

Where W_0, W_1 and W_2 are weight of sodium alginate, final weight of the

50

grafted polymer and weight of monomers respectively.

3.4.2   Infrared Spectroscopy (FTIR)

FTIR test was run using FTIR Perkin Elmer, model Spectrometer Spectrum RX1 within the wave number 4000-400 cm^{-1}. FTIR analysis on AA and all the grafted polymers (different ratio of AA and AM and different concentration of $CaCl_2$) were examined directly on the sample surface using Attenuated Total Reflectance (ATR) technique. FTIR spectra of pure NaAlg and extra pure AM were obtained using KBr techniques. Pure NaAlg or extra pure AM was mixed with KBr powder in the mass ratio 1:10 (NaAlg:KBr or AM:KBr) and pressed using hydraulic press to obtain a translucent and homogenous KBr pellets for the analysis.

3.4.3   Thermogravimetric Analysis (TGA)

Thermal decomposition temperature and weight loss of pure NaAlg and its grafted polymers with different ratio of AA and AM and different concentration of $CaCl_2$ were determined using Mettler Toledo TGA analyzer, model SDTA851^e. Approximately 10 mg of grafted polymers were weighed into 70μL alumina crucible and heated from room temperature to 550 ºC at a heating rate of 10 ºC/min under minimum 99.9995% purity nitrogen purge of 10 mL/min.

3.4.4 Differential Scanning Calorimetry Analysis (DSC)

The glass-transition temperature (T_g) and melting temperature (T_m) of pure NaAlg and its grafted polymers with different ratio of AA and AM and different concentration of $CaCl_2$ were determined using Mettler Toledo differential scanning calorimeter, model DSC823^e. Approximately 10 mg of grafted polymers were sealed in a standard 40μL alumina crucible and were analysed under minimum 99.9995% purity of nitrogen purge at a flow rate of 10 ml/min. The temperature range investigated was from room temperature to 300 ºC at a heating rate of 10 ºC/min.

3.4.5 X-ray Diffraction Study (XRD)

Wide angle X-ray diffraction analysis was carried out by using Shimadzu X-ray Diffractometer, model LabX XRD-6000, in step scan mode using Cu kα radiation. The grafted polymer was analyzed at 1º/min scan speed in 10-80º scan range.

3.4.6 Study of Surface Morphology using Scanning Electron Microscopy

The surface morphology of the grafted polymers and fertilizer-imbedded grafted polymers was investigated using the Field Emission Scanning Electron Microscopy (FESEM, JOEL, model JSM 7601F, Japan) at accelerating voltage of 3.0 kV. The grafted polymers were coated using platinum before scanning.

3.4.7 Swelling Capacity of SAPs

A known mass of each grafted polymers were immersed in tap water inside the beaker with a glass cover and allowed to swell for 8 hours at room temperature. The swollen sample was then removed from distilled water at 1 hour interval by filtering through a 100-mesh sieve to remove non-absorbed water. The samples were then dried in conventional oven overnight at 60°C and weighed. The water absorbency was calculated gravimetrically as shown in Equation 3.3 (Liang, Liu and Wu, 2007; Zhang and Wang, 2007; Wu and Liu, 2008; Phang *et al*., 2011).

$$Q = \frac{m_2 - m_1}{m_1} \qquad \ldots\ldots\ldots\ldots\ldots (3.3)$$

where m_1 and m_2 are the mass of the dry samples and the swollen samples, respectively. Q is grams of water per gram of dried sample.

3.4.8 Soil Burial Test

3.4.8.1 Collection of Soil

Malaysia oil palm soil is a type of loamy soil which contains a combination of microorganisms and some organic materials such as rooted leaves, wood chips, old manure, compost and etc, which help in the growth of oil palm trees. The oil palm soil was found to be slightly acidic, pH 5.78.

By employing random sampling method, four oil palm soil samples were collected from four different oil palm plantations, Felda Trolak Selatan Perak, Felda Sungai Klah Perak, Felda Gunung Besout 1 Perak and Felda Gunung Besout 2 Perak. A plastic pail was used to enclose the soil samples up to two third of its volume. The pail was loosely capped using pins-holed aluminium foil for gas exchange; the samples were kept at room temperature for one week.

3.4.8.2 Microbial Degradation Using Weight Loss Test

Soil burial test to evaluate the biodegradation of superabsorbent grafted polymers was conducted for 90 days. The grafted polymers were weighed and wrapped with stainless steel wire mesh (325#) in order to minimize the loss of the polymer fragments during the soil burial process. Each grafted polymer was buried approximately 5cm beneath the surface of the soil as shown in Figure 3.5 and the oil palm soil was maintained at 30 wt.% of water holding capacity by weighing and adding water if necessary throughout the test (Phang *et al.*, 2011).
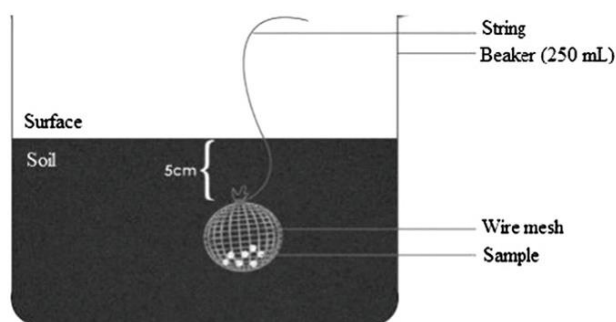
Figure 3.5:   Soil Burial Test Set-up (Phang *et al.*, 2011)

At least three grafted polymers of each sample were used in the test to obtain its average reading. The grafted polymers were transferred out from soil at different time intervals (10, 20, 30 , 50, 70 and 90 days).The grafted polymers were then put in an oven at 60ºC overnight after washed to remove all the debris and plankton microorganism. The weight of dried grafted polymers was taken.

The weight loss was determined using the Equation 3.4:

$$WL\% = \frac{m_0 - m_t}{m_0} \qquad \text{................} \qquad (3.4)$$

Where *WL%* is weight loss in percentage, m_0 is the initial mass and m_t is the final mass. An average of three measurements was taken (Franco *et al*., 2004).

3.4.8.3 Rate of Release of Fertilizer in Soil

To study the controlled-release behavior of fertilizer-imbedded graft polymer beads in oil palm soil. 10 grafted polymer samples with different ratio of AA and AM with different concentration of $CaCl_2$ was buried in palm soil. The samples were kept in a 500 ml beaker and properly covered (Figure 3.5) and incubated for different periods at room temperature. Throughout the test, the oil palm soil was maintained at 30 wt. % of water holding capacity by weighing and adding water if necessary.

After 3, 7, 14, 21, 28, 35, 42, 49, 54 and 60 days of incubation periods,

the remaining of grafted polymers were removed from oil palm soil and washed with distilled water to remove all debris and plankton microorganism and then dried at room temperature overnight to estimate the content of N, P and K. For 10 measurements, 10 beakers were prepared at the same time. The remaining amount of N, P and K was estimated using Kjeldahl method of distillation (Abraham and Rajasekharan, 1996) and atomic absorption spectrophotometer (AAS), respectively.

The release results were analyzed by using an empirical equation to estimate the value n and K as follows (Al-Zahrani, 1999; Peng, Zhang and Kennedy, 2006):

$$\frac{M_t}{M} = Kt^n$$

.... (3.5)

$$\log\left(\frac{M_t}{M}\right) = \log(K) + n \log(t)$$

.... (3.6)

Where M_t/M is the release fraction at time t, n is the release exponent and K is the release factor.

3.4.8.4 Measurement of Water Retention in Soil

5 grams of fertilizer-imbedded grafted polymers was well mixed with 200 g of dry soil (below 2mm in diameter) and kept in a cup and then 200 g of tap water was slowly added into the cup and weighed (W_1). A controlled experiment, i.e., without fertilizer-imbedded grafted polymer (plain soil

sample), was also carried out. The cups were maintained at room temperature and weighed every 5 days (W_i) over a period of 20 days. The water retention percentage (*WR%*) of soil was determined using the following equation (Liang, Liu and Wu, 2007; Wu and Liu, 2007; Wu, Liu and Liang, 2008):

$$WR\% = \frac{W_i}{W_1}$$

………………… (3.7)

CHAPTER 4.0

RESULTS AND DISCUSSION

4.1 Grafting of AA and AM onto NaAlg (NaAlg: AA+AM = 6:21) and its Grafting Percentage and Grafting Efficiency

In this research study, AA and AM were successfully crosslinked by *N*-MBA and grafted onto NaAlg backbone. *N*-MBA (crosslinker) is a material that can form a strong polymeric network in the SAPs and it can help SAPs to retain the water more effectively. The formation of the interpenetrating network is shown in Figures 4.1 (a) and (b). The grafting percentage (G%) and grafting efficiency (E%) of AA and AM are shown in Table 4.1. The results show that the G% and E% increases as AM ratio increases in formulation. The increment of E% with increment of AM concentration might due to two reasons. First of all, AA alone may prefer to produce homopolymer rather than becoming a grafted copolymer onto NaAlg backbone compared to AM (Lanthong *et al*., 2006). Secondly, grafting efficiency could be enhanced on the charge transfer from a donor (Oxidant) to an acceptor (reductant); from electron rich AM to the electron poor AA (Wu *et al*., 2012). Thus, the AA could be easily grafted to NaAlg backbone in the presence of AM.
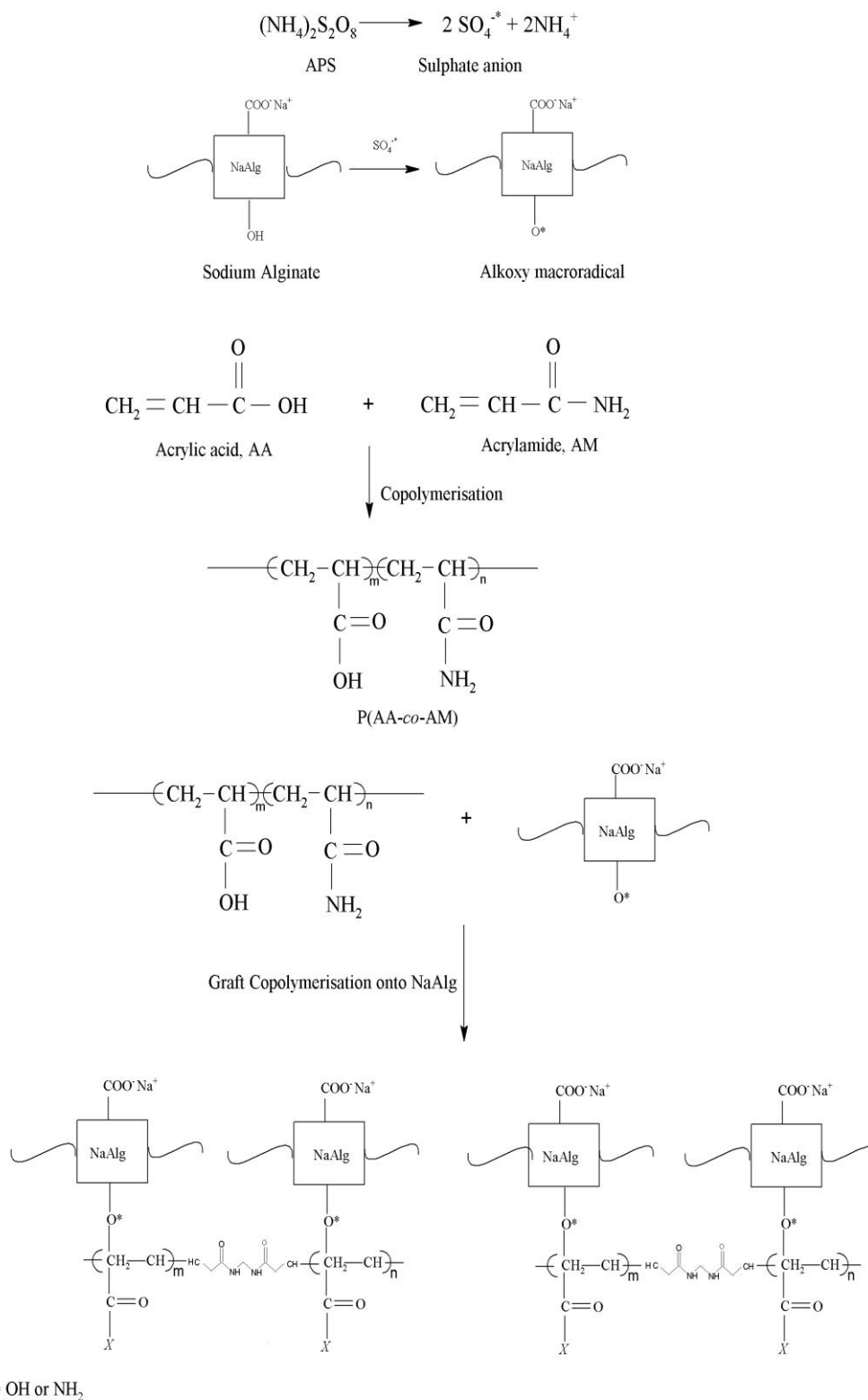
Figure 4.1(a): Schematic diagram of grafting of AA and AM onto NaAlg in the presence of *N*-MBA

CH₂ = CH — C — OH + CH₂ = CH — C — NH₂

Acrylic acid, AA

Acrylamide, AM

N-MBA

Copolymerisation

P(AA-*co*-AM)

X = OH or NH₂   ⟿ = Copolymer Chain

Figure 4.1(b): **Schematic diagram of crosslinking of P(AA-*co*-AM)**

copolymers using *N*-MBA

Table 4.1: **Grafting percentage and grafting efficiency of AA and AM onto NaAlg (NaAlg: AA+AM = 6:21)**

Grafted Polymer	AA:AM	Grafting percentage (G%)	Grafting efficiency (E%)
A	85:15	28.0	8.0
B	70:30	95.5	27.3
C	55:45	159.8	46.0
D	40:60	185.5	53.0
E	25:75	290.5	83.0
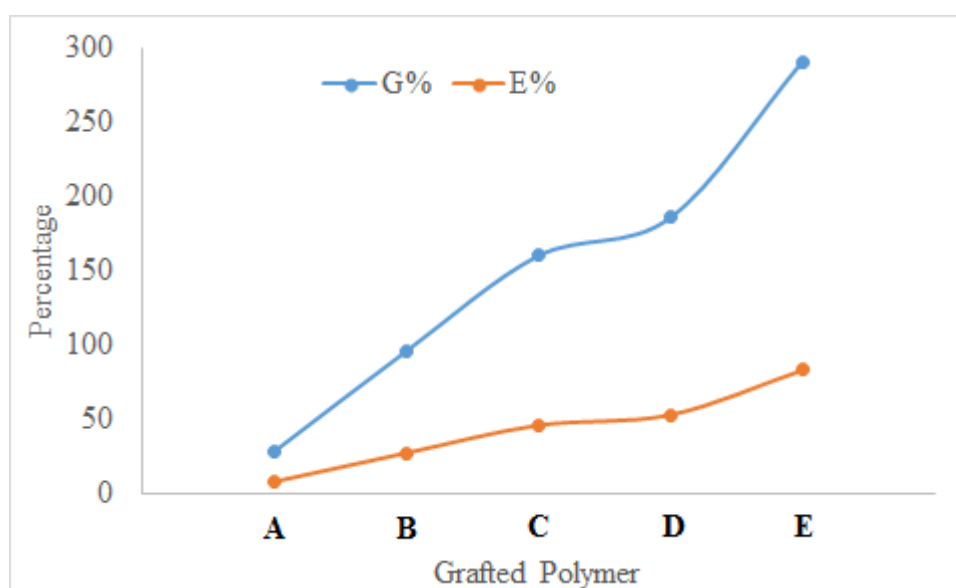
Figure 4.2 **Grafting percentage and grafting efficiency of AA and AM onto NaAlg**

4.2   Identification Codes

In the result and discussion, grafted polymers A3, B3, C3, D3 and E3 are grafted polymers selected for the comparison of different ratio of AA and AM with constant concentration of $CaCl_2$ at 3M whereas grafted polymers A1, A2 and A3 are chosen for the comparison of different concentration of $CaCl_2$ with fixed ratio of AA and AM of 85:15. On the other hands, NPK fertilizers-imbedded grafted polymers were designated starting with the letter F. For example, FA3 indicates the NPK-imbedded grafted polymers, with ratio of AA:AM = 85:15 and 3M concentration of $CaCl_2$,

4.3   Fourier Transform Infrared Spectroscopy (FTIR)

IR analysis was carried on pure NaAlg, AA, extra pure AM and selected copolymers which are copolymer A, B, C, D and E with their three different concentration of $CaCl_2$ solution. IR Spectra of all the starting material and products are obtained in the range of $400 - 4000$ cm^{-1}. IR spectrum of pure NaAlg was illustrated in Figure 4.3 whereas Figure 4.4 and 4.5 depict the IR spectra of extra pure AM and AA respectively.

In the IR spectrum of pure NaAlg, the broad peak observed at the region between $3600 - 3100$ cm^{-1} is assigned as the H-bonded O-H stretching (Xu *et al*., 2006). Small band at approximately 2900 cm^{-1} is known as C-H stretching. The regions from $1000 - 750$ cm^{-1} are the fingerprint bands for carbohydrates and has been discussed extensively by Leal and coworkers in

2008. The weak peaks at 1300, 1100, and 1029 cm^{-1} are due to stretching vibration of C-O and the peak at 950 cm^{-1} is contributed by stretching vibration of C-O-C both from glycosidic bonds respectively.

In addition, there are two peaks at 1632 and 1414 cm^{-1} indicating the COO^- stretching group attached to the sodium ion. This is caused by the asymmetric stretching vibration of the carboxylate COO^- for the former while the latter is due to the C-OH deformation vibration with contribution of COO^- symmetric stretching vibration of the carboxylate group (Soares *et al*., 2004; Xu *et al*., 2006; Wang and Wang, 2010).

In the IR spectrum of extra pure AM, a broad band at region between 3300 – 3000 cm^{-1} indicates –NH stretching of acrylamide unit. Peaks at 2816 and 1715 cm^{-1} are assigned as C-H stretching and C=O stretching of acrylate unit respectively. Carbonyl moiety of acrylamide unit is found at the peak at 1615 cm^{-1} and peak at 1135 cm^{-1} which corresponds to –CO-O- stretching of acrylate unit.

Meanwhile, the IR spectrum of AA exhibits the characteristic band at the 2500 – 3000 cm^{-1} due to the –OH stretching of carboxylic group. The peak around 1634 cm^{-1} attributed to the stretching of carbonyl group of carboxylic acid. The peak at 1430 cm^{-1} shows the C=O symmetric stretching vibration of the carboxylic groups whereas the peaks at 1292 and 1237 cm^{-1} are assigned as –CO-O stretching of carboxylate group.
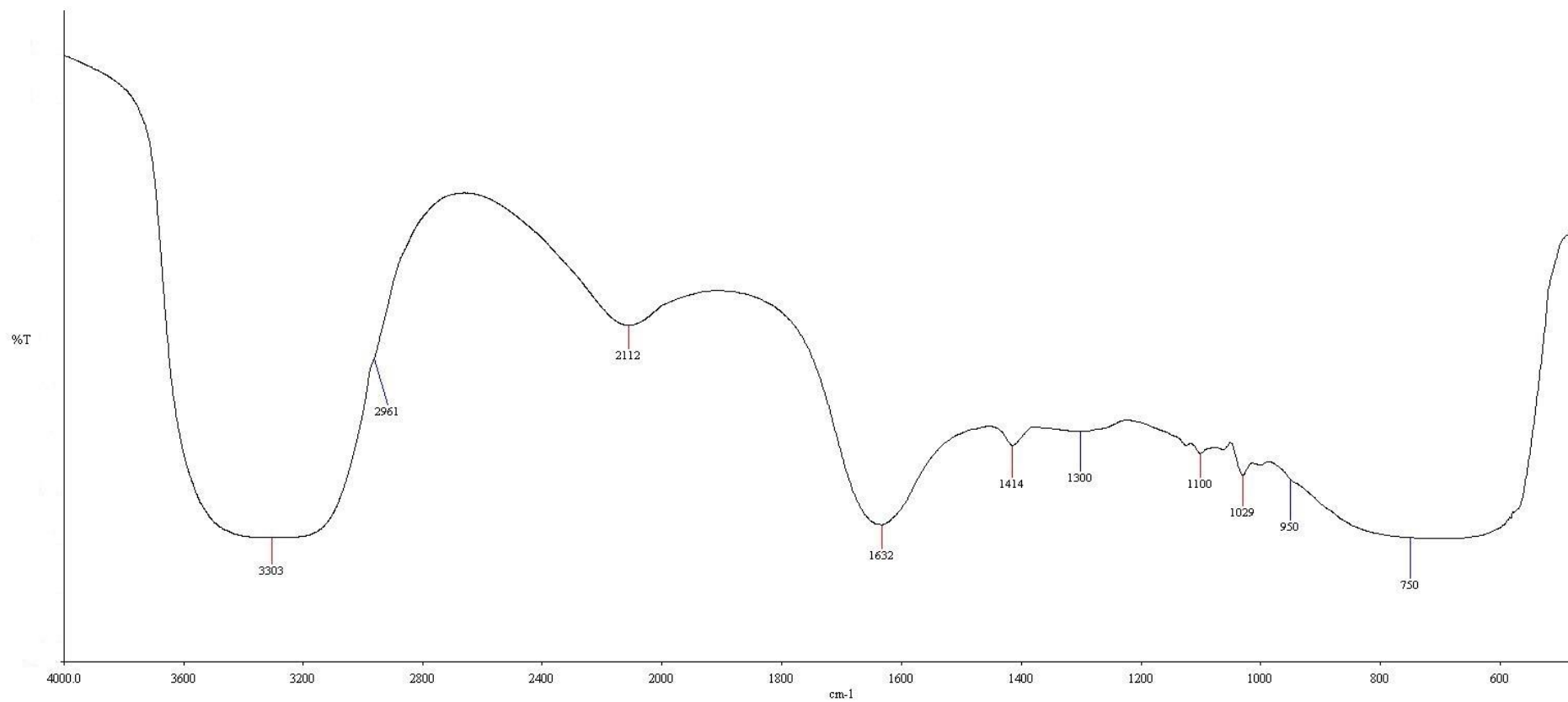
Figure 4.3: **IR spectrum of Pure NaAlg**
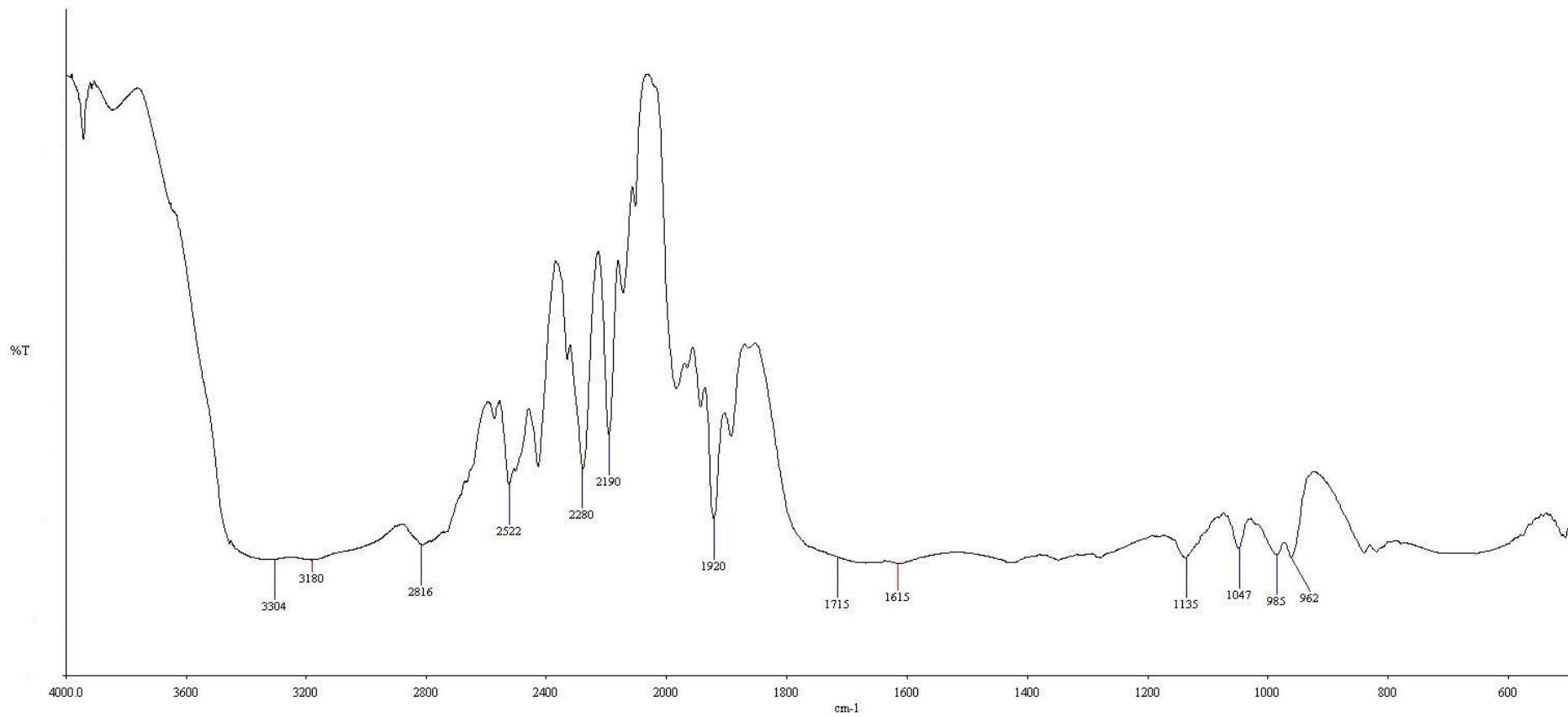
Figure 4.4: **IR spectrum of extrapure AM**
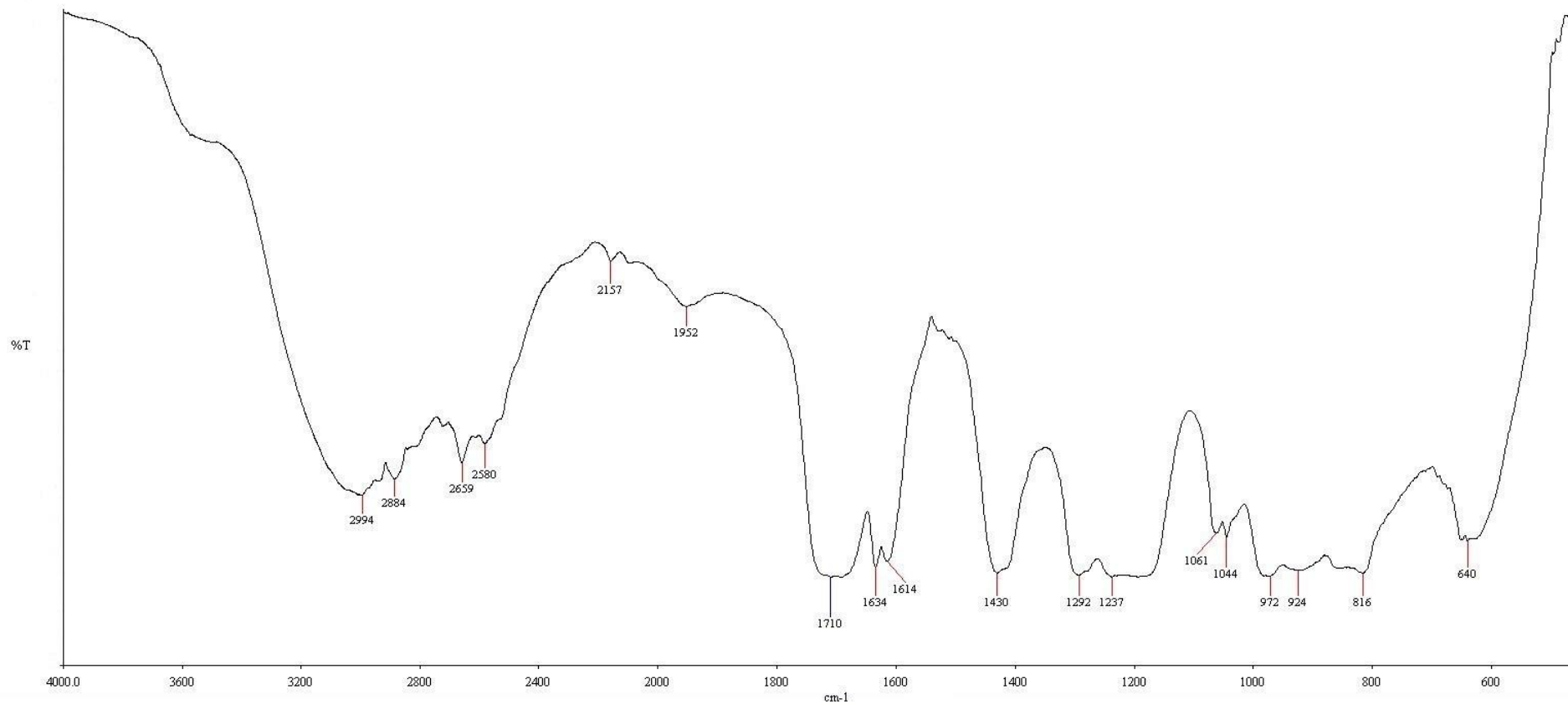
Figure 4.5: IR spectrum of AA

Figure 4.6 - 4.10 illustrates the IR spectra of grafted polymers A3, B3, C3, D3 and E3 respectively. From the spectra, the effect of different molar ratio of monomers on pure NaAlg can be explored.

Generally, the wavenumber of H-bonded O-H stretching vibrations of NaAlg has been shifted from 3303 to the range of $3148 - 3390$ cm^{-1} in all the grafted polymers A3, B3, C3, D3 and E3. This can be concluded that all the grafted polymers still maintain their hydrophilic characteristic. In addition, the intensity of H-bonded O-H stretching vibrations increases from A3 to E3 and this shows that the hydrogen bonding increases as the concentration of AM increases. Weak signals in between $2951 - 2799$ cm^{-1} shown in the IR spectra are actually due to the C-H stretching vibrations of the all the grafted polymers.

As can be seen in the IR spectra of NaAlg and all the grafted polymers, the comparison shows that the peak region $1000 - 985$ cm^{-1} which attributed to the C-H of on NaAlg still exists, suggesting the NaAlg ring was not opened in the reaction (Yang, Ma and Guo, 2011).

In the IR spectra of all the grafted polymers, the peak at 1414 cm^{-1} which represents the COO^{-} symmetric stretching vibration of NaAlg has shifted to 1400, 1402, 1416, 1402 and 1427 cm^{-1} for grafted polymers A3, B3, C3, D3 and E3 respectively. This is due to the presence of C-N group in $-CONH_2$ (Wang and Wang 2010) and this also indicates AM has successfully grafted onto NaAlg backbone.

Figure 4.6: IR Spectrum of grafted polymer A3

Figure 4.7:   IR Spectrum of grafted polymer B3

Figure 4.8:   IR Spectrum of grafted polymer C3

Figure 4.9: **IR Spectrum of grafted polymer D3**

Figure 4.10: IR Spectrum of grafted polymer E3

Furthermore, there is a small double peak at 1455 and 1400 cm^{-1} found in IR spectrum of grafted polymer A3 and 1447 and 1402 cm^{-1} in IR spectrum of grafted polymer B3. As the concentration of AM increases, the double peak has changed to one single peak as shown in Figure 4.11. This peak-overlapping is due to the higher amount of AM is grafted onto NaAlg polymer backbone than AA. However, further investigation need to be carried out to double confirm this.
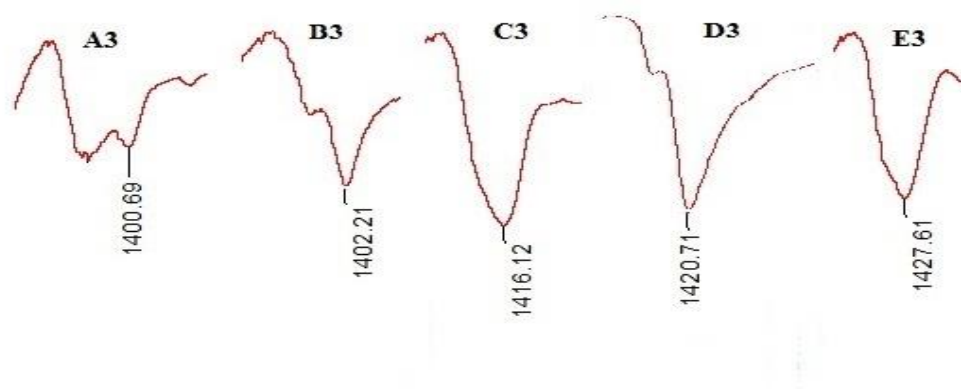
Figure 4.11: Peaks overlapping vs concentration of AM between the wavenumber of 1427 – 1400 cm^{-1}

There is another difference between the IR spectra of NaAlg and grafted polymers A3, B3, C3, D3 and E3. Compared with the peak for the asymmetric stretching of the COO$^-$ group attached to the sodium ion in NaAlg at 1632 cm^{-1}, the peak has been shifted to the range of 1615 to 1657 cm^{-1} for all the grafted polymers.

The shift mentioned above is further indicating the grafting of AA and AM onto the NaAlg backbone and is serving as a proof of the SAPs formation.

73

This is due to the strong hydrogen bond interaction between the –COOH and –C=O groups (Lin *et al.*, 2009, as cited by Wang and Wang, 2010), which is accentuated by the C-N group of –C(=O)NH$_2$ of AM. It is noteworthy that this peak is shifted more towards the wavenumber of C=O stretching of amide bands compared to C=O stretching of carbonyl group. This may be due to the better grafting efficiency of AM compared to AA to the NaAlg backbone (discussed in Table 4.1). Peaks were also observed around 3340 cm^{-1} in IR spectra of all grafted polymers. This also deduced that all the grafted polymers are successfully crosslinked by *N*-MBA.

The IR spectra of grafted polymers A1, A2 and A3 are shown in Figure 4.12– 4.14. From the spectra, the effect of different concentration of calcium chloride on pure NaAlg can be determined.

When the grafted polymers are dropped to CaCl$_2$ solution, hydrogel grafted polymer beads were formed instantaneously by electrostatic interaction between negatively charged NaAlg and positively charged Ca^{2+}. The precipitating process with Ca^{2+} caused an obvious shift of symmetric –COO- stretching from 1414 cm^{-1} to higher wavenumber in Figure 4.12 – 4.14. This indicates the formation of ionic bonding between Ca^{2+} and –COO$^-$ of NaAlg (Xu *et al.*, 2007) and the strength of Ca^{2+} protective layer is slightly stronger. The peaks at 1455 – 1445 cm^{-1} show that all grafted polymers are successfully precipitated by Ca^{2+} to form a protective layer.
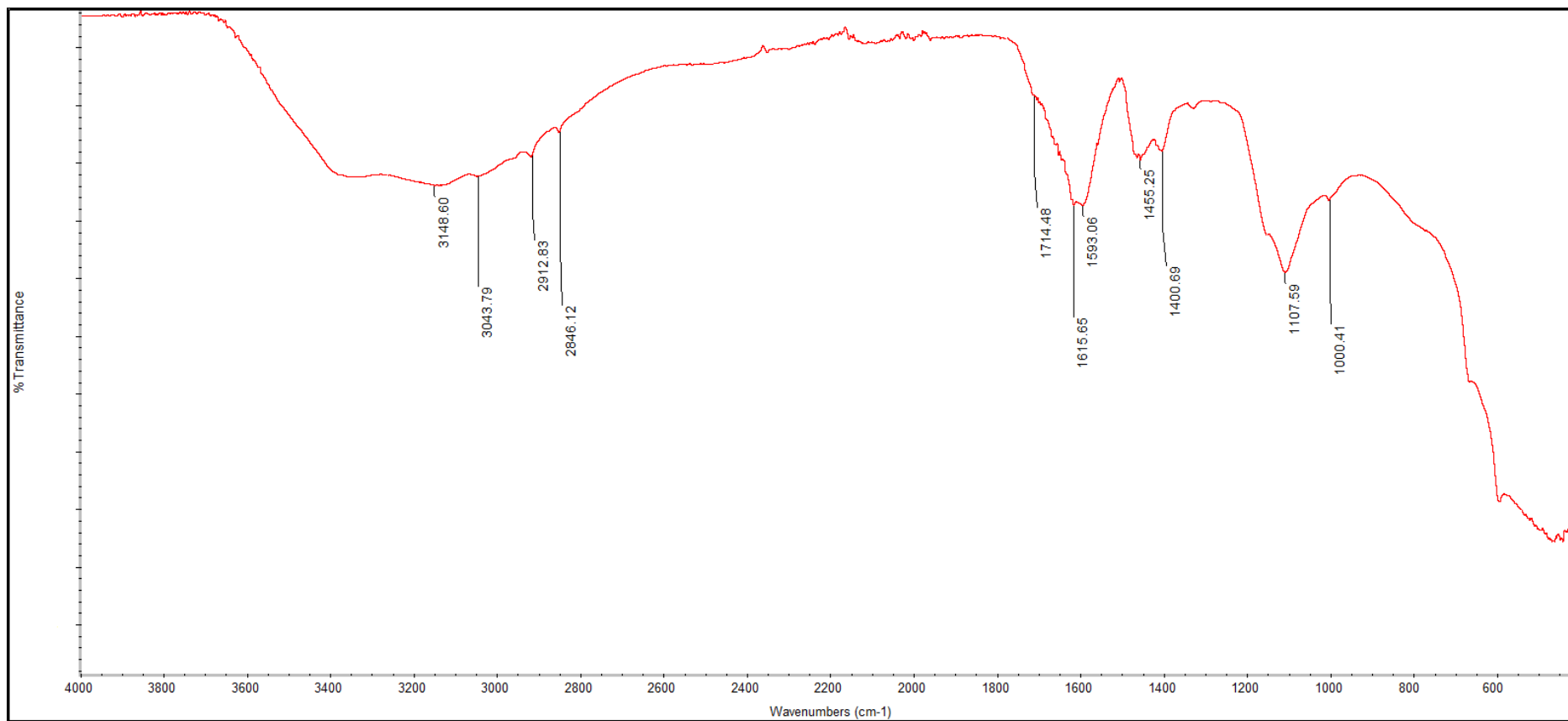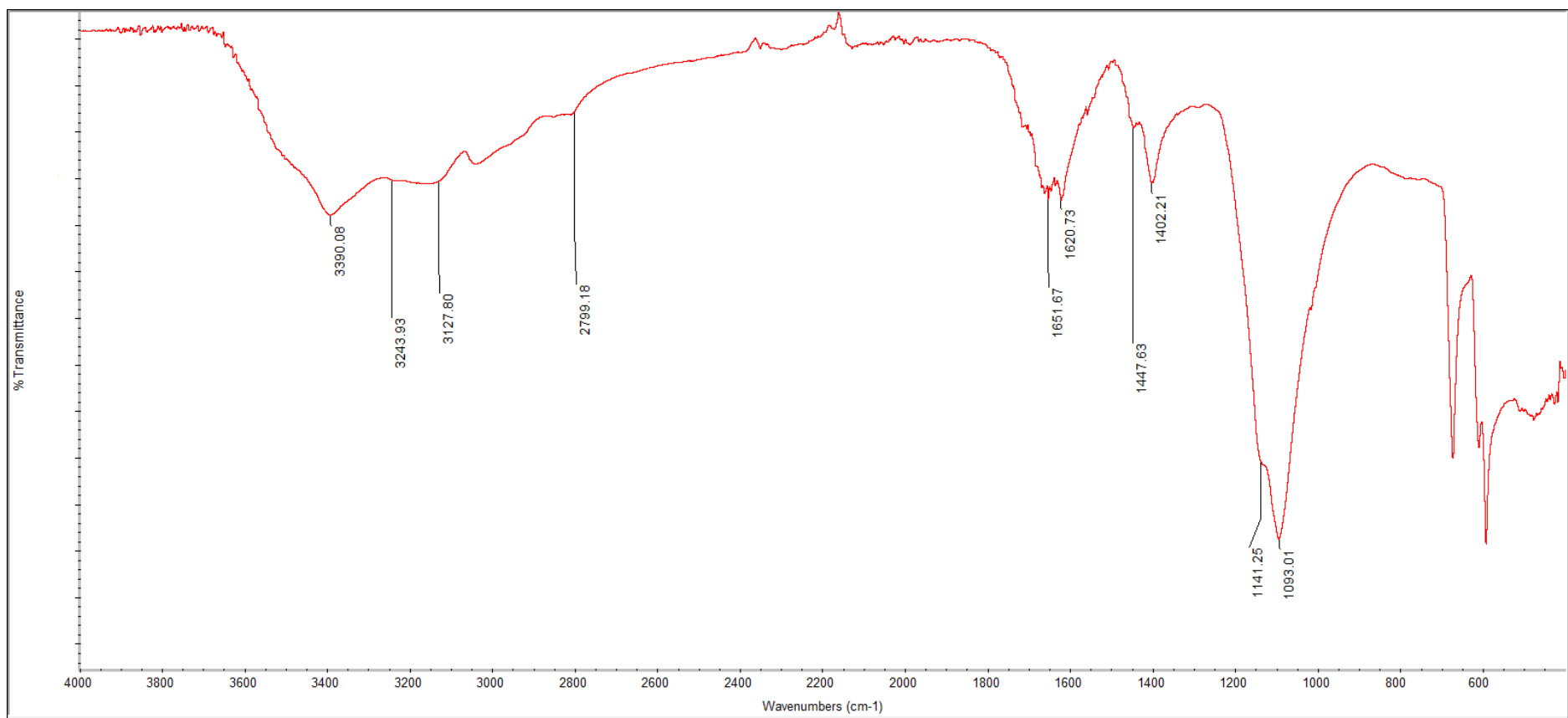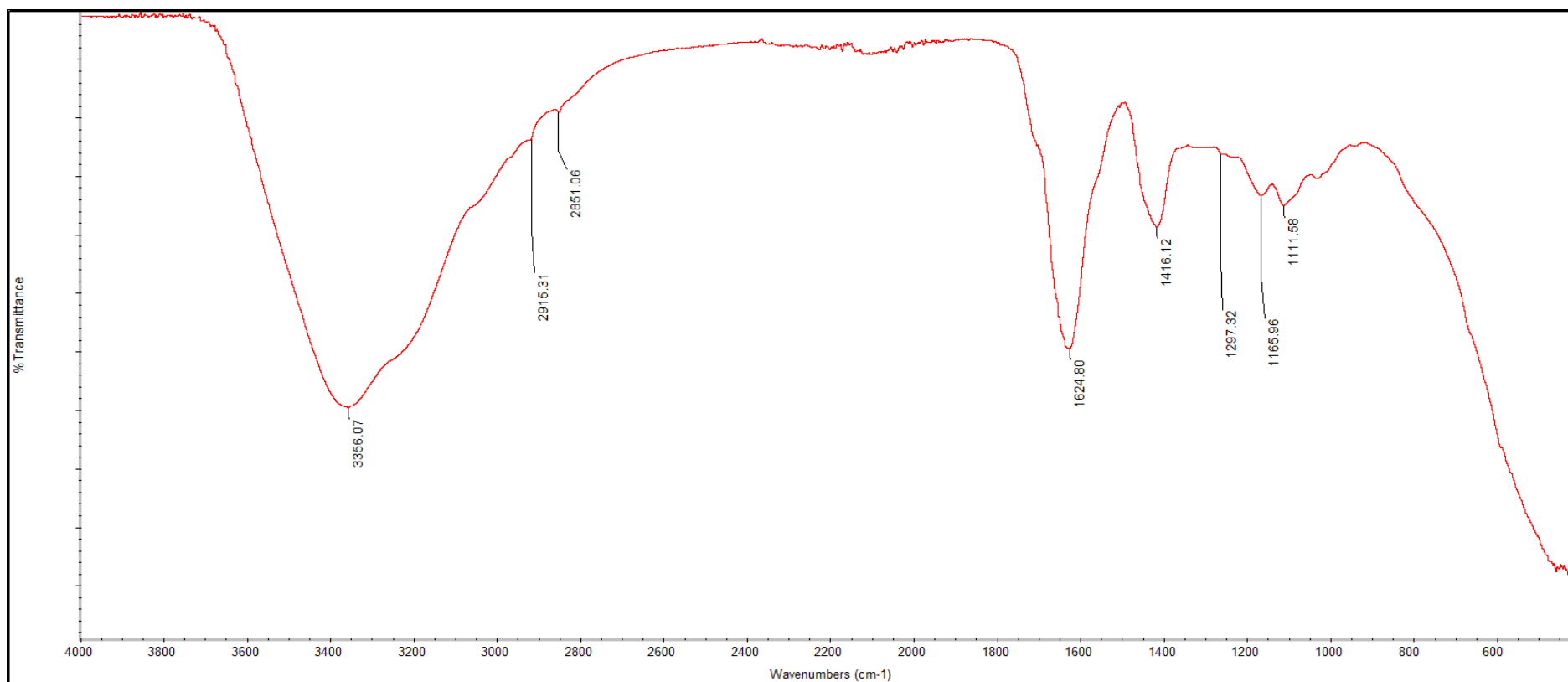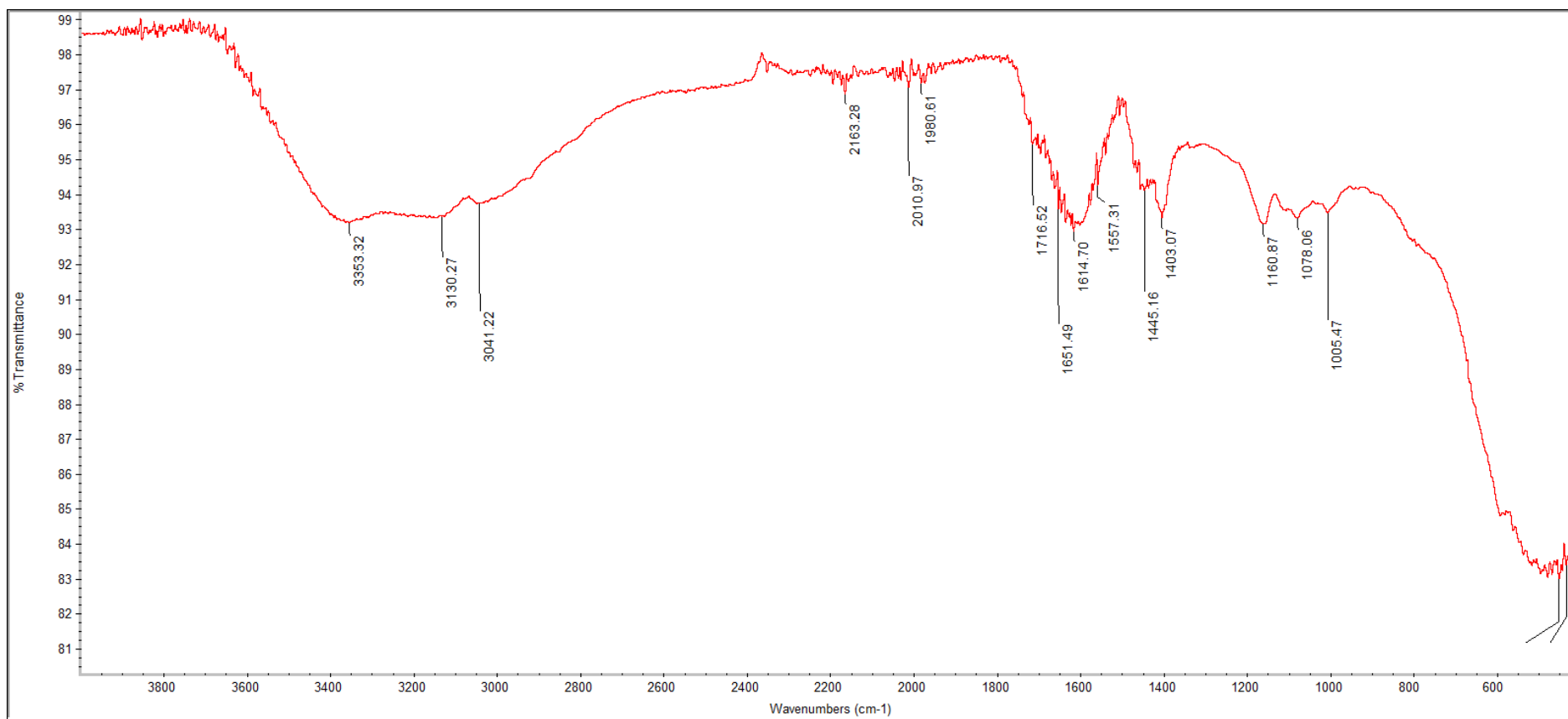
Figure 4.12:   IR Spectrum of grafted polymer A1
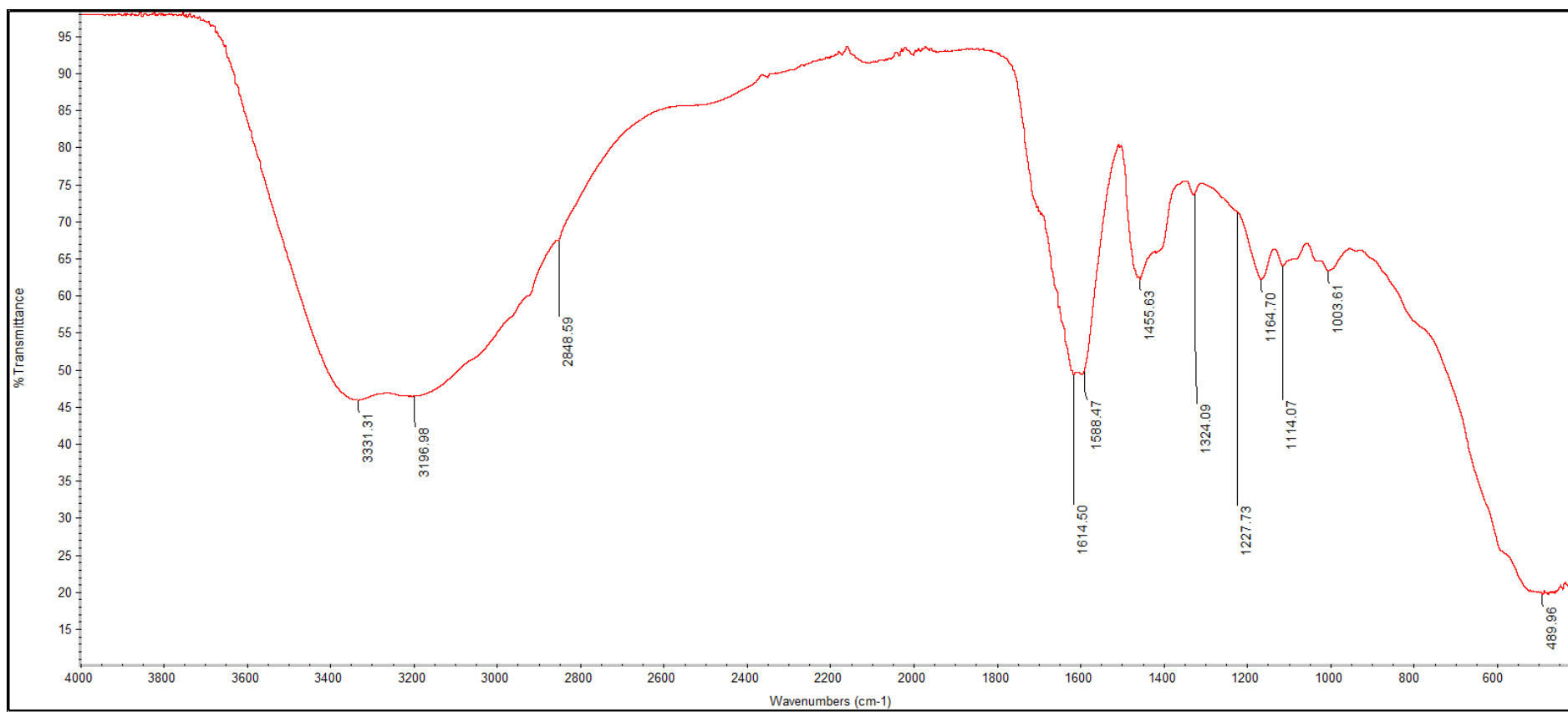
Figure 4.13:   IR Spectrum of grafted polymer A2

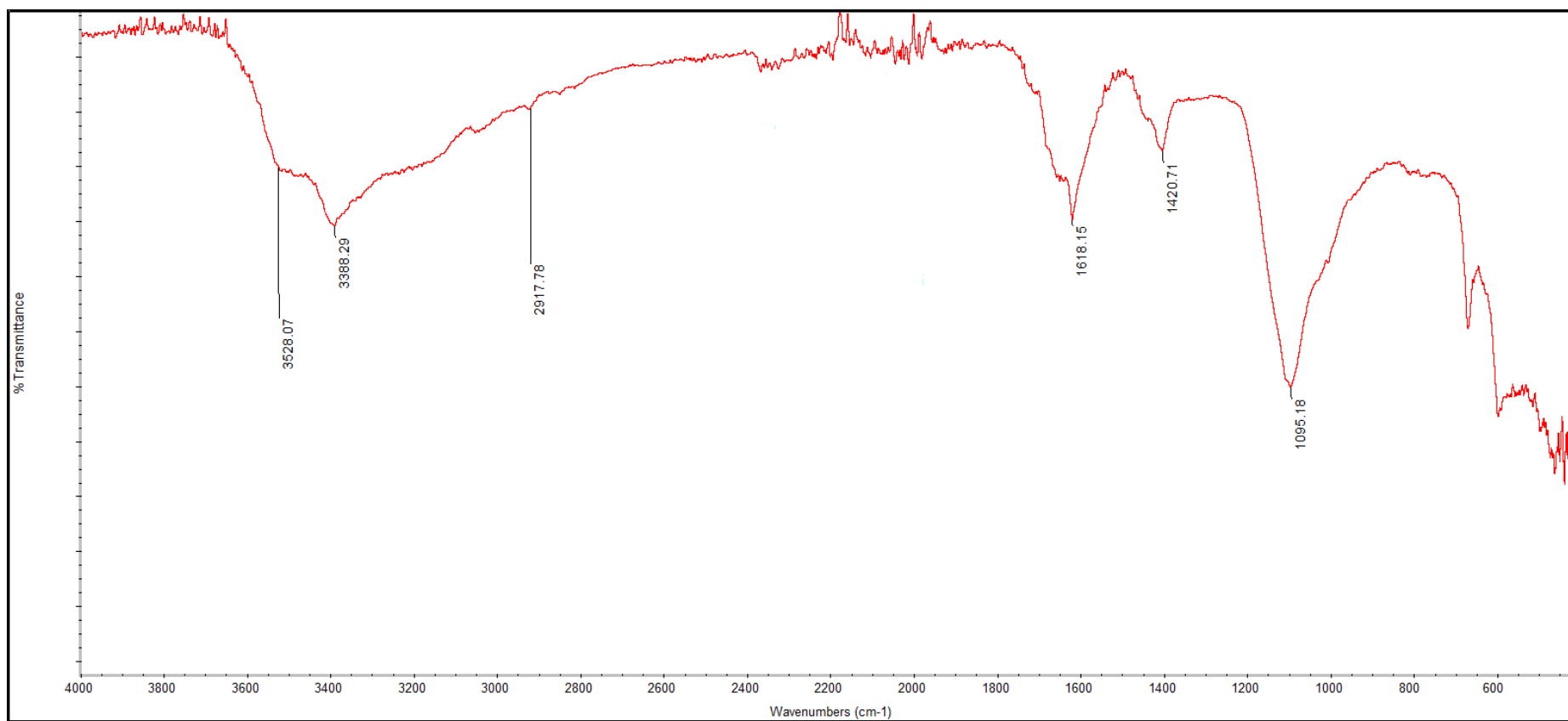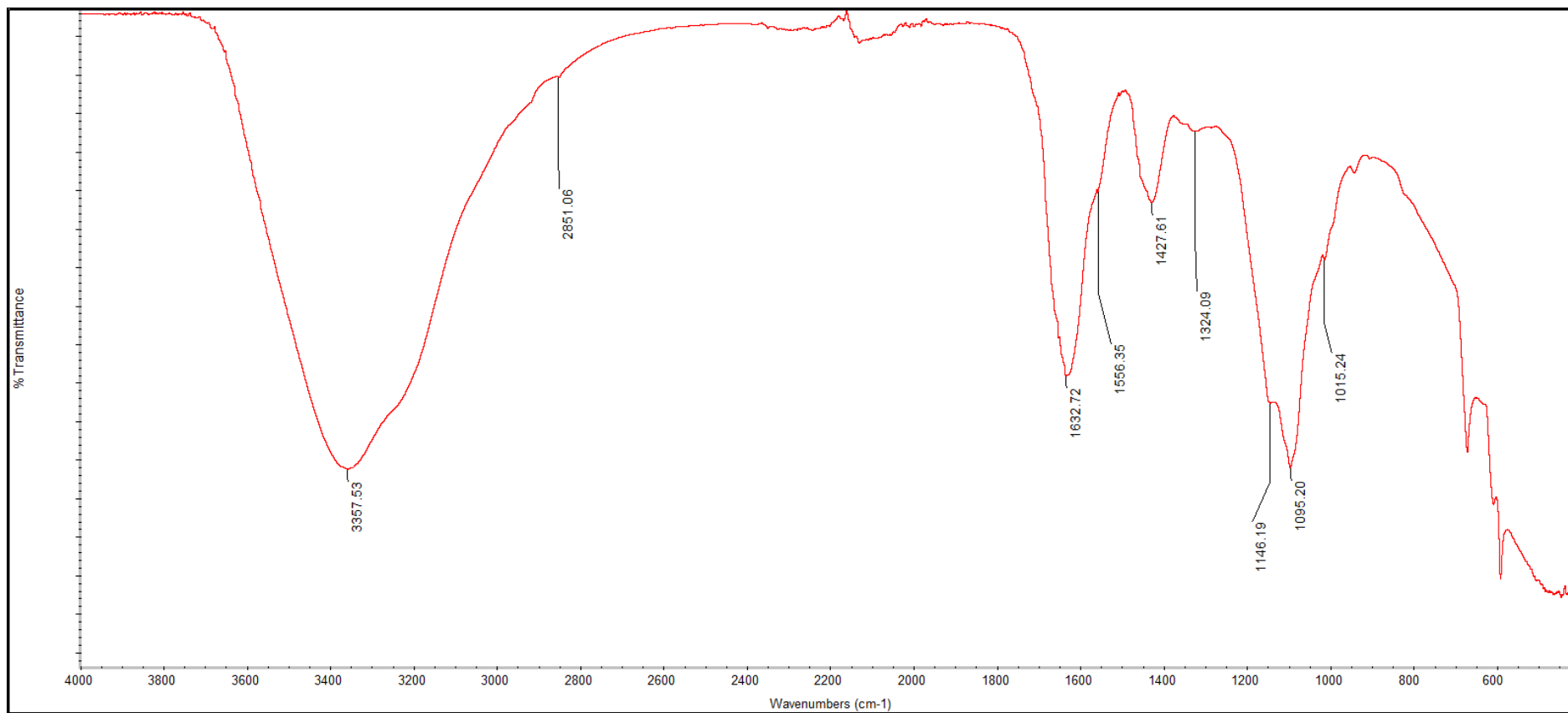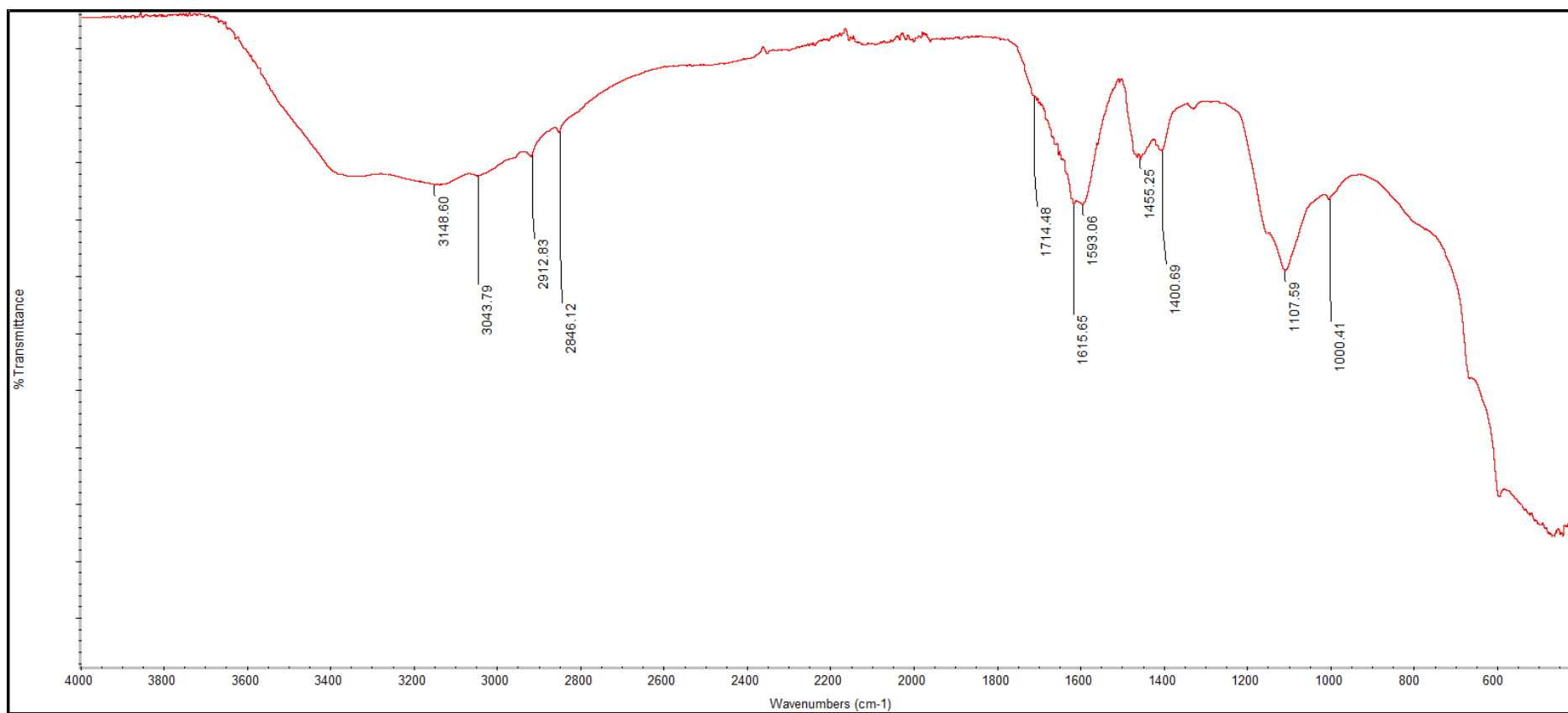**Figure 4.14:   IR Spectrum of grafted polymer A3**

4.4   Thermogravimetric Analysis (TGA)

Figure 4.15 illustrates the weight loss in percentage of pure NaAlg and 5 selected grafted polymers with different ratio of AA and AM (A3, B3, C3, D3 and E3) whereas Figure 4.16 shows the weight loss in percentage of 3 selected grafted polymers (A1, A2 and A3) with different concentration of $CaCl_2$.
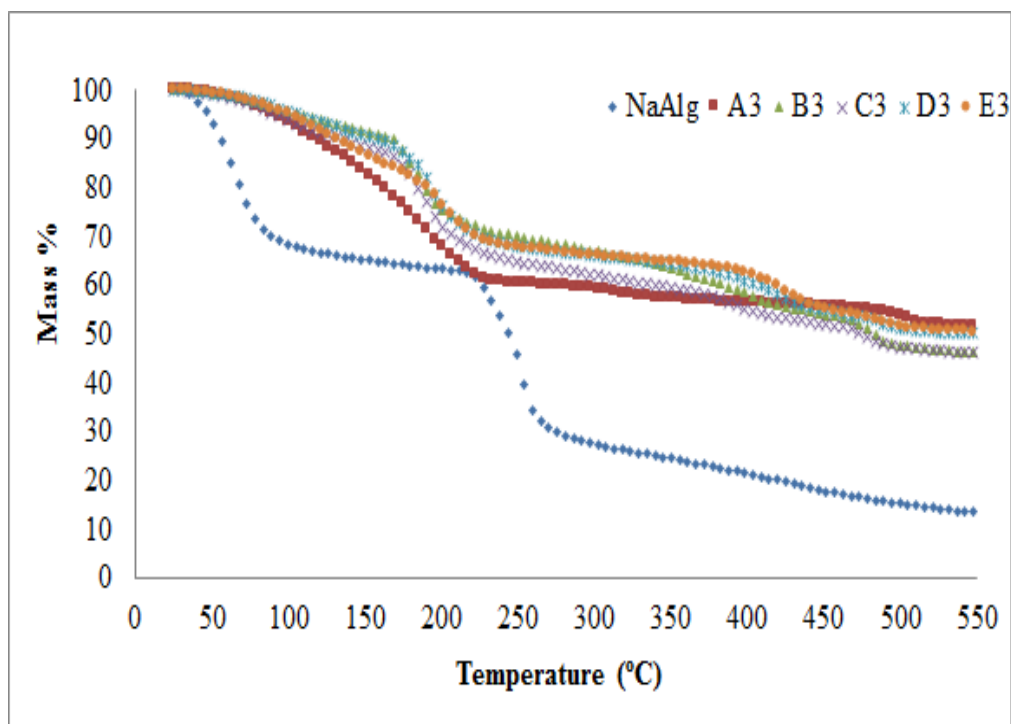
Figure 4.15:   Weight loss of pure NaAlg and 5 selected grafted polymers

(A3, B3, C3, D3, and E3)

From the TGA results, the weight loss of pure NaAlg started at 55°C and this is due to the removal of moisture and surface bound water from pure NaAlg. For the graft polymers, the weight loss at temperature below 100°C is minimal compared to pure NaAlg.

The TGA result of pure NaAlg shows one-step of degradation. The degradation started at inflection point of 252.60 °C. It indicates the degradation of NaAlg in nitrogen atmosphere through the decomposition process of the saccharide rings by breaking up the C-H and C-O-C glycosidic bonds in the main chain of the polysaccharides (Phang *et al.*, 2011). As the result of this decomposition process, Na_2CO_3 and other carbonaceous materials were left as residue (Soares *et al.*, 2004). The remaining residue weight is about 20.53% at 550ºC for pure NaAlg.

For all the grafted polymers selected; A3, B3, C3, D3 and E3, 3 degradation steps were observed. All inflection points, weight loss percentage and residue of copolymers were summarised in Table 4.2.

The first degradation step at the first inflection point of all the grafted polymers refers to the side chain breakdown or decomposition of the carboxyl group of AA and AM together with the thermal degradation of NaAlg (Lanthong *et al.*, 2006; Yang *et al.*, 2009; Phang *et al.*, 2011) whereas the second degradation step at the second inflection point is due to the breakage of the C-C bonds in PAA and PAM chain (Chen and Tan, 2006; Phang *et al.*, 2011) and the complex decomposition of NaAlg backbone including dehydration of the saccharide rings, breaking of C-O-C bonds in the chain of NaAlg, depolymerisation with the formation of water, carbon dioxide and methane (Laurienzo *et al.*, 2005; Lanthong *et al.*, 2006; Phang *et al.*, 2011). Lastly, the third degradation step at the third inflection point might be due to the further degradation of the additional of C-C bonds of crosslinker and all the

left-over copolymers (Phang *et al*., 2011).

Table 4.2:   Inflection points and weight loss percentage of NaAlg and its 5 selected grafted polymers

Sample / Parameters	NaAlg	A3	B3	C3	D3	E3
Inflection Point 1	252.60	173.99	173.99	171.04	176.89	180.98
Weight loss (%)	35.72	39.92	30.67	37.26	33.73	34.00
Inflection Point 2	-	298.56	385.98	380.17	401.28	408.56
Weight loss (%)	-	3.55	14.57	9.51	11.11	11.27
Inflection Point 3	-	480.95	499.63	456.92	464.66	465.65
Weight loss (%)	-	4.67	8.17	6.18	4.63	3.75
Residue (%) at 550 °C	20.53	51.81	45.68	46.79	50.53	50.87

There is an obvious variance between the TGA results of NaAlg and all the grafted polymers. From Table 4.2, there is only 20.53% residue of the NaAlg left after TGA analysis whereas 51.81%, 45.68%, 46.79%, 50.53% and 50.87% residues are left for grafted polymers A3, B3, C3, D3 and E3 respectively.

Thus, it can be concluded that the grafting of AA and AM onto NaAlg backbone had obviously increased thermal stability as NaAlg is protected by copolymers. Moreover the decomposition pathway is also altered when NaAlg was grafted with AA and AM.

From Figure 4.16, the remaining residue of A1, A2 and A3 are 51.20%, 52.46% and 51.81% respectively.
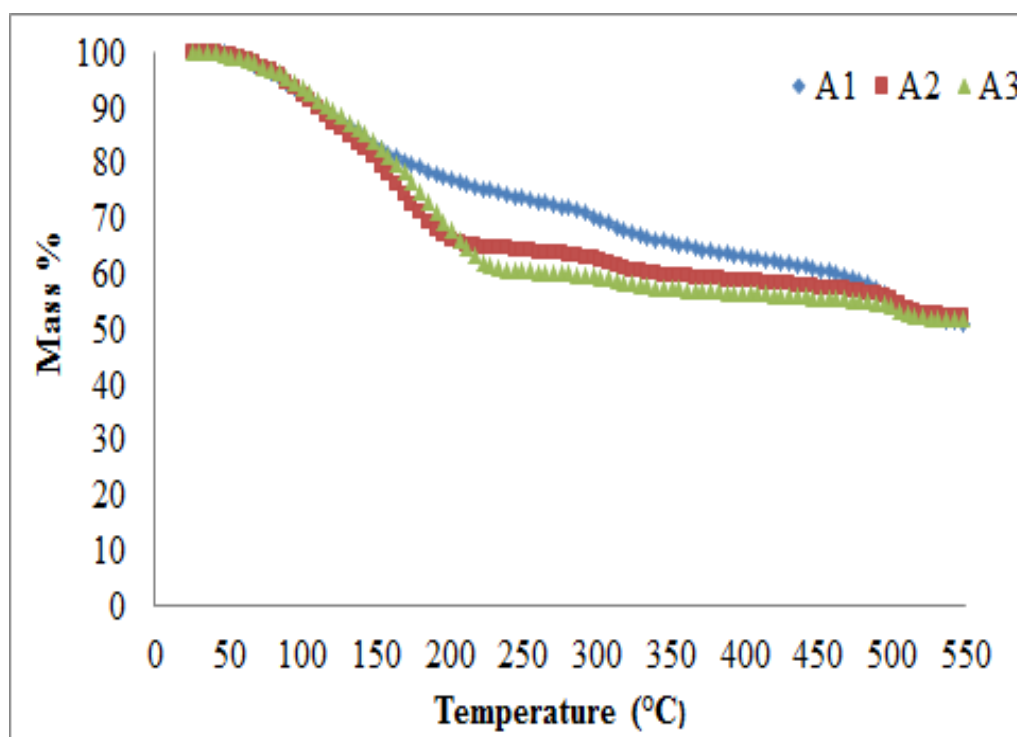
Figure 4.16:   Weight loss of 3 selected grafted polymers (A1, A2 and A3)

It can be observed that first inflection point, which refers to side chain breakdown or decomposition (Lanthong *et al.*, 2006; Yang *et al.*, 2009; Phang *et al.*, 2011), increases from 129.97 to 173.99 °C. This is due to $CaCl_2$, which acts as protective layer, can protect the grafted polymers from being further decomposed at higher temperature. Table 4.3 shows the summary of all

inflection points, weight loss percentage and residue of grafted polymers from TGA thermograms.

Table 4.3: **Inflection points and weight loss percentage of NaAlg and its 3 selected grafted polymers**

Parameters \ Sample	A1	A2	A3
Inflection Point 1	129.97	154.08	173.99
Weight loss (%)	35.72	35.88	39.92
Inflection Point 2	289.61	298.05	298.56
Weight loss (%)	11.48	5.27	3.55
Inflection Point 3	479.28	483.16	484.95
Weight loss (%)	12.05	6.49	4.67
Residue (%)	51.20	52.46	51.81

4.5 Differential Scanning Calorimetry Analysis (DSC)

Figure 4.17 illustrates the T_g (glass transition temperature) and T_m (melting temperature) of pure NaAlg and 5 selected grafted polymers with different ratio of AA and AM. The T_g and T_m values are summarized in Table 4.4.

From Figure 4.17, the DSC traces of sodium alginate exhibit an endothermic peak at 77.50 ℃. The endothermic peak represents T_g for NaAlg,

whereas, the exothermic peak are due to decomposition of NaAlg at temperature 248.24 ℃ which is also supported by first inflection temperature of NaAlg at 252.60 ℃ in TGA result. Many other literatures also support this finding. Research done by Yang *et al*. (2011) also recorded an exothermic peak at temperature around 250℃ for sodium alginate.
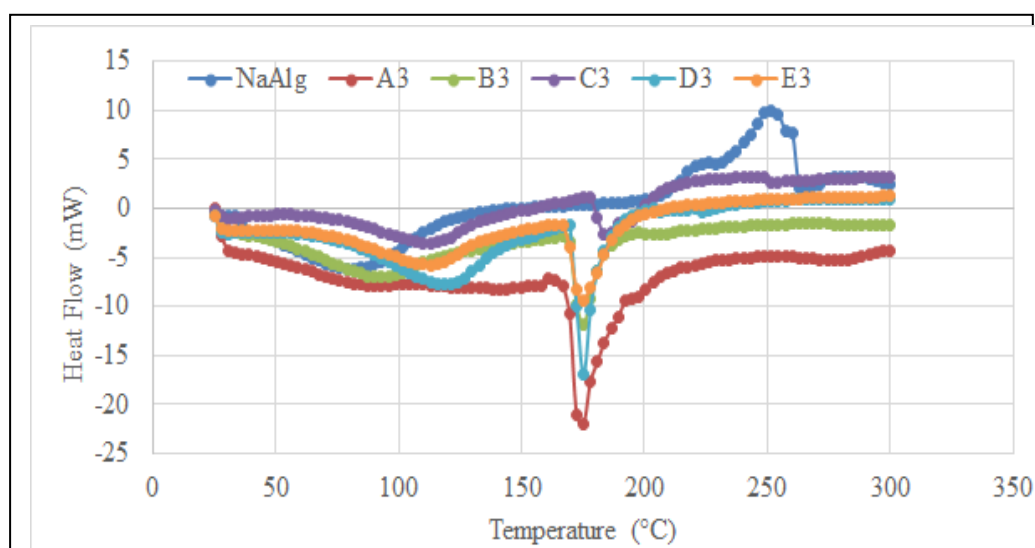
Figure 4.17: T_g and T_m values of pure NaAlg and 5 selected grafted polymers

This exothermic peak was not observed for the crosslinked grafted polymers. According to literature study, in Ca^{2+} crosslink beads, the decomposition peak was not observed due to the formation of "egg box" structure with calcium ions (Sarmento *et al*., 2006). Moreover the crosslink network formation between the polymer chains also will contribute to this enhancement. According to previous research pure NaAlg exhibit semi crystalline structure (Xiao *et al*., 2014). However in our case, the T_m value or a second endothermic peak was not observed in DSC thermogram. The reason

for this might due to decomposition which takes place as soon as melting happens, thus, the endothermic and exothermic reaction overlaps and only the net heat flux could be observed. The amorphous nature of NaAlg is further supported by XRD results in Section 4.6.

All grafted polymers exhibit two endothermic peaks; T_g and T_m. Both T_g and T_m are affected by restriction of segmental movement of polymeric chain of polymers whereas T_m alone is affected by crystallinity, which means the measurement of temperature at which amorphous region has been destructed.

Different crystallinity has different types of hydrogen bonding that occur in all these grafted polymers due to different concentration of AA and AM. Each of this hydrogen bonds exhibits different strength.

Grafted polymer C3 exhibits the highest T_m value, due to the $O-H\cdots:N$ type of hydrogen bond formation as the concentration of AA and AM are almost similar. The T_m value increases from grafted polymer A3 to B3, as the possibility for the formation of $O-H\cdots:N$ type of hydrogen bond increase as the concentration of AM increases. However, for grafted polymers D3 and E3, the T_m value is lower than grafted polymer C3 when the concentration of AM exceeds 50%, more $N-H\cdots:N$ type of hydrogen bond will be formed and these bonds are relatively weak compared to $O-H\cdots:N$ bonds (Gilli and Gilli, 2009).

In contrast, the T_g value increases proportionally as the concentration of AM increases. This is due to the reduction in segmental mobility of polymeric chain and this reduction is caused by crosslinking of grafted polymeric chain. Furthermore, the formation of interpenetrating crosslink structure in the amorphous region might contribute to this increment. AA exhibits an ionic characteristic, whereas AM shows non-ionic characteristic. Thus, the grafted polymers with higher concentration of AA will be acidic and the grafted polymers with higher concentration of AM will be more neutral.

Previous research study shows that neutralized grafted polymers can be crosslinked much faster than non-neutralized, as the initiator and crosslinking agent are activated much faster in neutralized condition (Merlin and Sivasankar, 2009). Hence, in the grafted polymers with high concentration of AM, more crosslinks can be formed in the reaction.

In addition, the theoretical T_g values of AA (379K or 106ºC) and AM (438K or 165ºC) can also support the increment of T_g values as the concentration of AM increases (Brandrup *et al.*, 1999). The grafted polymers with higher concentration of AM, the T_g value must be less than the theoretical T_g value (165ºC) and from Table 4.4, the T_g values are less than the theoretical, and hence it can be concluded that the experimental T_g values are acceptable.

Table 4.4: Values of T_g and T_m of NaAlg and 5 selected grafted polymers

Sample	T_g (°C)	T_m (°C)
NaAlg	78	-
A3	82	172
B3	89	174
C3	111	185
D3	118	173
E3	118	178

Figure 4.18 shows the T_g (glass transition temperature) and T_m (melting temperature) of 3 selected grafted polymers with different concentration of CaCl$_2$ and T_g and T_m values are recorded in Table 4.5.
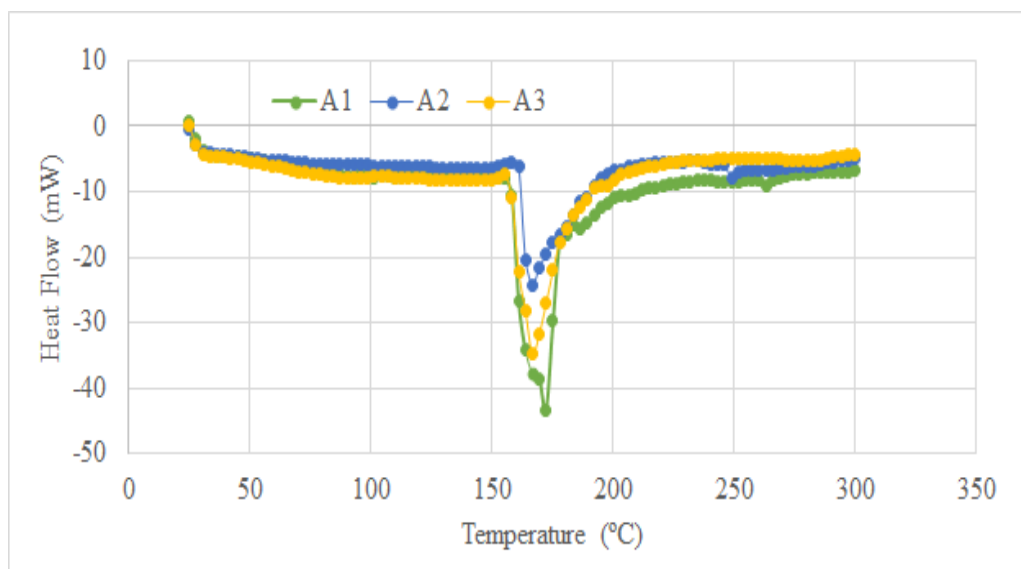
Figure 4.18: T_g and T_m values of 3 selected grafted polymers

From the figure above, it can be concluded that the T_g value slightly

decreases as the concentration of $CaCl_2$ increases. This is due to the influence of close electrostatic interaction force between Ca^{2+} and grafted polymers. However, based on Table 4.5, Ca^{2+} does not affect much on T_g of grafted polymer and this can be supported by XRD result in section 4.6.

Table 4.5: Values of T_g and T_m of 3 selected grafted polymers

Sample	T_g (ºC)	T_m (ºC)
A1	86	169
A2	83	166
A3	82	166

4.6   X-ray diffraction Analysis (XRD)

The effect of AA and AM ratio and the concentration of $CaCl_2$ on the crystallinity of the grafted polymers were evaluated and recorded in Figure 4.19 and 4.20 respectively.

From Figure 4.19, some peaks were observed in XRD pattern of pure NaAlg and it shows that the pure NaAlg used in this research study is amorphous. The diffractogram of all grafted polymers shows a broad area between the 2θ ranges of 10 to 30º with some new peaks. This indicate the formation of new loosely packed crystalline region with very high interlayer spacing. As the concentration of AM increases no intense peak was observed in this area indicating there are no significant amount of loosely packed

crystalline region. Other sharp and intense peaks were observed at 2θ range of 30 to 45° and 65° to 80°. Grafted polymers A3, B3 and D3 have similar peaks (similar crystallinity) at 65° to 80° whereas grafted polymers C3 and E3 have similar sharp peaks (similar crystallinity) at 65° to 80°. This is proven by T_m values from DSC results.

The peak intensity at 30° to 45° increases as the concentration of AM increases. This also shows that the grafting of AA and AM onto NaAlg does affect the semi crystalline structure of the grafted polymers by changing the nature of polymer.

On the other hand, Figure 4.20 shows the XRD patterns of grafted polymers A1, A2 and A3. The diffractogram of all selected grafted polymers shows a broad peak between the 2θ ranges of 10 to 30° and this indicates amorphous region (Liu, wang and Chen, 2001). However, the pattern changed from pyramid pattern to normal broad pattern when the concentration of $CaCl_2$ increases. This shows that the crystallinity is affected by the concentration of $CaCl_2$. Some crystalline peaks were obtained at 2θ range of 30 to 45° from XRD patterns. Crystalline peaks at 2θ range of 12 to 50° are getting less and this result indicates that the concentration of Ca^{2+} solution does affect the crystallinity of the superabsorbent polymer. This kind of change might be due to the close electrostatic interaction force between Ca^{2+} and grafted polymers.
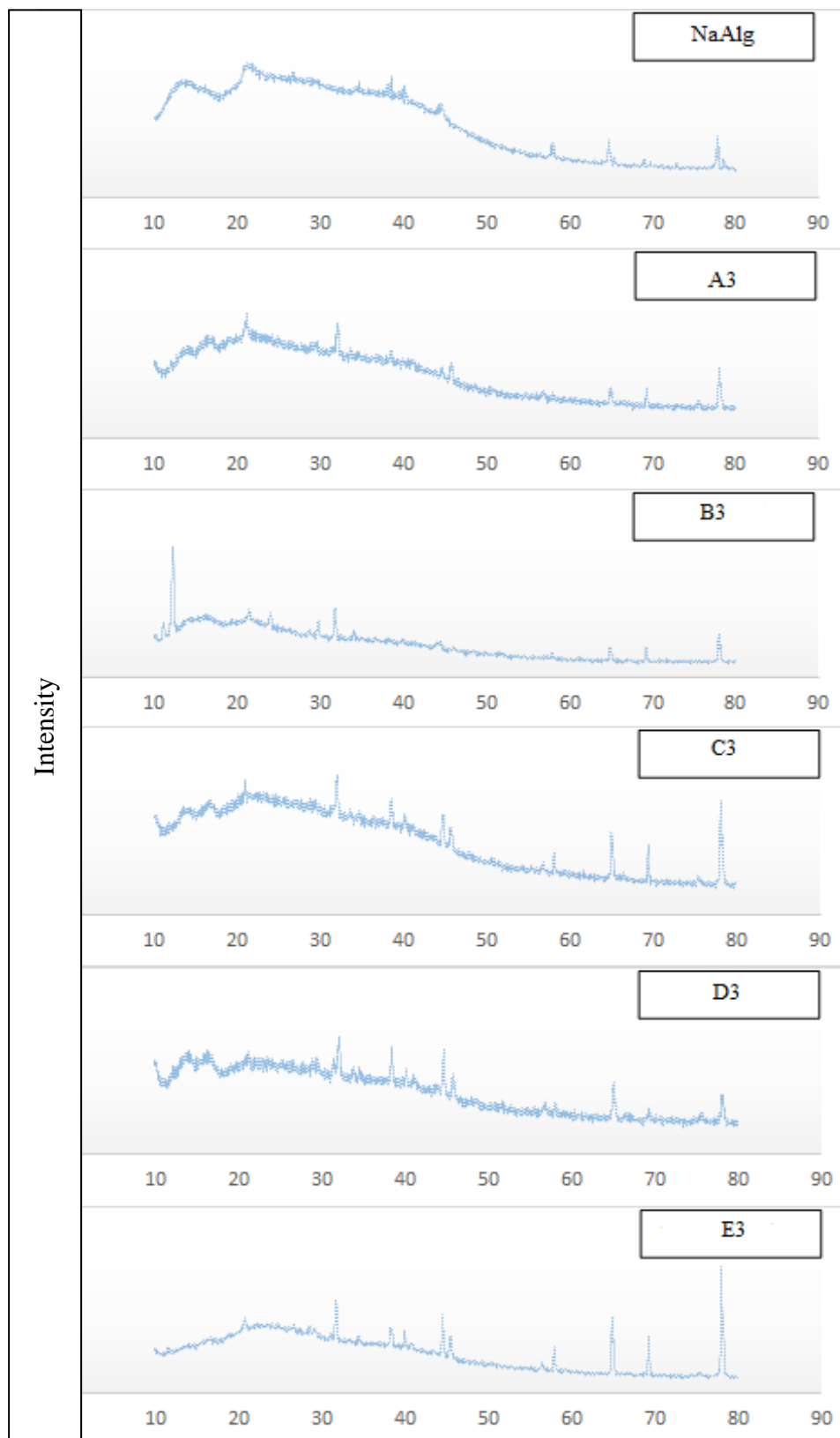
Figure 4.19: X-ray diffraction patterns of pure NaAlg and 5 selected grafted polymers
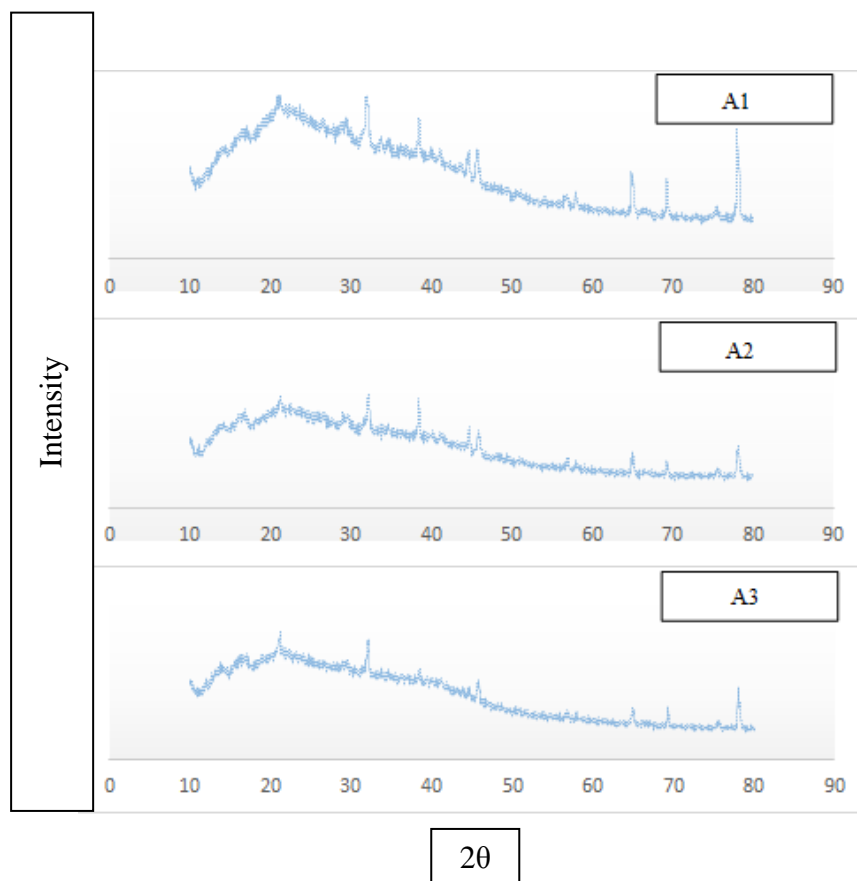
Figure 4.20:   X-ray diffraction patterns of 3 selected grafted polymers

4.7   Morphological Analysis

4.7.1   Surface morphology of grafted polymers without NPK fertilizers

FESEM micrographs of selected grafted polymers (A3, B3, C3, D3 and E3) with different ratio of AA and AM at the magnification of x1000 were shown in Figure 4.21 respectively whereas Figure 4.22 illustrate the FESEM micrograph of another selected grafted polymers (A1, A2 and A3) with different concentration of $CaCl_2$. Different magnification (x350) of all the grafted polymers were shown in Appendix B.
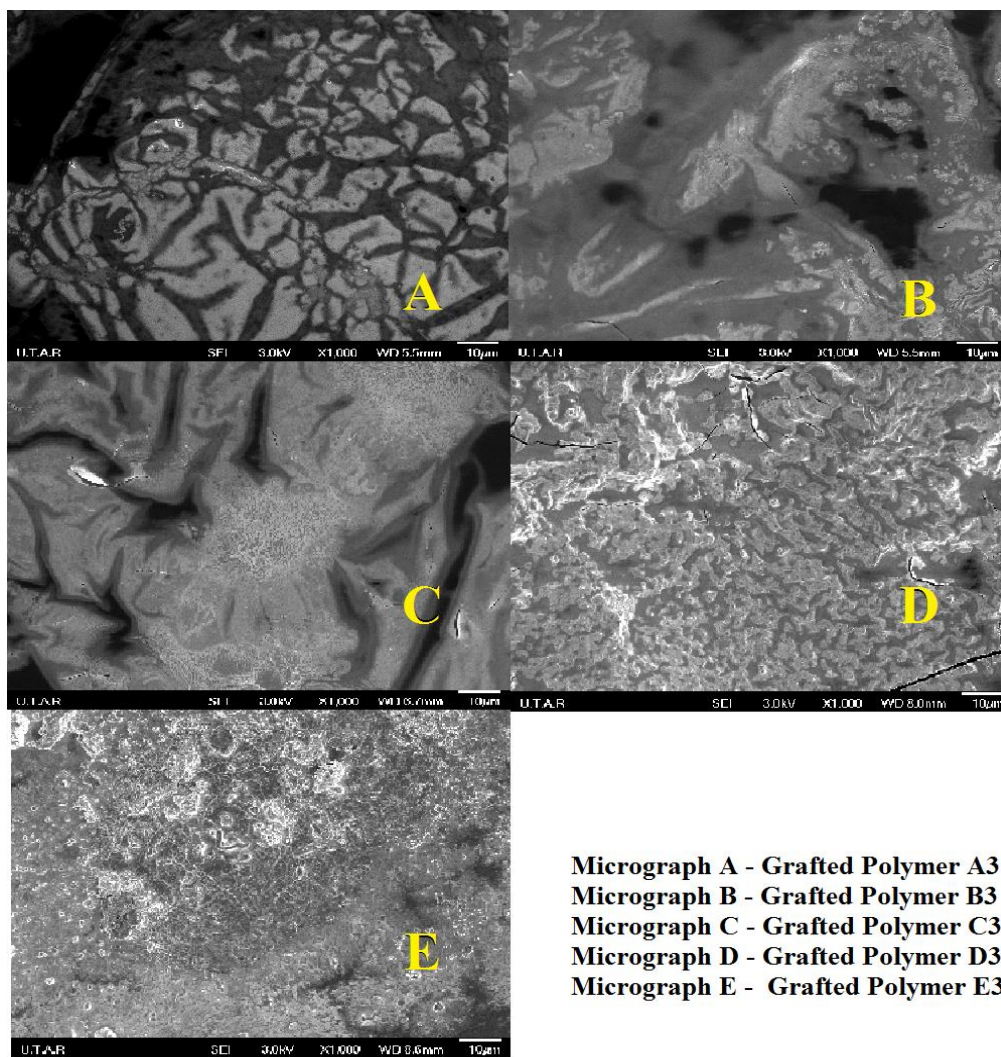
Figure 4.21: FESEM micrograph of 5 selected grafted polymers

From FESEM micrographs shown in Figure 4.21, it can be observed that all the selected grafted polymers (A3, B3, C3, D3 and E3) present an undulant, coarse and porous surface which structurally increases the surface area. This kind of surface facilitates the permeation of water into the polymeric network to form a swollen hydrogel (Zheng *et al*., 2007).

The FESEM micrographs also show that fewer folds were observed and voids on the surface have been reduced as the concentration of AM increases. A less wavy surface can be observed with higher concentration of AM as shown

by FESEM micrographs for grafted polymers D3 and E3. Less wavy surface of sample D3 and E3 is expected to decrease the surface area and directly decrease the swelling capacity of the grafted polymers. This will be further discussed in section 4.8.

Furthermore, the surface is getting more compact and exhibit less folds with higher concentration of AM. This is due to the hydrogen bonding interaction between the functional groups. The functional group "$-CONH_2$" of AM has more effective hydrogen-bonding interaction than the functional group "$-COOH$" of AA.

According to the FESEM micrographs, grafted polymer A3 exhibits the most void and folds if compare to other four grafted polymers. As a result, it causes the grafted polymer A3 having the weakest gel strength and the strongest swelling capacity whereas grafted polymer E3 possesses the strongest gel strength which leads weakest swelling capacity. This will be further discussed in section 4.8.

On the other hand, from FESEM micrographs shown in Figure 4.22, the selected grafted polymers (A1, A2 and A3) present an undulant, coarse and porous surface which allows the penetration of water into the polymeric network. It is very obvious that less folds and porous structure are found on the surface of the grafted polymers as the concentration of $CaCl_2$ increases. This is due to the formation of stronger Ca^{2+} continuous protective layer on the surface of the copolymers as concentration of $CaCl_2$ increases.

Micrograph A - Grafted polymer A1
Micrograph B - Grafted polymer A2
Micrograph C - Grafted polymer A3
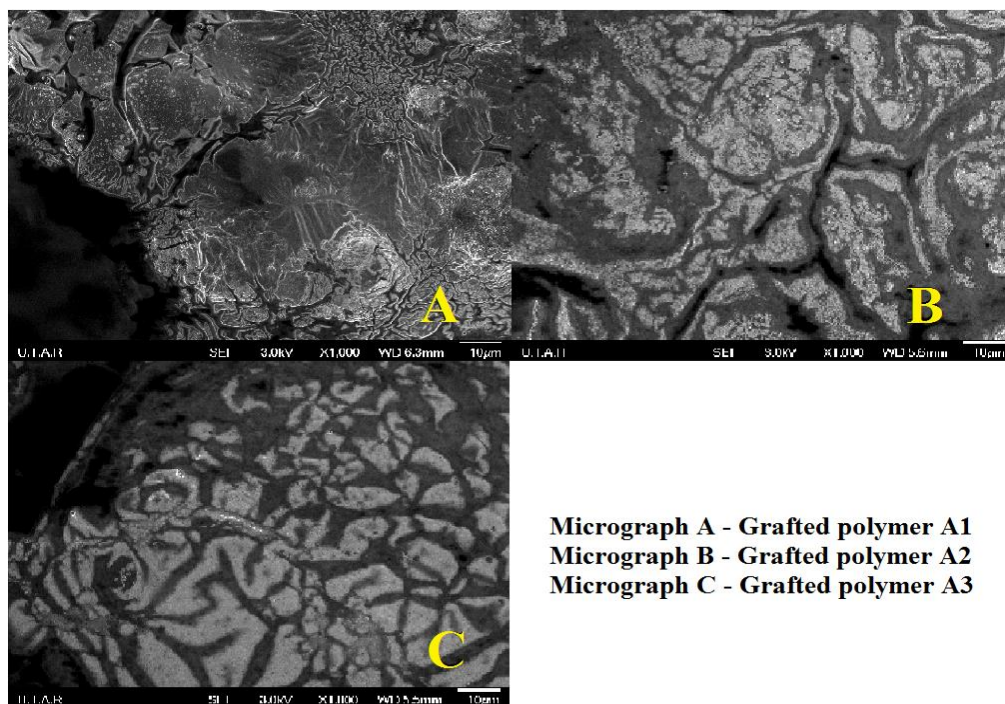
Figure 4.22: FESEM micrograph of 3 selected grafted polymers

4.7.2 Surface morphology of NPK fertilizer imbedded grafted polymers

SEM micrographs of 5 selected NPK fertilizer-imbedded grafted polymers (FA3, FB3, FC3, FD3 and FE3) with different ratio of AA and AM at the magnification of x2500 are shown in Figure 4.23. Different magnification (x350) of all the grafted polymers were shown in Appendix C.

Important note: Letter F represents the grafted polymer contains NPK fertilizer; A-E indicates the sample with different ratio of AA and AM; number 1-3 is the concentration of $CaCl_2$.

From FESEM micrographs shown in Figure 4.23, it can be observed that all the selected grafted polymers (FA3, FB3, FC3, FD3 and FE3) present

an undulant and coarse surface which allows diffusion of water into the polymeric network (Zheng *et al*., 2007). Fewer folds and more compact surface are observed as the concentration of AM increases in the grafted polymers.

Micrograph A - Grafted Polymer FA3
Micrograph B - Grafted Polymer FB3
Micrograph C - Grafted Polymer FC3
Micrograph D - Grafted Polymer FD3
Micrograph E - Grafted Polymer FE3
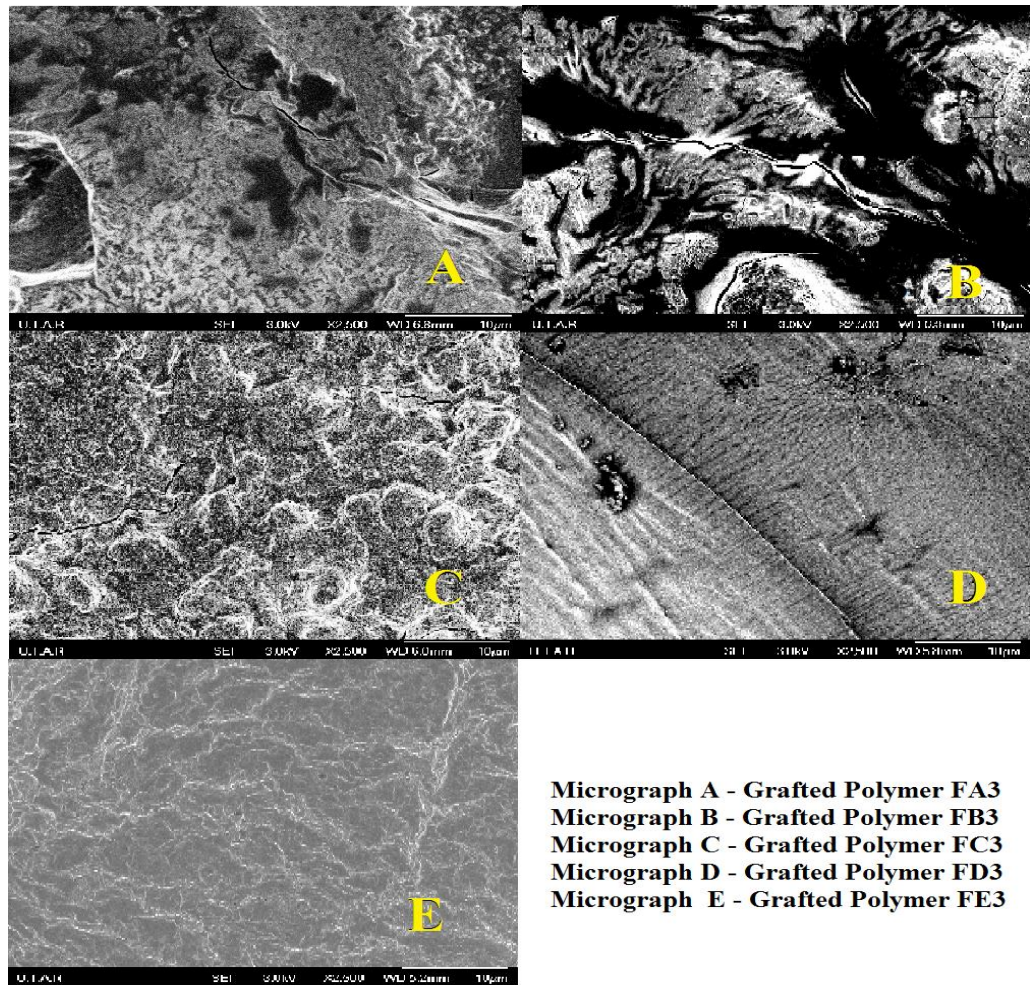
Figure 4.23: FESEM micrograph of 5 selected fertilizer-imbedded grafted polymers

Furthermore, from FESEM micrographs shown in Figure 4.24, the selected grafted polymers (FA1, FA2 and FA3) present an undulant and porous surface which allows the penetration of water into the polymeric network.
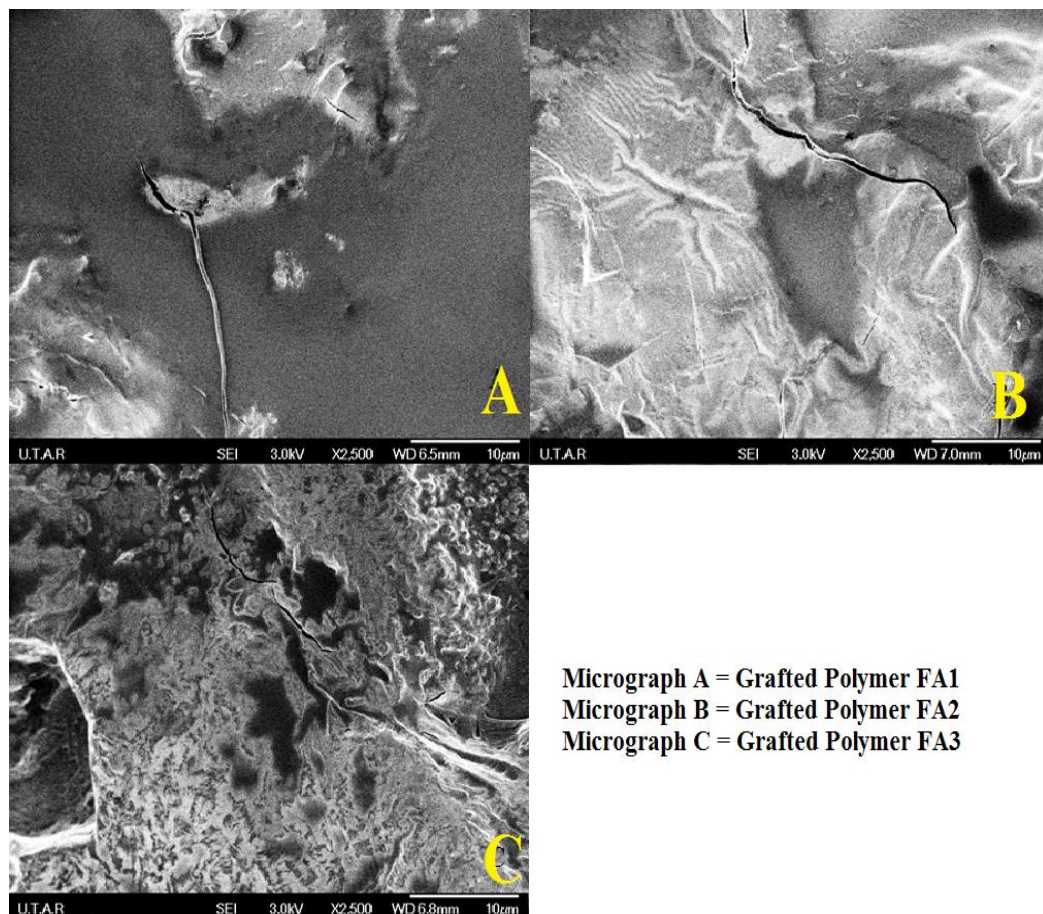
Figure 4.24: FESEM micrograph of 5 selected fertilizer-imbedded grafted polymers

It can be seen that less pinholes and cracks found on the surface of the grafted polymers as the concentration of $CaCl_2$ increases. This is due to the stronger Ca^{2+} protective layer which can decrease the swelling capacity and the rate of release of fertilizer.

4.8 Measurement of Swelling Capacity

Figure 4.25 explains the swelling capacity of grafted polymers with different ratio of AA:AM with respect to the duration of swelling. The results

indicated that the swelling capacity decreases as the AM concentration increases and this could be attributed to the synergistic effect of -$CONH_2$ of AM and –COO^- group of AA which leads to different surface morphology and structure of grafted polymers as indicated in FESEM and XRD results.

The -COO^- group has better hydrophilic ability than the -$CONH_2$ group due to higher number of hydrophilic group, so the swelling capacity decreases with the further increase of AM concentration (Liang, Liu and Wu, 2007; Wu and Liu, 2008). Additionally, AM is a non-ionic monomer, and it almost does not ionize in solution, so the ions in the solution have little influence on it.

Moreover, the swelling capacity is also dependent on the hydrogen bonding interaction between the functional groups. The functional group "–$CONH_2$" of AM has stronger hydrogen-bonding interaction than the functional group "–COOH" of AA. Thus, the hydrogen bonding interaction, which affects the surface morphology of grafted polymers (discussed in section 4.7), will be stronger as the concentration of AM increases (Kim and Park, 2004). Wavy surface, cracks and pin holes do affect the swelling capacity of grafted polymers too. As evidenced from FESEM images, as concentration of AM increases the surface becomes more compact with less folds and pin holes.
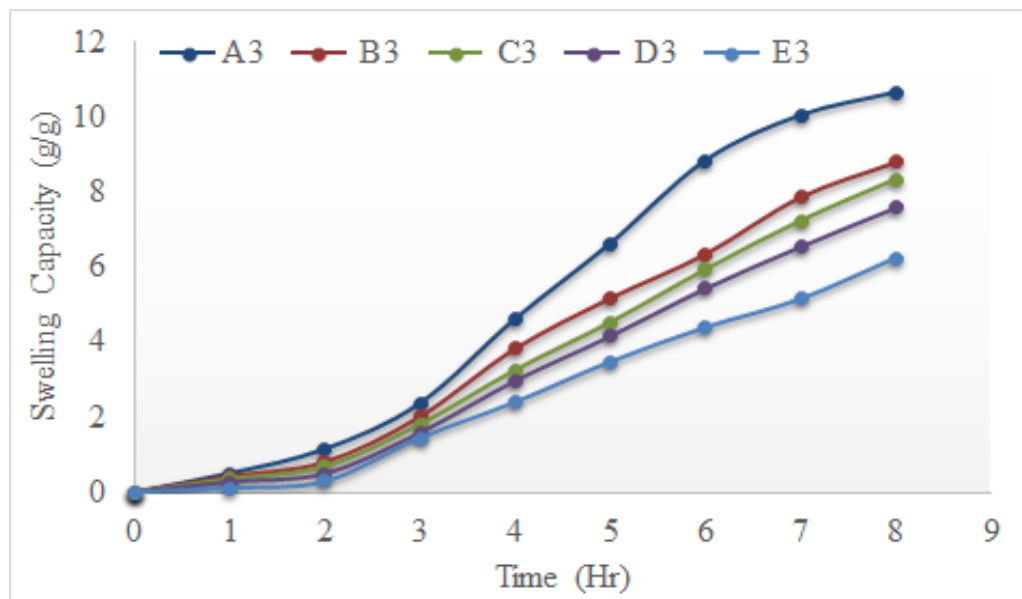
Figure 4.25: Swelling capacity of 5 selected grafted polymers as a function of time

Figure 4.26 shows the swelling capacity of grafted polymers with different concentration of $CaCl_2$ against the duration of swelling. The results indicated that the swelling capacity decreases as the concentration of $CaCl_2$ increases.

The decrease in water absorbency as concentration of $CaCl_2$ increases can be due to three reasons. First reason is maybe due to the amount of Ca^{2+}-CO_2^- bond to form a well-crosslinked network. Higher concentration of $CaCl_2$ produce bigger amount of Ca^{2+}-CO_2^- bond and directly form a better crosslinked network.

Second reason is due to the surface of copolymers (discussed in section 4.7). Wavy surface shown on copolymer with lower concentration of $CaCl_2$ will have larger surface area to allow more water penetrate into polymeric

network, hence the swelling capacity of copolymer will be higher as shown by grafted polymer A1. As the concentration of $CaCl_2$ increases in grafted polymer A3, the surface becomes more compact and no wavy surface observed. Thus the swelling capacity decreases.

The third reason is due to existence of more folds, voids and pin holes on the surface of grafted polymers with lower concentration of $CaCl_2$. Because of this, a large volume of water can penetrate into the grafted polymer easily. Hence, grafted polymer A3 with highest concentration of Ca^{2+} showed the lowest swelling capacity compared to grafted polymers A1 and A2.
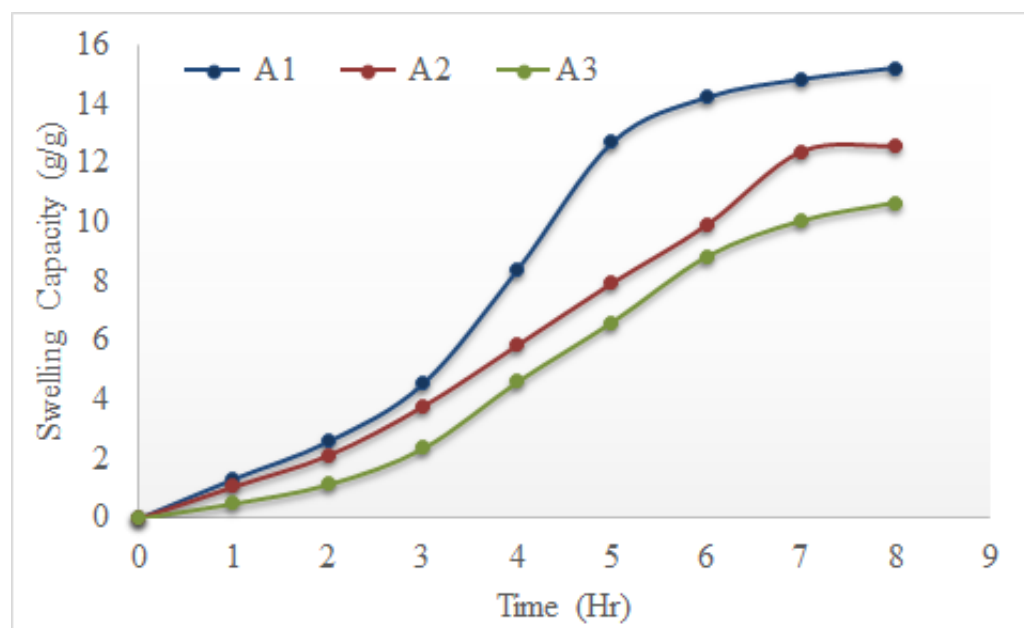
Figure 4.26: Swelling capacity of 3 selected grafted polymers as a function of time

4.9 Biodegradability Test (Weight Loss Test)

One of the imporant factors that can affect the release rate of fertilizer in soil is the biodegradability of the grafted polymers over period. Figures 4.27 and 4.28 illustrate the weight loss percentage of selected grafted polymers (A3, B3, C3, D3, E3 and A1, A2, A3 respectively), through the soil burial method, in the soil sample obatined from several points of location of Oil Palm Field at Trolak Selatan, Perak, Malaysia. The soil sample was found slightly acidic at pH 5.78.
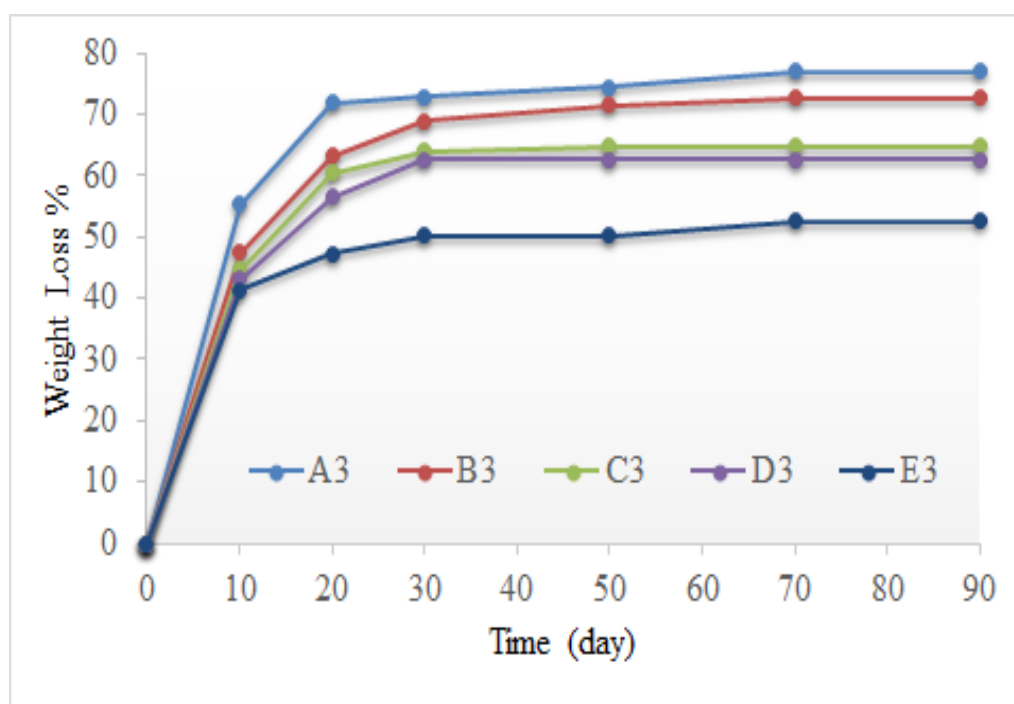
Figure 4.27: **Percentage weight loss of 5 selected grafted polymers as a function of time through soil burial**
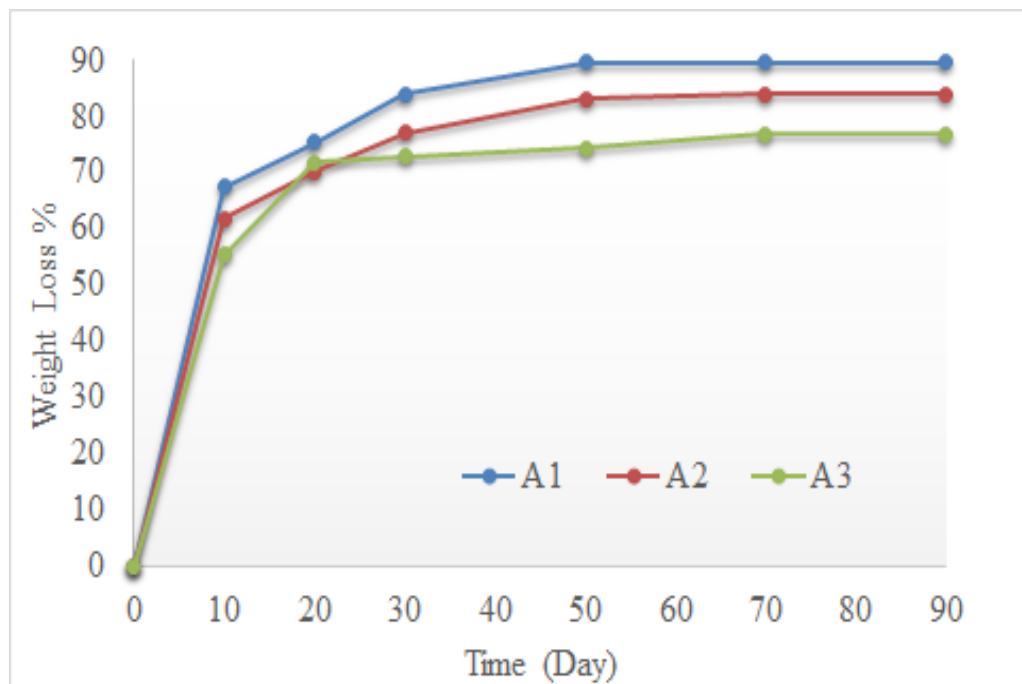
Figure 4.28: **Percentage weight loss of 3 selected grafted polymers as a function of time through soil burial**

During the first 30 days of soil burial test, the grafted polymers showed a drastic loss in weight, in which the weight loss was 76.9% for grafted polymer A3, 72.6% for grafted polymer B3, 64.7% for grafted polymer C3, 62.5% for grafted polymer D3 and 50.2% for grafted polymer E3 (as shown in Figure 4.27) and 89.7% for grafted polymer A1, 84.0% for grafted polymer A2 and 76.9% for grafted polymer A3 as (shown in Figure 4.28).

However, the weight loss persisted with slower rate from 30th day onwards. This could be due to the depletion of nutrients that support the microbial growth and lack of bacterial activity in the soil sample, therefore, the rate of biodegradation decreases (Phang *et al.*, 2011). The biodegradability can be improved if the grafted polymers are buried in plantation area with natural condition.

Moreover, the interpenetrating network formation among the copolymer chains is also one of the factor that could slower down the rate of biodegradation. It is noteworthy to mention that the crosslinked grafted polymer chains will not biodegrade easily. Furthermore, the Ca^{2+}, which acts as a protective layer on the surface of the grafted polymers, can prevent the direct penetration of microorganism to attack the polymer chain. In addition, the grafted polymers with higher concentration of AM will have lower biodegradability and this due to the compact surface with no fold and pin hole which gives the limitation for bacteria to penetrate into grafted polymer for biodegradation process.

4.10   Rate of Release Behaviour of NPK Fertilizer In Soil

The most important characteristic of this research work is the controlled-release property of this research's product − fertilizer-imbedded grafted polymer beads (Figure 4.29) to be applied in agriculture field, especially for fighting with loss of nutrient during rain that mentioned in the main objective. Figure 4.30 indicates the proposed controlled-release mechanism of the imbedded-fertilizer grafted polymers.

Figure 4.29:   Fertilizer-imbedded grafted polymer beads

101

Diffusion of water
soluble nutrients

The polymer
encapsulation material
start to biodegrade and
micro pores are formed

Water

Micro organism

Biodegradable
Superabsorbent Polymer

Fertilizer

The biodegradable
superabsorbent polymer is
swollen by water in the
soil.

The water
soluble
nutrients
from
fertilizer will
dissolve in
water and
diffuse to the
soil

The water
will penetrate
further in and
more
nutrients will
be dissolve
and diffuse to
the soil. The
concentration
of nutrient
will become
lower with
time.

The polymer
encapsulation material
will biodegrade with
time. Micro organism
can penetrate and
degrade the insoluble
part of fertilizer. This
part can diffuse into
the soil.

Figure 4.30:   The controlled-release mechanism of fertilizer-imbedded grafted polymers

102

Figures 4.31, 4.32 and 4.33 represent the rate of release of N, P and K fetilizer from 5 selected grafted polymers (different ratio of AA and AM) in soil whereas Figures 4.34, 4.35 and 4.36 depict the rate of release of N, P and K fertilizer from 3 selected grafted polymers (different concentration of $CaCl_2$) in soil.

Figure 4.31: Release behaviours of nitrogen from 5 selected grafted polymers in soil as a function of time

It could be seen from Figure 4.31 that the amount of nitrogen (N) released from fertilizer-imbedded grafted polymer beads are 28.2%, 18.3%, 12.1, 5.4%, 1.6% for grafted polymer FA3, FB3, FC3, FD3 and FE3 respectively on 3rd day, 60.3%, 40.6%, 19.2%, 16.0%, 12.3% for grafted polymer FA3, FB3, FC3, FD3 and FE3 respectively on 7th day and 95.0%, 86.3%, 63.1%, 43.6%, 39.2% for grafted polymer FA3, FB3, FC3, FD3 and FE3 respectively on 28th day.

Figure 4.32: **Release behaviours of phosphorus from 5 selected grafted polymers in soil as a function of time**

From Figure 4.32, the amount of phosphorus (P) released from fertilizer-imbedded grafted polymer beads are 26.8%, 18.5%, 10.7, 5.6%, 1.9% for grafted polymer FA3, FB3, FC3, FD3 and FE3 respectively on 3rd day, 58.9%, 35.3%, 17.6%, 16.0%, 5.8% for grafted polymer FA3, FB3, FC3, FD3 and FE3 respectively on 7th day and 97.5%, 79.3%, 53.7%, 41.6%, 34.9% for grafted polymer FA3, FB3, FC3, FD3 and FE3 respectively on 28th day.

Figure 4.33: Release behaviours of potassium from 5 selected grafted polymers in soil as a function of time

It could be observed from Figure 4.33 that the amount of potassium (K) released from fertilizer-imbedded grafted polymer beads are 24.9%, 18.3%, 9.7, 4.4%, 1.3% for grafted polymer FA3, FB3, FC3, FD3 and FE3 respectively on 3rd day, 56.4%, 33.6%, 11.9%, 12.8%, 12.3% for grafted polymer FA3, FB3, FC3, FD3 and FE3 respectively on 7th day and 94.0%, 76.3%, 50.9%, 37.6%, 29.6% for grafted polymer FA3, FB3, FC3, FD3 and FE3 respectively on 28th day.

With the sum of nutrients release lower than 15% on the 3rd day and not above 75% on the 30th day, this indicates that only grafted polymers FC3, FD3 and FE3 prepared are in compliance with the standard of slow release fertilizers criteria of the Committee of European Normalization (CEN) (Trenkel, 1997). This means these grafted polymers having excellent controlled
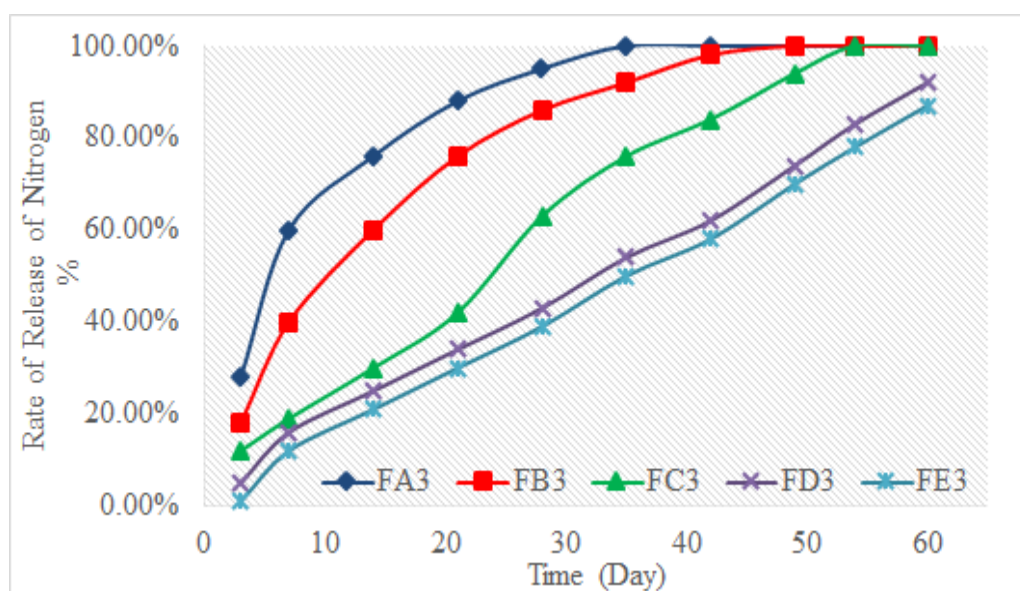
105

release property in soil.
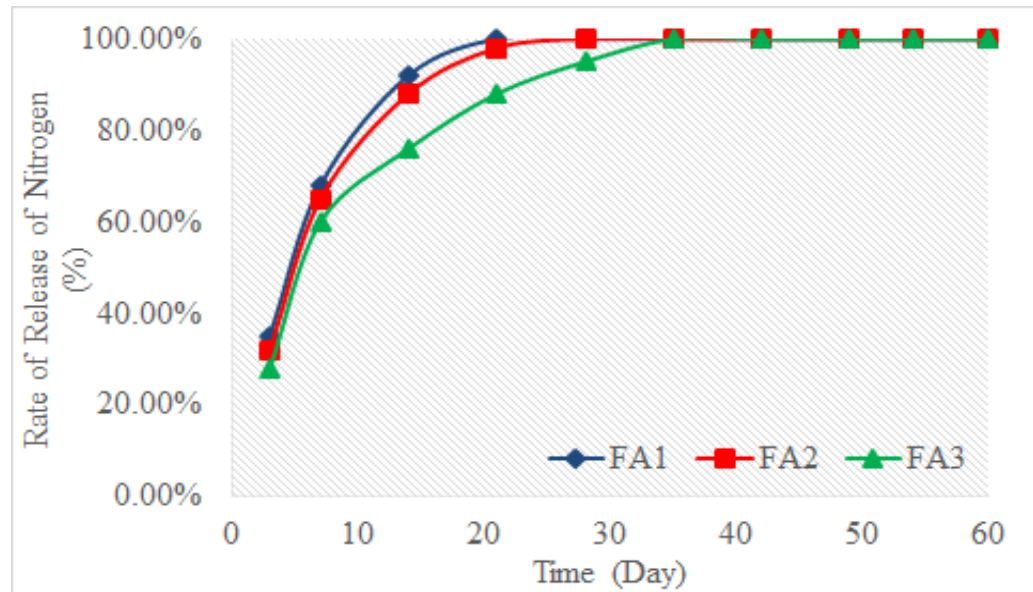
Figure 4.34: **Release behaviours of nitrogen from 3 selected grafted polymers in soil as a function of time**

It could be seen from Figure 4.34 that nitrogen (N) released 35.4%, 32.7%, 28.2% for grafted polymer FA1, FA2 and FA3 respectively on 3rd days, 68.7% 65.3%, 60.3% for grafted polymer FA1, FA2 and FA3 respectively on 7th days and 100, 100% and 95.0% for grafted polymer FA1, FA2 and FA3 respectively on 28th days.
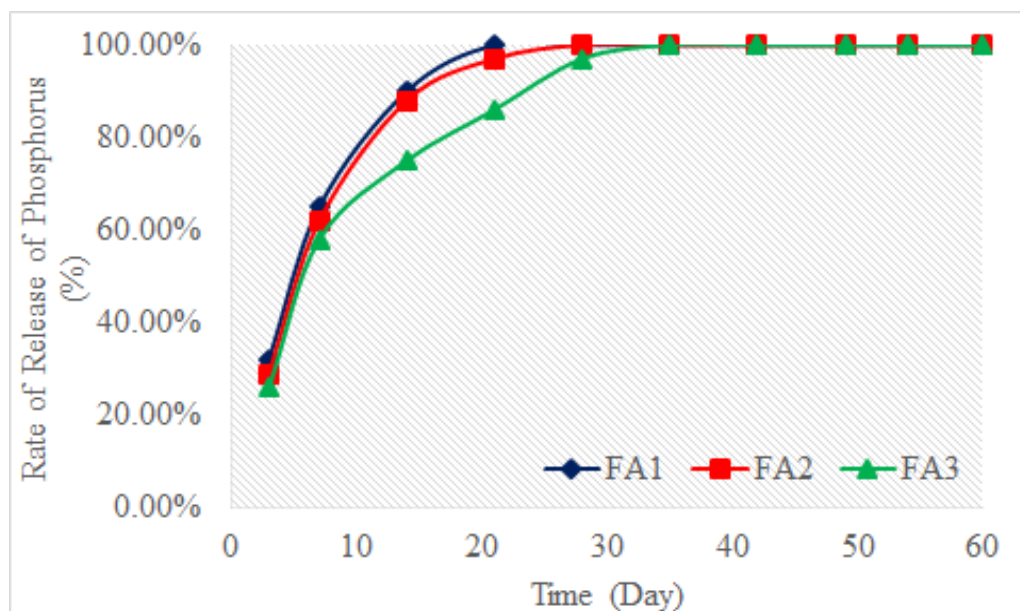
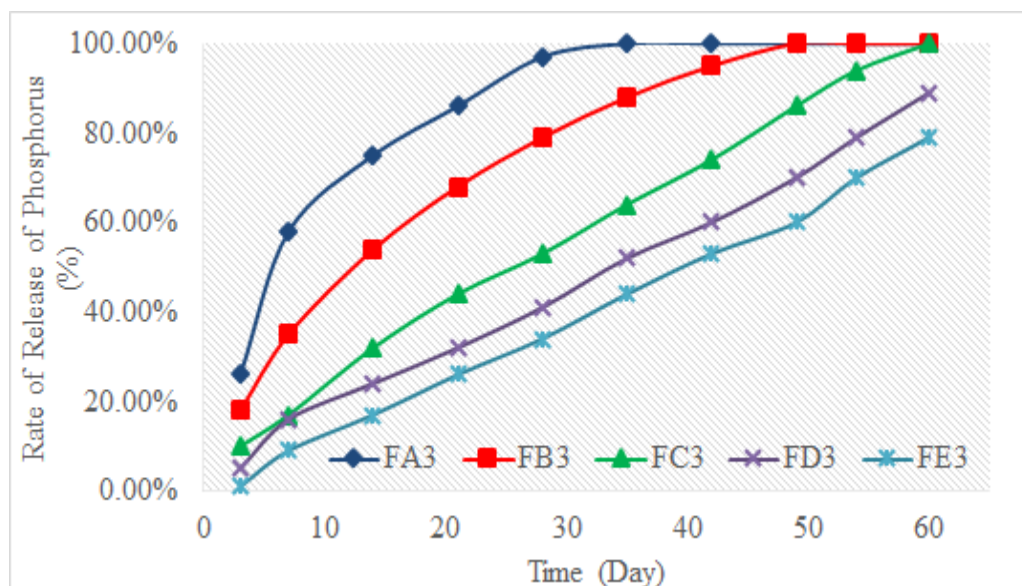**Figure 4.35: Release behaviours of phosphorus from 3 selected grafted polymers in soil as a function of time**

From Figure 4.35, phosphorus (P) released 32.9%, 29.2%, 26.8%, for grafted polymer FA1, FA2 and FA3 respectively on 3rd days, 65.1%, 62.4%, 58.9%, for grafted polymer FA1, FA2 and FA3 respectively on 7th days and 100%, 100%, 97.5% for grafted polymer FA1, FA2 and FA3 respectively on 28th days.
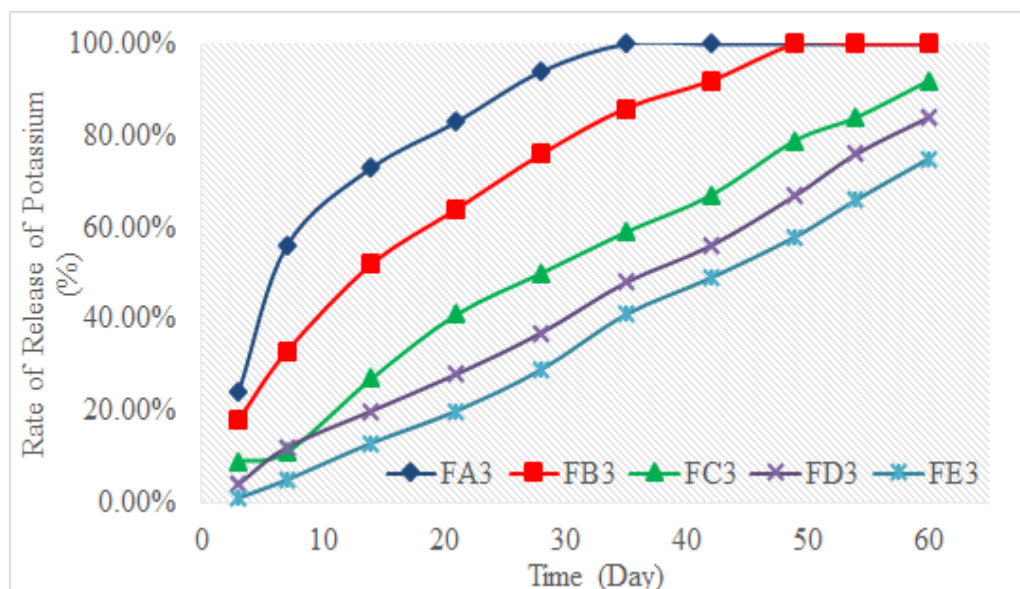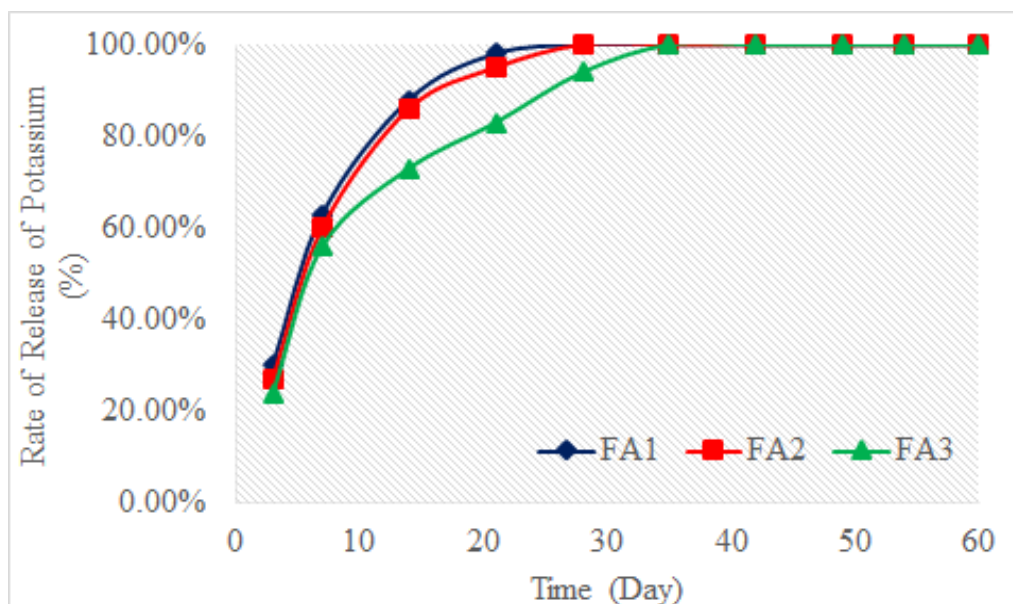
Figure 4.36: **Release behaviours of potassium from 3 selected grafted polymers in soil as a function of time**

From Figure 4.36, potassium (K) released 30.5%, 27.1%, 24.9% for grafted polymer FA1, FA2 and FA3 respectively on 3rd days, 63.7%, 60.1%, 56.4%, for grafted polymer FA1, FA2 and FA3 respectively on 7th days and 100%, 100%, 94.0%, for grafted polymer FA1, FA2 and FA3 respectively on 28th days.

According to standard slow release fertilizers of the Committee of European Normalization (CEN) (Trenkel, 1997), none of grafted polymer A1, A2 and A3 agreed with the standard which the sum of nutrients release must be lower than 15% on the 3rd day and not above 75% on the 30th day.

The nutrient release mechanism is described by the following steps:

i) The Ca^{2+} protective layer of copolymers is attacked by water in the soil and caused NaAlg-*g*-P(AA-*co*-AM) layer swollen slowly and transforms to hydrogel. A dynamic exchange between the free water in the hydrogel and the water in soil will develop (David and Mark, 1994; Smyth, Francis and Vincent, 1998).

ii) When the free water contacts with NaAlg-*g*-P(AA-*co*-AM) layer, the water will penetrate into the layer slowly through the apperture and holes in the initial stage and dissolved NPK fertilizer. Diffusion would be the release rate –limiting step.

iii) Under the effect of water, ions and microorganism in soil, NaAlg layer will slowly degrade and continue dissolve the leftover NPK fertilizer. Degradation rate determines the nutrient release rate.

iv) The dissolved NPK fertilizer diffuses out and releases into the soil through the dynamic exchange of free water.

From Figures 4.30, 4.31 and 4.32, it can be concluded that the release rate of NPK fertilizer from grafted polymer beads decreases with the increment of concentration of AM whereas from figures 4.33, 4.34 and 4.35, it can be decuded that the release rate of NPK fertilizer from grafted polymer beads decreases as the concentration of $CaCl_2$ increases.

The discussions above agree with the statements discussed in Section 4.7, 4.8, and 4.9. As the concentration of AM increases, the grafting efficiency will be higher and the surface of grafted polymers will be more compact and

less folds if compare to those with higher concentration of AA. This causes the grafted polymers with high concentration of AM having weaker swelling capacity. As the swelling capacity is weak, it is harder for water or other biological fluids to penetrate through the surface of grafted polymers in order to dissolve the fertilizer nutrients and undergo diffusion of nutrients into soil.

Furthermore, the higher AM concentration grafted polymers with compact surface will have lower biodegradability due to difficulty of bacterial attacking the surface of grafted polymers. This will also slower down the release rate since the surface is much harder to be penetrated to allow the nutrient to diffuse out from grafted polymers.

On the other hand, grafted polymers with higher concentration of $CaCl_2$ will have slower rate of release. This is due to the Ca^{2+} protecive layer is much stronger with higher concentration of $CaCl_2$. This protective layer is also one of the factors which influence the release rate of fertilizer.

The n value is an emperical parameter characterzing the release mechanism (Shaviv, 2000). On the basis of the diffusion exponent, n value of 0.5 indicates the nutrient release to a Fickian diffusion controlled release, whereas n equal to 1.0 indicates the nutrient release mechanism approaches to zero-order release. The n value from 0.5 to 1.0 is a nutrient release mechanism for non-Fickian diffusion or chain relaxation control release. The release exponent (n) and release factor (K) were calculated from the plots of log (M_t/M) versus log (t) (Appendix D) and summarized in Table 4.6

Table 4.6: The release factors (K), release exponents (n) and determination coefficients (r^2) from release data of 5 selected fertilizer-imbedded grafted polymers

Grafted Polymers	Nutrients	n	K	r^2
A3	N	0.3869	23.79	0.8738
	P	0.4106	21.82	0.8744
	K	0.4355	19.76	0.8828
B3	N	0.5543	12.20	0.9454
	P	0.5736	10.91	0.9778
	K	0.5800	10.43	0.987
C3	N	0.7654	4.59	0.9859
	P	0.7843	4.00	0.9977
	K	0.8397	2.95	0.9765
D3	N	0.9125	2.15	0.988
	P	0.8968	2.18	0.9865
	K	0.9756	1.51	0.9942
E3	N	1.000	0.47	0.929
	P	1.000	0.41	0.9541
	K	1.000	0.28	0.991

From Table 4.6, it can be concluded that the nutrients release mechanism of grafted polymers B3 and C3 is non-Fickian diffusion. This release mechanism is controlled by a combination of diffusion of fertilizers and degradation rate of grafted polymers.

111

4.11 Water Retention of Soil

Another important characteristic for this research work is to be applied in agriculture field, especially for saving water to fight with drought in oil palm plantation. Figure 4.37 shows the water retention behaviours of soil without (Blank) and with different ratio of AA and AM of grafted polymers (FA3, FB3, FC3, FD3 and FE3) whereas Figure 4.38 the water retention behaviours of soil without (Blank) and with different concentration of $CaCl_2$ of grafted polymers (FA1, FA2 and FA3). It is very obvious that the addition of fertilizer-imbedded grafted polymers could increase the water retention of soil.
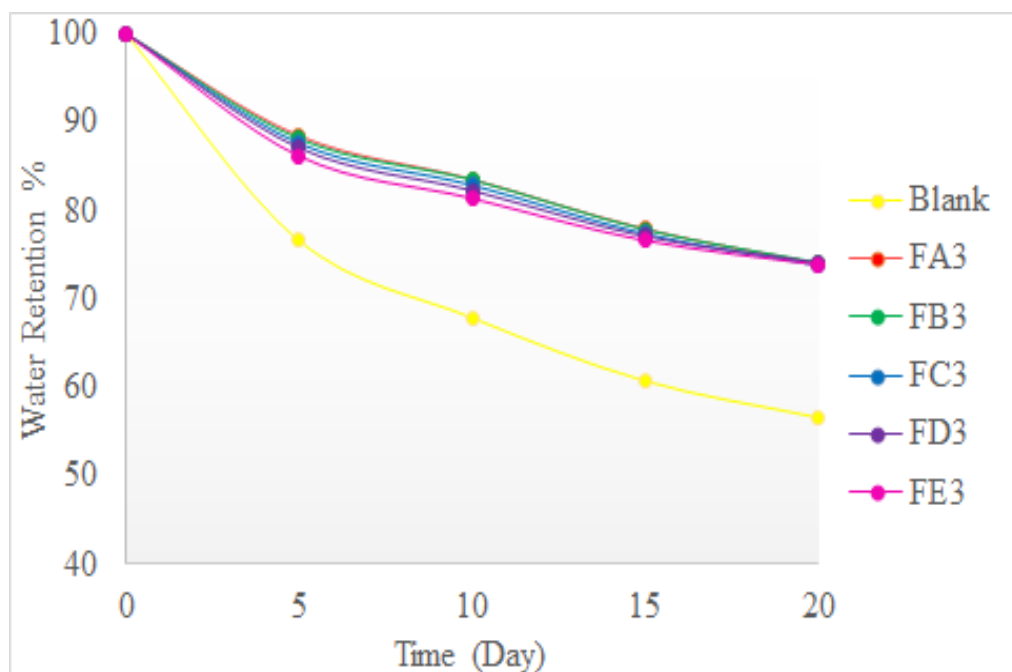

Figure 4.37: **Water retention behaviours of soil sample with fertilizer-imbedded grafted polymers (FA3, FB3, FC3, FD3 and FE3) and plain soil sample (Blank) as a function of time**
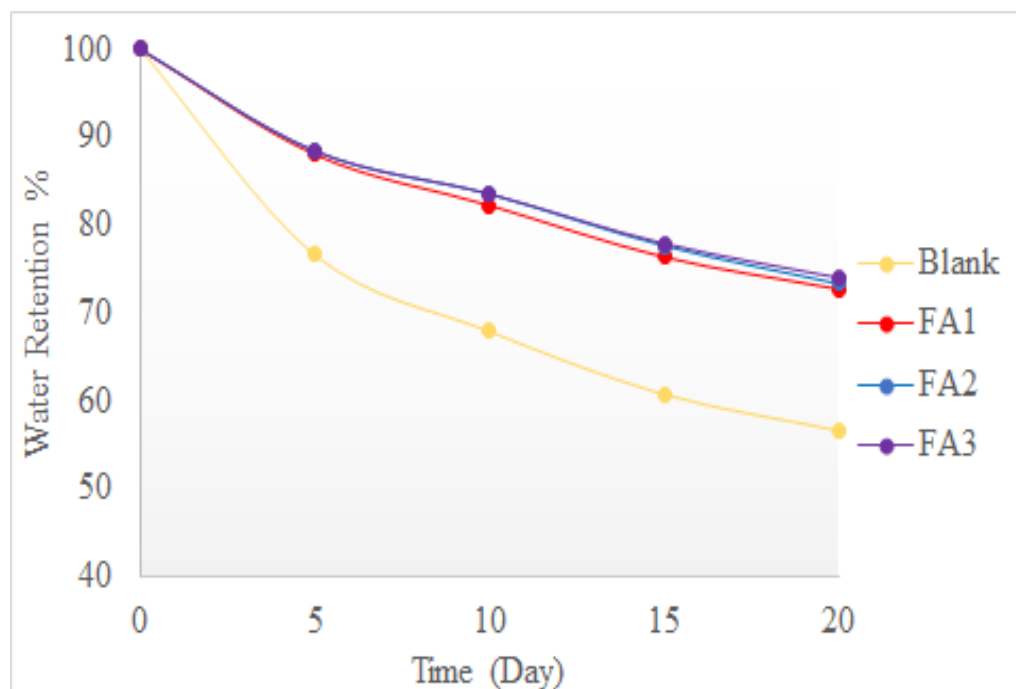
Figure 4.38: Water retention behaviours of soil sample with fertilizer-imbedded grafted polymers (FA1, FA2 and FA3) and plain soil sample (Blank) as a function of time

The water retention percentage of soil without fertilizer-imbedded grafted polymers (Blank) had remained 67.88% and 56.59% on the 10th day and 20th day respectively whereas the water retention of soil with fertilizer-imbedded grafted polymers still could remain at least 80% and above. This can be concluded that the water retention of soil sample can be improved with the help of fertilizer-imbedded grafted polymers, allowing the water to be saved and managed so that the water and ferilizer can be effectively used for the growth of oil palm.

In addition, from this study, it could also be inferred that the soil sample in Malaysia has better water retention ratio, which is up to 56.59% on the 20th

day, if compared to other countries.

Hence, NaAlg-*g*-poly(AA-*co*-AM) are safe to use and not harmful to soil since the copolymers AA and AM can be biodegraded in soil (Ye, Zhao and Zhang, 2004). Besides that, NaAlg is a food-based material and it provides nutrient to support the bacterial activity in soil for further biodegradation.

CHAPTER 5.0

CONCLUSIONS

Acrylic acid (AA) and acrylamide (AM) were successfully grafted on sodium alginate (NaAlg) using ammonium persulfate (APS) as initiator and *N,N'*-methylenebisacrylamide (NMBA) as crosslinking agent. Spherical beads were successfully formed using calcium chloride ($CaCl_2$) as precipitating agent. NPK fertilizer with ratio 15:15:15 was calculated and successfully imbedded in alginate-based superabsorbent polymer beads.

Upon investigation, it was found that different ratio of AA and AM and different concentration of $CaCl_2$ affected several characteristics and properties of NaAlg-*g*-P(AA-*co*-AM) superabsorbent polymer. As concentration of AM increases in the graft copolymerization reaction, the grafting efficiency of AA and AM onto NaAlg increases.

The obtained results of FTIR analysis showed that the monomers were successfully grafted onto NaAlg in the presence of crosslinking agent to form grafted polymers. According to TGA results, the thermal stability increased from 20.53% to the range from 45.68% to 51.81%. This shows that grafting of monomers on NaAlg has better thermal stability if compared to the non-grafted NaAlg. On the other hand, if the concentration of $CaCl_2$ increases, the decomposition temperature increases due to the strong protective layer which could prevent further decomposition of grafted polymers. T_g value is found

increasing as the concentration of AM increases. According to XRD result, it can be concluded that as the concentration of AM increases, the crystallinity will change from amorphous (NaAlg) to semi-crystalline (grafted polymers) whereas crystallinity will slightly change if concentration of $CaCl_2$ increases.

Furthermore, the effect of AA and AM ratio and concentration of $CaCl_2$ on the surface morphology of grafted polymers as well as their swelling capacity, biodegradability and release rate of NPK fertilizer were investigated. As the concentration of AM increases, the surface of grafted polymers becomes more compact with less folds, cracks and pinholes. This directly affect the swelling capacity, biodegradability and release rate of fertilizer.

As the concentration of AM and $CaCl_2$ increase, the swelling capacity and biodegradability of grafted polymers decreases. However, all grafted polymers are able to absorb water or any biological fluids and swell and those polymers are able to degrade at least 50% in 1 month.

According to standard of slow release fertilizers criteria of the Committee of European Normalization (CEN) (Trenkel, 1997), fertilizer-imbedded grafted polymer C (AA:AM; 55:45) and D(AA:AM; 40:60) are suitable to be applied in oil palm plantations in Malaysia or other agriculture purpose. This is because the release rate of NPK fertilizer has fullfilled the standard of slow release which is less than 15% on 3rd day and 75% on 30th day and these two fertilizer-imbedded grafted polymers have a non-Fickian diffusion. This release mechanism is controlled by a combination of diffusion

116

of fertilizers and degradation rate of grafted polymers. In addition, the water retention of soil had been improved up to 80% with fertilizer-imbedded grafted polymers added into soil. Therefore, the objectives of this reseaerch work are achieved.

REFERENCES

Abraham, J. and Rajasekharan, P. Y. N. (1996). Membrane-encapsulated controlled-release urea fertilizers based on acrylamide copolymers. *Journal of Applied Polymer Science*, 60, 2347–2351.

Al-Zahrani, S. M. (1999). Controlled-release of fertilizers: Modeling and simulation. *International Journal of Engineering Science*, 37, 1299-1307.

Baker, K. L., Langenhede, S., Nicol, G.W., Ricketts, D., Killham, K., Campbell, C. D. and James, I. P. (2009). Environmental and spatial characterisation of bacterial community composition in soil to inform sampling strategies. *Soil Biology & Biochemistry*, 41, 2292–2298.

Bhattacharya, S. S., Mazahir, F., Banerjee, S., Verma, A. and Ghosh, A. (2013). Preparation and in vitro evaluation of xanthan gum facilitated superabsorbent polymeric microspheres. *Carbohydrate Polymers*, 98, 64–72.

Brandrup, J., Immergut, E. H., Grulke, E. A. (Eds.). Abe, A. and Bloch, D. R. (Assoc. Eds.). (1999). *Polymer Handbook Volume 1* (pp. VI/198; VI/201). Fourth Edition. New York: Wiley-Interscience.

Braun, D., Cherdron, H., Rehahn, M., Ritter, H. and Voit, B. (2005). *Polymer synthesis: theory and practice* (pp. 5; 123; 149–150; 164; 166; 175–176; 257–259). 4th Edition. Germany: Springer-Verlag.

Buchhloz, F. L. and Graham, A. T. (Eds.). (1998). *Modern superabsorbent polymer technology* (pp. 7–8; 20–21; 30–31; 55–58; 147; 158–159; 187). New York: Wiley-VCH.

Chandia, N. P., Matsuhiro, B., Ortiz, J. S. and Mansilla, A. (2005). Carbohydrates from the sequential extraction of Lessonia vadosa (phaeophyta). *Journal of the Chilean Chemical Society*, 50, 501–504.

Chang, C. Y., Duan, B., Cai, J. and Zhang, L. N. (2010). Superabsorbent hydrogels based on cellulose for smart swelling and controllable delivery. *European Polymer Journal*, 46, 92–100.

Chen, Y. and Tan, H. (2006). Crosslinked carboxymethylchitosan-*g*-poly(acrylic acid) copolymer as a novel superabsorbent polymer. *Carbohydrate Research*, 341, 887–896.

Cosgrove, L., McGeechan, P. L., Robson, G. D. and Handley, P. S. (2007). Fungal communities associated with degradation of polyester polyurethane in soil. *Applied and Environmental Microbiology*, 73, 5817–5824.

Crini, G. (2005). Recent developments in polysaccharide-based materials used as adsorbents in wastewater treatment. *Progress in Polymer Science*, 30, 38–70.

Cui, S. W. and Wang, Q. (2006). Functional properties of carbohydrates: polysaccharide gums. In H. H. Yiu (Ed.), *Handbook of food science technology, and engineering* (pp. 4–11). UK: CRC Press.

119

Da Silva, D. A., de Paula, R. C. M. and Feitosa, J. P. A. (2007). Graft copolymerisation of acrylamide onto cashew gum. *European Polymer Journal*, 43, 2620–2629.

Davis, T. A., Volesky, B. and Mucci, A. (2003). A review of the biochemistry of heavy metal biosorption by brown algae. *Water Research*, 37, 4311–4330.

Draget, K. I. (2009). Alginates. In G. O. Philips and P. A. Williams (Eds.), *Handbook of hydrocolloids* (pp. 380). 2nd Edition. UK: CRC Woodhead Publishing Limited.

Draget, K. I., Smidsrød, O. and Skjåk-Bræk, G. (2005). Alginates from algae. In Steinbuchel, A. and Rhee, S. K. (Eds.), *Polysaccharides and polyamides in the food industry, properties, production and patents* (pp. 1–30). Weinheim: Wiley-VCH.

Ebewele, R. O. (2000). *Polymer science and technology* (pp. 8; 182; 363; 431–432). Boca Raton: CRC Press.

Ge, H. and Wang, S. (2014). Thermal preparation of chitosan-acrylic acid superabsorbent: Optimization, characteristic and water absorbency. *Carbohydrate Polymers*, 113, 296–303.

Gilli, G. and Gilli, P. (2009). *The nature of hydrogen bond* (pp. 222–225). New York: Oxford University Press Inc.

Glicksman, M. (1953). Natural polysaccharide gums in the food industry. In E. M. Mrak and G. F. Stewart (Eds.), *Advances in food research* (pp.

138). US: Academic Press.

Han, T. L., Kumar, R. N., Rozman, H. D. and Noor, M. A. M. (2003). GMA grafted sago starch as a reactive component in ultra violet radiation curable coatings. *Carbohydrate Polymers*, 54, 509–516.

Hemvichian, K., Chanthawong, A. and Suwanmala, P. (2014). Synthesis and characterization of superabsorbent polymer prepared by radiation-induced graft copolymerization of acrylamide onto carboxymethyl cellulose for controlled release of agrochemicals. *Radiation Physics and Chemistry*, 103, 167–171.

Huang, M., Shen, X., Sheng, Y. and Fang, Y. (2005). Study of graft copolymerization of *N*-maleamic acid-chitosan and butyl acrylate by γ-ray irradiation. *International Journal of Biological Macromolecules*, 36, 98–102.

Huang, Y. H., Yu, H. Q. and Xiao, C. B. (2007). pH-sensitive cationic guar gum/poly (acrylic acid) polyelectrolyte hydrogels: Swelling and in vitro drug release. *Carbohydrate Polymers*, 69, 774–783.

Işıklan, N., Kurşun, F. and İnal, M. (2010). Graft copolymerization of itaconic acid onto sodium alginate using benzoyl peroxide. *Carbohydrate Polymers*, 79, 665–672.

Kabiri, K., Omidian, H., Hashemi, S. A. and Zohuriaan-Mehr, M. J. (2003). Synthesis of fast-swelling superabsorbent hydrogels: effect of crosslinker type and concentration on porosity and adsorption rate.

European Polymer Journal, 39, 1341–1348.

Karadag, E. and Saraydin, D. (2002). Swelling of superabsorbent acrylamide/sodium acrylate hydrogels prepared using multifunctional crosslinkers. *Turkish Journal of Chemistry*, 26, 863–875.

Kiatkamjornwong, S., Mongkolsawat, K. and Sonsuk, M. (2002). Synthesis and property characterization of cassava starch grafted poly[acrylamide-*co*-(maleic acid)] superabsorbent via γ-irradiation. *Polymer*, 43, 3915–3924.

Kim, D. and Park, K. (2004). Swelling and mechanical properties of superporous hydrogels of poly(acrylamide-*co*-acrylic acid)/polyethylenimine interpenetrating polymer networks. *Polymer*, 45, 189–196.

Lanthong, P., Nuisin, R. and Kiatkamjornwong, S. (2006). Graft copolymerization, characterization and degradation of cassava starch-*g*-acrylamide/itaconic acid superabsorbents. *Carbohydrate Polymers*, 66, 229–245.

Larsen, B., Smidsrød, O., Painter, T. J. and Haug, A. (1970). Calculation of the nearest-neightbour frequencies in fragments of alginate from the yields of free monomers after partial hydrolysis. *Acta Chemica Scandinavica*, 24, 726–728.

Laurienzo, P., Malinconico, M., Motta, A. and Vicinanza, A. (2005). Synthesis and characterization of a novel alginate-poly(ethylene glycol) graft

copolymer. *Carbohydrate Polymers*, 62, 274–282.

Leal, D., Matsuhiro, B., Rossi, M. and Caruso, F. (2008). FT-IR spectra of alginic acid block fractions in three species of brown seaweeds. *Carbohydrate Research*, 343, 308–316.

Lee, J. S., Kumar, R. N., Rozman, H. D. and Azemi, B. M. N. (2005a). Pasting, swelling and solubility properties of UV initiated starch-graft-poly(AA). *Food Chemistry*, 91, 203–211.

Lee, Y. H., Kim, J. S. and Kim , H. D. (2005b). A sudy of biodegradable superabsorbent materials based on acrylonitrile grafted sodium alginate. *Key Engineering Materials*, 277–279, 450–454.

Lewis, J. G., Stanley, N. F. and Guist, G. G. (1988). Commercial production and applications of algal hydrocolloids. In C. A. Lembi and J. R., Waaland, *Algae and human affairs* (pp. 206). UK: Cambridge University Press.

Li, A. and Wang, A. (2005). Synthesis and properties of clay-based superabsorbent composite. *European Polymer Journal*, 41, 1630–1637.

Liang, R., Liu, M. and Wu, L. (2007). Controlled release NPK compound fertilizer with the function of water retention. *Relative and Functional Polymers*, 67, 769–779.

Lin, W., Guan, Y., Zhang, Y. J., Xu, J. and Zhu, X. X. (2009). Salt-induced erosion of hydrogen-bonded layer-by-layer assembled films. *Soft Matter*, 5, 860–867.

Liu, S. Z., Wang, F. and Chen, T. L. (2001). Synthesis of poly(ether ether ketone)s with high content of sodium sulfonate groups as gas dehumidification membrane materials. *Macromolecular Rapid Communications*, 22, 579–582.

Liu, T., Qian, L., Li, B., Li, J., Zhu, K., Deng, H., Yang, X. and Wang, X. (2013). Homogenous synthesis of chitin-based acrylate superabsorbents in NaOH/urea solution. *Carbohydrate Polymers*, 94, 261–271.

Lynda Merlin, D. and Sivasankar, B. (2009). Synthesis and characterization of semi-interpenetrating polymer networks using biocompatible polyurethane and acrylamide monomer. *European Polymer Journal*, 45, 165–170.

Mahdavinia, G. R., Pourjavadi, A., Hosseinzadeh, H. and Zohuriaan, M. J. (2004). Modified chitosan. 4. Superabsorbent hydrogels from poly(acrylic acid-*co*-acrylamide) grafted chitosan with salt- and pH-responsiveness properties. *European Polymer Journal*, 40, 1399–1407.

Moe, S. T., Draget, K. I., Skjåk-Bræk, G. and Smidsrød, O. (1995). Alginates. In A. M. Stephen (Ed.), *Food polysaccharides and their applications* (pp. 245–286). New York: Marcel Dekker.

Mogoşanu, G. D. and Grumezescu. (2014). Natural and synthetic polymers for wounds and burns dressing. *International Journal of Pharmaceutics*, 463, 127–136.

Murray, P. R. S. (1977). *Principles of Organic Chemistry*. 2nd Edition (pp. 297–306). London: Heinemann Educational Books.

Odian, G. (1991). *Principles of polymerization* (pp. 143; 212–213; 219; 311; 313; 454). 3rd Edition. US: John Wiley & Sons Inc.

Omidian, H., Hashemi, S. A., Sammes, P. G. and Meldrum, I. G. (1998). Modified acrylic-based superabsorbent polymers. Effect of temperature and initiator concentration. *Polymer*, 39, 3459–3466.

Omidian, H., Rocca, J. G. and Park, K. (2005). Advances in superporous hydrogels. *Journal of Controlled Release*, 102, 3–12.

Orive, G., Hernández, R. M., Gascón, A. R. and Pedraz, J. L. (2006). Encapsulation of cells in alginate gels. In J. M. Guisan, *Immobilization of enzymes and cells* (pp. 345–348). US: Humana Press.

Özeroglu, C. and Birdal, A. (2009). Swelling properties of acrylamide-N,N'-methylene bis(acrylamide) hydrogels synthesized by using meso-2,3-dimercaptosuccinic acid-cerium(IV) redox couple. *eXPRESS Polymer Letters*, 3, 168–176.

Painter, T. J., Smidsrød, O. and Haug. A. (1968). A computer study of the changes in composition-distribution occurring during random depolymerisation of a binary linear heteropolysaccharide. *Acta Chemica Scandinavica*, 22, 1637–1648.

Patel, G. M., Patel, C. P. and Trivedi, H. C. (1999). Ceric-induced grafting of

methyl acrylate onto sodium salt of partially carboxymethylated sodium alginate. *European Polymer Journal*, 35, 201–208.

Peng, X. H., Zhang, L. N. and Kennedy, J. F. (2006). Release behavior of microspheres from cross-linked *N*-methylated chitosan encapulsated ofloxacin. *Carbohydrate Polymers*, 65, 288-295.

Phang, Y. N., Chee, S. Y., Lee, C. O. and Teh, Y. L. (2011). Thermal and microbial degradation of alginate-based superabsorbent polymer. *Polymer Degradation and Stability*, 96, 1653–1661.

Pourjavadi, A., Zeidabadi, F. and Barzegar, S. (2010b). Alginate-based biodegradable superabsorbents as candidates for diclofenac sodium delivery systems. *Journal of Applied Polymer Science*, 118, 2015–2023.

Pourjavadi, A. and Zohuriaan-Mehr, M. J. (2002). Modification of carbohydrate polymers via grafting in air. 2. Ceric-initiated graft copolymerization of acrylonitrile onto natural and modified polysaccharides. *Starch*, 54, 482–488.

Ramazani-Harandi, M. J., Zohuriaan-Mehr, M. J., Yousefi, A. A., Ershad-Langroudi, A. and Kabiri, K. (2006). Rheological determination of the swollen gel strength of superabsorbent polymer hydrogels. *Polymer Testing*, 25, 470–474.

Rioux, L. E., Turgeon, S. L. and Beaulieu, M. (2007). Characterization of polysaccharides extracted from brown seaweeds. *Carbohydrate*

Polymers, 69, 530–537.

Robyt, J. F. (1998). *Essentials of carbohydrates chemistry. With 370 Illustrations* (pp. 180–183). US: Springer.

Rudin, A. (1999). *The elements of polymer science and engineering: an introductory text and reference for engineers and chemists* (pp. 90–102; 277–297). 2nd Edition. US: Academic Press.

Saboktakin, M. R., Maharramov, A. and Ramazanov, M. A. (2009). pH-sensitive starch hydrogels via free radical graft copolymerization, synthesis and properties. *Carbohydrate Polymers*, 77, 634–638.

Sabra, W. and Deckwer, W. D. (2004). Alginate – a polysaccharide of industrial interest and diverse biological functions. In S. Dumitriu, *Polysaccharides: structural diversity and functional versatility* (pp. 515–529). UK: CRC Press.

Safaa, G. A. A., Murat, S. and Abdel Wahab, M. E. (2012). Swelling and mechanical properties of superabsorbent hydrogels based on Tara gum/acrylic acid synthesized by gamma radiation. *Carbohydrate Polymers*, 89, 478–485.

Saigusa, M. (2000). The evaluation of mode purity for ECCD using single fertilizer on green peppers grown. *Journal of Plant Nutrition*, 23, 1485.

Sarmento, B., Ferreira, D., Veiga, F. and Ribeiro, A. (2006). Characterization of insulin-loaded alginate nanoparticles produced by ionotropic pre-

gelation through DSC and FTIR studies. *Carbohydrate Polymers*, 66, 1–7.

Shaviv, A. (2000). Advances in controlled-release fertilizer. *Advances in Agronomy*, 71, 1–49.

Singh, B., Chauhan, G. S., Kumar, S. and Chauhan, N. (2007) Synthesis, characterization and swelling responses of pH sensitive psyllium and polyacrylamide based hydrogels for the use in drug delivery (I). *Carbohydrate Polymers*, 67, 190-200.

Smidsrød, O. and Whittington, S. G. (1969). Monte Carlo investigation of chemical inhomogeneity in copolymers. *Macromolecules*, 2, 42–44.

Soares, J. P., Santos, J. E., Chierice, G. O. and Cavalheiro, E. T. G. (2004). Thermal behavior of alginic acid and its sodium salt. *Ecletica Quimica*, 29, 53–56.

Spagnol, C., Rodrigues, F. H. A., Pereira, A. G. B., Fajardo, A. R., Rubira, A. F. and Muniz, E. C. (2012). Superabsorbent hydrogel composite made of cellulose nanofibrils and chitosan-*graft*-poly(acrylic acid). *Carbohydrate Polymers*, 87, 2038–2045.

Thomas, S. (2004). Wound dressings. In D. T. Rovee and H. I. Maibach, *The epidermis in wound healing* (pp. 219–220). UK: CRC Press.

Torres, M. R., Sousa, A. P. A., Filho, E. T. A. S., Melo, D. F., Feitosa, J. P. A., de Paulab, R. C. M. and Lima, M. G. S. (2007). Extraction and physicochemical characterization of Sargassum vulgare alginate from

Brazil. *Carbohydrate Research*, 342, 2067–2074.

Tripathy, T., Pandey, S. R., Karmakar, N. C., Bhagat, R. P. and Singh, R. P. (1999). Novel flocculating agent based on sodium alginate and acrylamide. *European Polymer Jounal*, 35, 2057–2072.

Trenkel, M. E. (1997). Slow- and controlled-release and stabilized fertilizers; an option for enhancing nutrient use efficiency in agriculture. *International Fertilizer Industry Association*.

Trivedi, J. H., Kalia, K., Patel, N. K. and Trivedi, H. C. (2005). Ceric-induced grafting of acrylonitrile onto sodium salt of partially carboxymethylated guar gum. *Carbohydrate Polymers*, 60, 117–125.

Upadhyaya, L., Singh, J., Agarwal, V. and Prakash Tewari, R. (2014). The implications of recent advances in carboxymethyl chitosan based targeted drug delivery and tissue engineering applications. *Journal of Controlled Release*, 186, 54–87.

Van de Velde, K. and Kiekens, P. (2002). Biopolymers: overview of several properties and consequences on their applications. *Polymer Testing*, 21, 433–442.

Wang, D., 2007. Superabsorbent polymers derived from kenaf. *International Symposium on Kenaf and Allies Fibres*. Xiamen, China, June 2007.

Wang, W. and Wang, A. (2010). Synthesis and swelling properties of pH-sensitive semi-IPN superabsorbent hydrogels based on sodium alginate-*g*-poly(sodium acrylate) and polyvinylpyrrolidone.

Carbohydrate Polymers, 80, 1028–1036.

Wong, M. (2004). Alginates in tissue engineering. In A. P. Hollander and P. V. Hatton, *Biopolymer methods in tissue engineering* (pp. 77–80). US: Humana Press.

Wu, F., Zhang, Y., Liu, L. and Yao, J. (2012). Synthesis and characterization of a novel cellulose-*g*-poly(acrylic acid-*co*-acrylamide) superabsorbent composite based on flax yarn waste. *Carbohydrate Polymers*, 87, 2519–2525.

Wu, L. and Liu, M. (2008). Preparation and properties of chitosan-coated NPK compound fertilizer with controlled-release and water-retention. *Carbohydrate Polymers*, 72, 240–247.

Wu, L., Liu, M. and Liang, R. (2008). Preparation and properties of a double-coated slow-release NPK compound fertilizer with superabsorbent and water-retention. *Bioresource Technology*, 99, 547–554.

Xu, K. Q., Xu, X. L., Ding, Z. J. and Zhou, M. H. (2006). Synthesis and flocculability of sodium alginate grafted with acrylamide. *China Particuology*, 4, 60–64.

Xu, Y., Zhan, C., Fan, L., Wang, L. and Zheng, H. (2007). Prepration of dual crosslinked alginate-chitosan blend gel beads and in vitro controlled release in oral site-specific drug delivery system. *International Journal of Pharmaceutics*, 336, 329–337.

Xiao, Q., Lu, K., Tong, Q. and Liu, C. (2014). Barrier properties and

microstructure of pullulan-alginate based films. *Journal of Food Processing Engineering*, 38, 155–161.

Yang, F., Li, G., He, Y. G., Ren, F. X. and Wang, G. X. (2009). Synthesis, characterization and applied properties of carboxymethyl cellulose and polyacrylamide graft copolymer. *Carbohydrate Polymers*, 78, 95–99.

Yang, L., Ma, X. and Guo, N. (2011). Synthesis and properties of sodium alginate/Na$^+$ rectorite grafted acrylic acid composite superabsorbent via ^{60}Coγ irradiation. *Carbohydrate Polymers*, 85, 413–418.

Ye, H., Zhao, J. Q. and Zhang, Y. H. (2004). Noel degradable superabsorbent materials of silicate/acrylis-based polymer hybrids. *Journal of Applied Polymer Science*, 91, 936-940.

Yin, Y. H., Ji, X. M., Dong, H., Ying, Y. and Zheng, H. (2008). Study of the swelling dynamics with overshooting effect of hydrogels based on sodium alginate-*g*-acrylic acid. *Carbohydrate Polymers*, 71, 682–689.

Zheng, Y., Li, P., Zhang, J. and Wang, A. (2007). Study on superabsorbent composite XVI. Synthesis, characterization and swelling behaviors of poly(sodium acrylate)/vermiculite superabsorbent composites. *European Polymer Journal*, 43, 1691–1698.

Zhong, K., Lin, Z., Zheng, X., Jiang, G., Fang, Y., Mao, X. and Liao, Z. (2013). Starch derivative-based superabsorbent with integration of water-retaining and controlled release fertilizers. *Carbohydrate Polymers*, 92, 1367–1376.

Zhong, K., Zheng, X., Mao, X., Lin, Z. and Jiang, G. (2012). Sugarcane bagasse derivative-based superabsorbent containing phosphate rock with water-fertilizer integration. *Carbohydrate Polymers*, 90, 820–826.

Zhu, S., Ma, M. and Zhou, W. (1996). Theory of non-random cross-linking: free-radical polymer grafting. *Macromolecules*, 29, 5688–5694.

Zohurian, M. J. and Shokrolahi, F. (2004). Thermal studies on natural and modified gums. *Polymer Testing*, 23, 575–579.

Appendix A

Preparation of 200wt.% NPK fertilizer in ratio 15:15:15 and its calculation

Urea, CH_4N_2O 60.06 g/mol

Phosphate rock, $Ca_3(PO_4)_2$ 310.17 g/mol

Potassium chloride, KCl   74.55 g/mol

Hence,

1 g of urea = 0.466 g of nitrogen (N)

1g of phosphate rock = 0.1997 g of phosphorus (P)

1g of potassium chloride = 0.5245 g of potassium (K)

In order to prepare 200 wt.% of fertilizer, we need to calculate the total solid content of SAP:

NaAlg = 6 g   AA+AM = 21 g H_2O = 380 g

TSC = (NaAlg + AA and AM) / NaAlg + (AA and AM + H_2O)

   = 27/407

   = 6.6%

Fertilizer required for 27g SAP = 27 g x 6.6%

= 1.782 g

200 wt.% fertilizer for this research study = 1.782 g x 2

= 3.546 g

In order to produce NPK fertilizer in ratio 15:15:15,

Amount of N needed = (15/45) x 3.546g

$\qquad$ = 1.188 g

Since the ratio is the same, amount of P needed = 1.188 g

$\qquad$ amount of K needed = 1.188 g

In order to prepare

$\qquad$ *15% of N which is 1.188g,

$\qquad$ 1.188 / 0.466 = 2.549 g of Urea required

$\qquad$ *15% of P which is 1.188g,

$\qquad$ 1.188 / 0.1997 = 5.949 g of phosphate rock required

$\qquad$ *15% of K which is 1.188g,

$\qquad$ 1.188 / 0.5245 = 2.265 g of potassium chloride required.

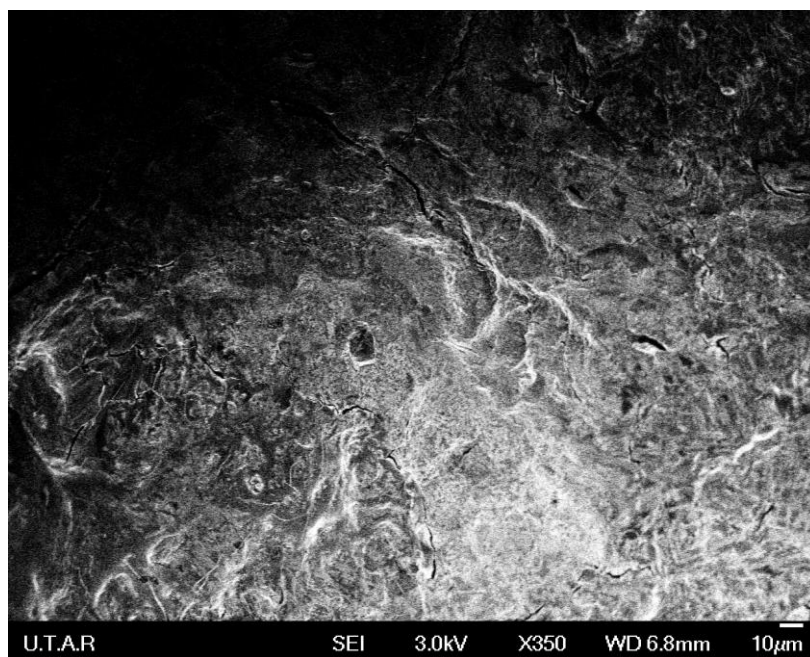**SEM of grafted polymers at x350 magnification**
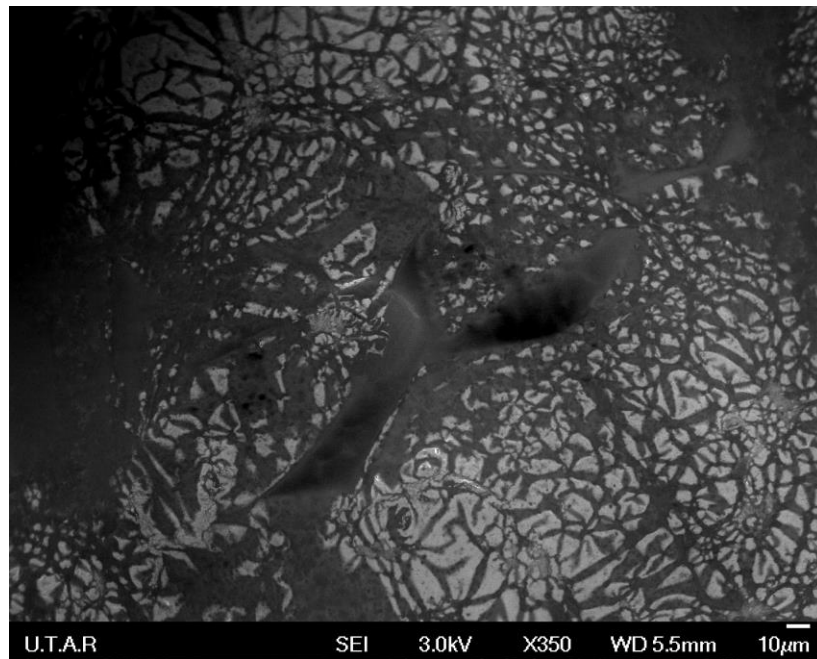
Figure 4.39: FESEM Micrograph of grafted polymer A3 at x350 magnification
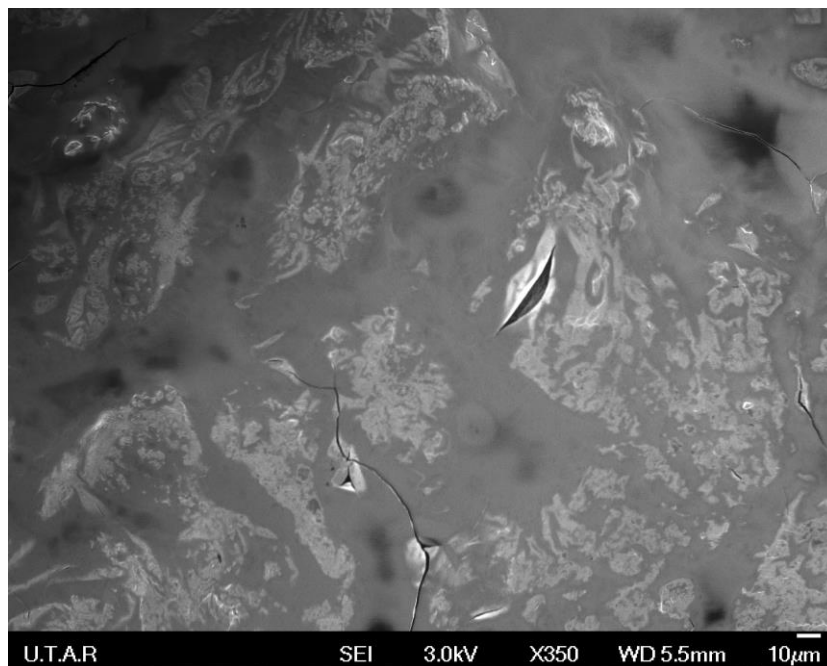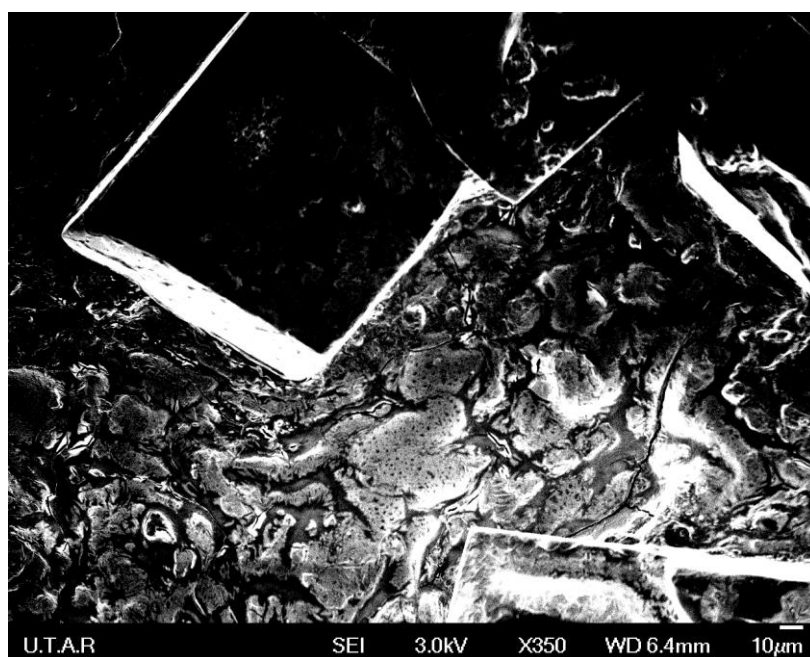

Figure 4.40: FESEM Micrograph of grafted polymer B3 at x350 magnification
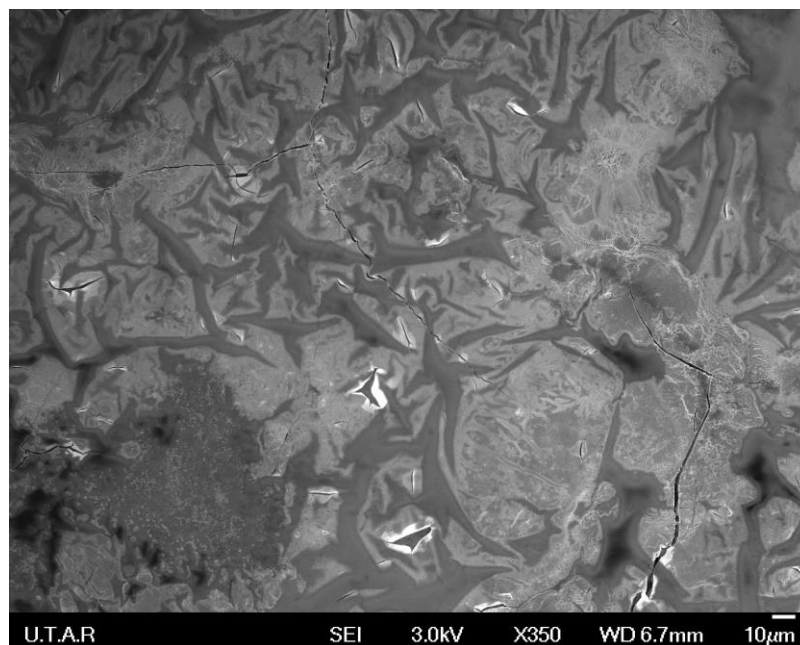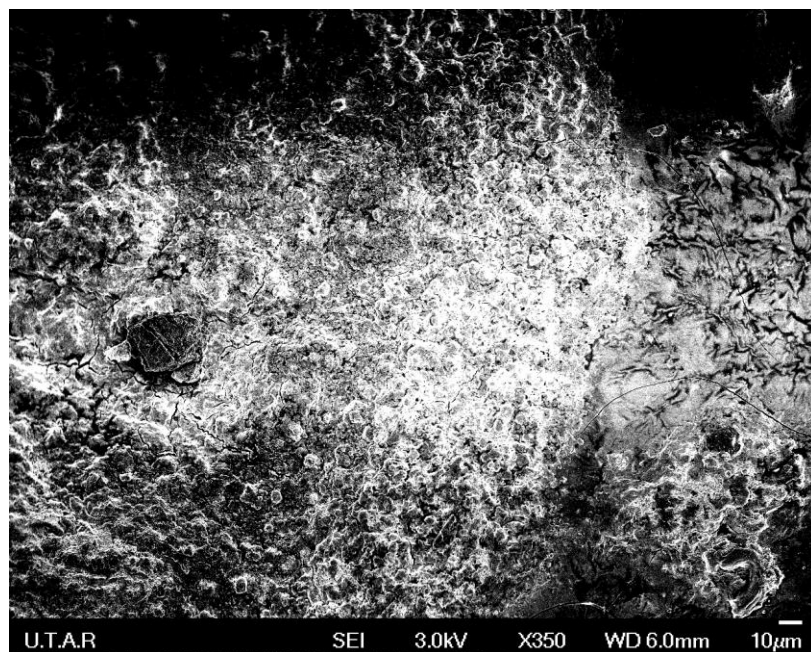
Figure 4.41: FESEM Micrograph of grafted polymer C3 at x350 magnification
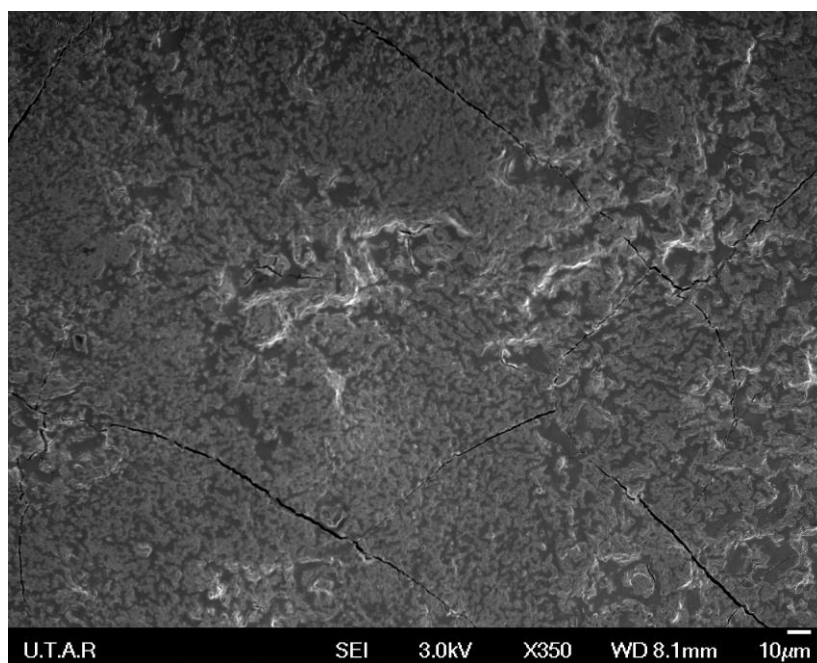
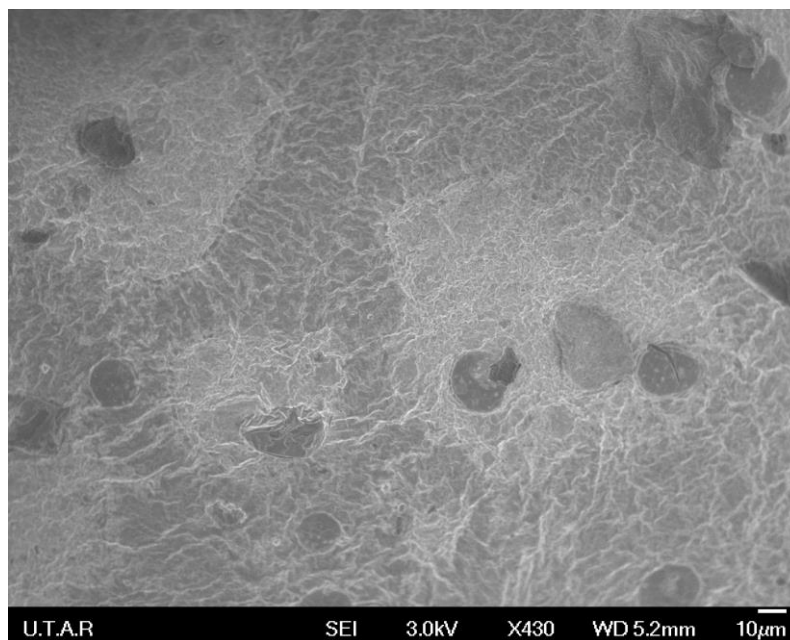**Figure 4.42: FESEM Micrograph of grafted polymer D3 at x350 magnification**
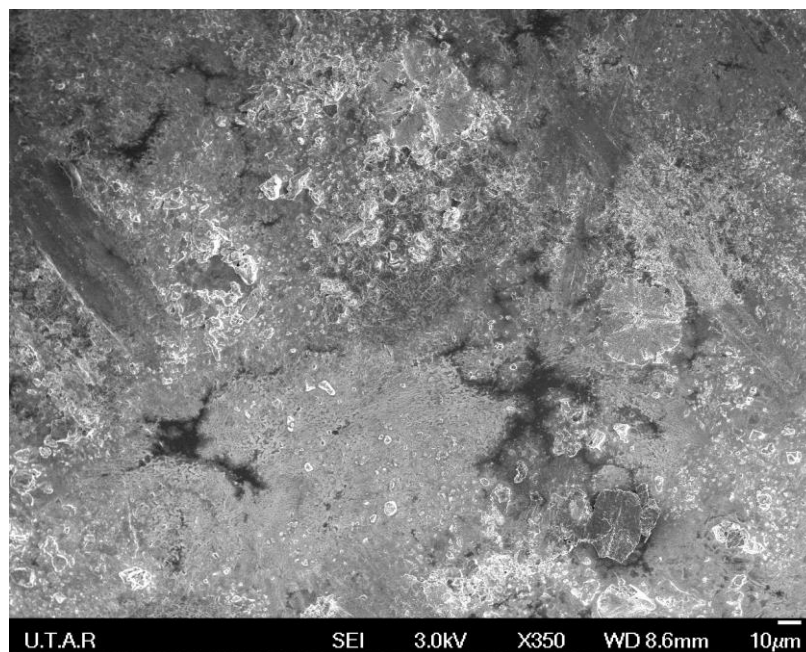
Figure 4.43: FESEM Micrograph of grafted polymer E3 at x350 magnification

SEM of NPK-imbedded grafted polymers at x350 magnification

Figure 4.44: FESEM Micrograph of grafted polymer FA3 at x350 magnification

Figure 4.45: FESEM Micrograph of grafted polymer FB3 at x350 magnification

Figure 4.46: FESEM Micrograph of grafted polymer FC3 at x350 magnification

Figure 4.47: FESEM Micrograph of grafted polymer FD3 at x350 magnification

Figure 4.48: FESEM Micrograph of grafted polymer FE3 at x350 magnification
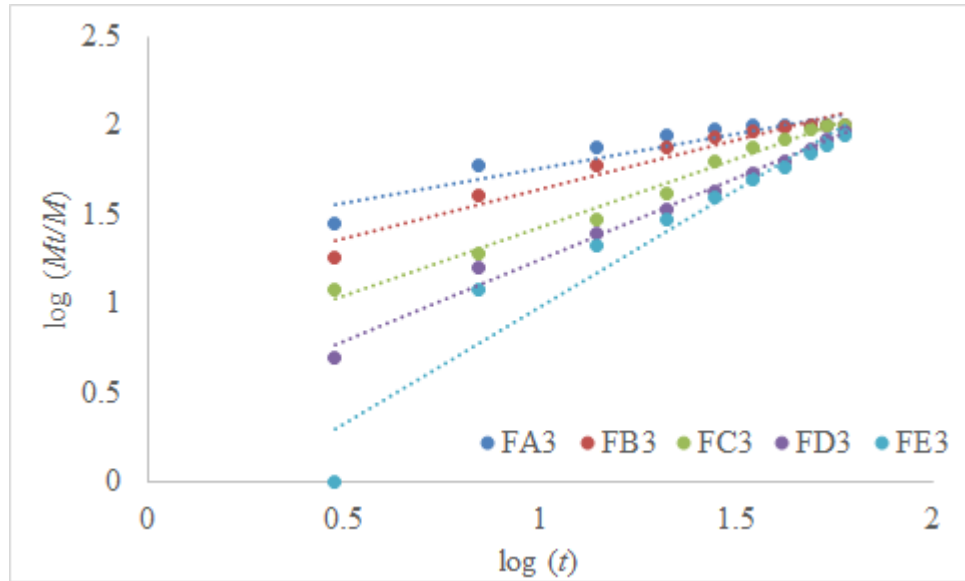
Plot of log (M_t/M) versus log (t) of nutrients

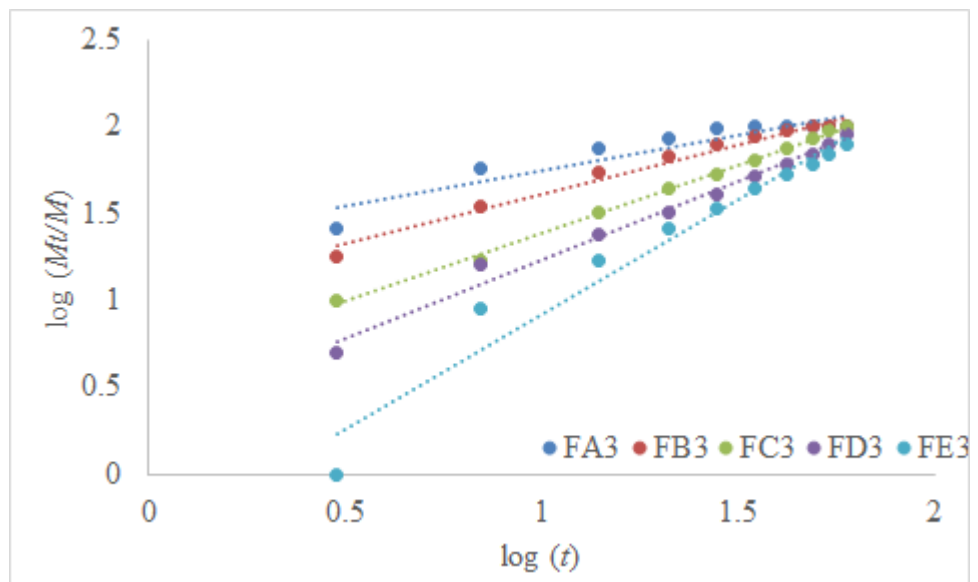**Figure 4.49: Plot of log (M_t/M) versus log (t) of nitrogen (N)**

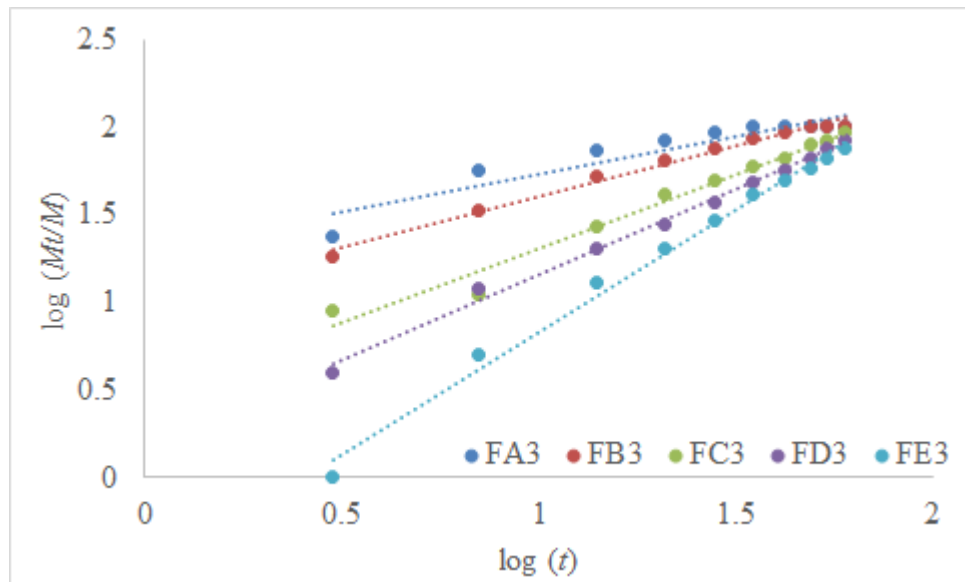**Figure 4.50: Plot of log (M_t/M) versus log (t) of phosphorus (P)**

Figure 4.51: Plot of log (M_t/M) versus log (t) of potassium (K)